# REFERENCES

Abthagir, P.S., Dhanalakshmi, K., and Saraswathi, R. (1998) Thermal studies on polyindole and polycarbazole. Synthetic Metals, 93, 1-7.

Abthagir, P.S. and Saraswathi, R. (2004) Charge transport and thermal properties of polyindole and polycarbazole and their derivatives. Thermochimica Acta, 424, 25-35.

Anandrao, R.K., Kumaresh, S.S., and Tejraj, M.A. (1999) Controlled release of diclofenac sodium from sodium alginate beads crosslinked with glutaraldehyde. Pharmaceutica Acta Helvetiae, 74, 29–36.

Bar-Cohen, Y. (2002, March, 17-19) Electro-active polymers: current capabilities and challenges. Proceeding of SPIE Smart Structures and Materials Symposium, EAPAD Conference, San Diego, CA.

Bar-Cohen, Y. (2004) Electroactive Polymer (EAP) Actuators as Artificial Muscles: Reality, Potential, and Challenges. 2nd ed. Bellingham, Wash: SPIE.

Baughman, R.H. (1996) Conducting polymer artificial muscles. Synthetic Metals, 79, 339-353.

Bhavana, G. and Prakash, R. (2010) Interfacial polymerization of carbazole: Morphology controlled synthesis. Synthetic Metals, 160, 523–528.

Chansai, P., Sirivat, A., Niamlang, S., Chotpattananont, D., and Viravaidya-Pasuwat, K. (2009) Controlled transdermal iontophoresis of sulfosalicylic acid from polypyrrole/poly(acrylic acid) hydrogel. Pharmaceutics, 381, 25-33.

Cianchetti M., Mattoli V., Mazzolai B., Laschi C., and Dario P. (2009) A new design methodology of electrostrictive actuators for bio-inspired robotics. Sensors and Actuators B: Chemical, 142, 288–297.

Del-Valle, L.J., Aradilla, D., Oliver, R., Sepulcre, F., Gamez, A., Armelin, E., Alema'n, C., and Estrany, F. (2007) Cellular adhesion and proliferation on poly(3,4-ethylenedioxythiophene): Benefits in the electroactivity of the conducting polymer. European Polymer Journal, 43, 2342–2349.

Gupta, B., Singh, A.K., and Prakash, R. (2010) Electrolyte effects on various properties of polycarbazole. Thin Solid Films, 519, 1016-1019.

Hall, K.K., Gattás-Asfura, K.M., and Stabler, C.L. (2011) Microencapsulation of islets within alginate/poly(ethylene glycol) gels cross-linked via Staudinger ligation. Acta Biomaterialia 7, 614–624.

Harun, M.H., Saion, E., Kassim, A., Yahya, N., and Mahmud, E. (2007) Conjugated conducting polymers: A brief overview. Journal for the Advancement of Science & Arts, 2, 63-68.

Hiamtup, P., Sirivat, A., and Jamieson, A.M. (2008) Electromechanical response of a soft and flexible actuator based on polyaniline particles embedded in a cross-linked poly(dimethyl siloxane) network. Materials Science and Engineering C: Materials for Biological Applications, 28, 1044–1051.

Hiamtup, P., Sirivat. A., and Jamieson, A.M. (2006) Electrorheological properties of polyaniline suspensions: Field-induced liquid to solid transition and residual gel structure. Journal of Colloid and Interface Science, 295, 270-278.

Inselt, G. (2003) Formation and redox behavior of polycarbazole prepared by electropolymerization of solid carbazole crystals immobilized on an electrode surface. Solid State Electrochem, 7, 503-510.

Ismail, Y.A., Martínezb, J.G., Harrasia, A.S., Kim, S.J., and Otero, T.F. (2011) Sensing characteristics of a conducting polymer/hydrogel hybrid microfiber artificial muscle. Sensors and Actuators B: Chemical, 160, 1180-1190.

Kuen, Y.L. and Mooneya, D.J. (2012) Alginate: Properties and biomedical applications. Polymer Science, 37, 106–126.

Kulkarni, A.R., Soppimath, K.S., Aminabhavi, T.M., Dave, A.M., and Mehta, M.H. (2000) Glutaraldehyde crosslinked sodium alginate beads containing liquid pesticide for soil application. Journal of Controlled Release, 63, 97-105.

Kunanuruksapong, R. and Sirivat, A. (2007) Poly(p-phenylene) and acrylic elastomer blends for electroactive application. Materials Science and Engineering A: Structural Materials : Properties Microstructure and Processing, 454, 453-460.

Kunchornsup, W. and Sirivat, A. (2012) Physically cross-linked cellulosic gel via 1-butyl-3-methylimidazolium chloride ionic liquid and its electrorheological response. Sensors and Actuators A: Physical, 155-164.

Macit, H., Sen, S., and Sacak, M. (2005) Electrochemical synthesis and characterization of polycarbazole. Journal of Applied Polymer Science, 96, 894-898.

Mirfakhrai, T., Madden, D.W., and Baughman, R.H. (2007) Polymer artificial muscles. Material Today, 10, 30-38.

Morin, J., Lecterc, M., Ades, D., and Siove, A. (2005) Polycarbazoles: 25 years of progress. Macromolecular Rapid Communication, 26, 761-778.

Murat A. (2013) A review study of (bio)sensor systems based on conducting polymers. Materials Science and Engineering C: Materials for Biological Applications, 33, 1853–1859.

Nathalie, K., Guimard, N.G., and Christine, E.S. (2007) Conducting polymers in biomedical engineering. Progress in Polymer Science, 32, 876–921.

Palakodeti, R. and Kessler, M.R. (2006) Influence of frequency and prestrain on the mechanical efficiency of dielectric electroactive polymer actuators. Materials Letters, 60, 3437-3440.

Pattavarakorn, D., Youngta, P., and Jaesrichai, S. (2013) Electroactive Performances of Conductive Polythiophene/hydrogel Hybrid Artificial Muscle. Energy Procedia, 34, 673–681.

Prissanaroon, W., Ruangchuay, L., Sirivat, A., and Schwank, J. (2000) Electrical conductivity response of dodecylbenzene sulfonic acid-doped polypyrrole film to $SO_2$-$N_2$ mixtures. Synthetic Metals, 114, 65-72.

Raj, V., Madheswari, D., and Ali, M. (2010) Chemical formation, characterization and properties of polycarbazole. Journal of Applied Polymer Science, 116, 147-154.

Richard, B., Nigel J., Cassidy, S., and Cartmell, H. (2014) Conductive polymers: Towards a smart biomaterial for tissue engineering. Acta Biomaterialia, 10, 2341–2353.

Saarai, A., Kasparkova, V., Sedlacek, T., and Saha, P. (2013) On the development and characterisation of crosslinked sodium alginate/gelatine hydrogels. The Mechanical Behavior of Biomedical Materials, 18, 152–166.

Shahinpoor, M. (2003) Ionic polymer/conductor composites as biomimetic sensors, robotic actuators and artificial muscles. Electrochimica Acta, 48, 2343-2353.

Sílvia, J.B., Barrias, C.C., and Granja, P.L. (2014) Injectable alginate hydrogels for cell delivery in tissue engineering. Acta Biomaterialia, 10, 1646–1662.

Siove, A. and Ades, D. (2004) Synthesis by oxidative polymerization with $FeCl_3$ of a fully aromatic twisted poly(3,6-carbazole) with a blue-violet luminescence. Polymer, 45, 4049-4054.

Tangboriboon, N., Sirivat, A., Kunanuruksapong, R., and Wongkasemjit, S. (2009) Electrorheological properties of novel piezoelectric lead zirconate titanate Pb(Zr0.5,Ti0.5)O3-acrylic rubber composites. Materials Science and Engineering C: Materials for Biological Applications, 29, 1913–1918.

Taoudi, H., Bernede, J.C., Del Valle, M.A., Bonnet, A., Molinie, P., Morsi, M., Diaz, F., Tregovet, Y., and Bereau, A. (2000) Polycarbazole obtained by electrochemical polymerization of monomers either in solution or in thin film form. Journal of Applied Polymer Science, 75, 1561-1568.

Thongsak, K., Kunanuruksapong, R., Sirivat, A., and Lerdwijitjarud, W. (2010) Electroactive styrene–isoprene–styrene triblock copolymer: Effects of morphology and electric field. Materials Science and Engineering A: Structural Materials : Properties Microstructure and Processing, 527, 2504–2509.

Tungkavet, T., Seetapan, N., Pattavarakorn, D., and Sirivat, A. (2012) Improvements of electromechanical properties of gelatin hydrogels by blending with nanowire polypyrrole: effects of electric field and temperature. Polymer International, 61, 825–833.

Verghese, M.M., Sundaresan, N.S, Basu, T., and Malhotra, B.D. (1995) Electroactivity and proton doping of polycarbazole. Materials Science Letters. 14, 401-404.

Wayne, H., Hill, J., and Brady D.G. (1976) Properties, environmental stability, and molding characteristics of polyphenylene sulfide. Polymer Engineering & Science, 16, 831- 835.

Wichiansee, W. and Sirivat, A. (2009) Electrorhrological properties of poly(dimethylsiloxane) and poly(3,4-ethylenedioxy thiophene)/poly(styrene sulfonic acid)/ethylene glycol blends. Materials Science and Engineering C: Materials for Biological Applications, 29, 78-84.

Yanyan, Z., Gao, S., Zhao S., Li, Y., Cheng, L., Li, J., and Yin, Y.    (2012) Synthesis and characterization of disulfide-crosslinked alginate hydrogel scaffolds. <u>Materials Science and Engineering C: Materials for Biological Applications,</u> 32, 2153–2162.

Zhuang, D.X. and Chen, P.Y.  (2009)  Electrochemical formation of polycarbazole films in air and water-stable room-temperature ionic liquids. <u>Journal of Electroanalytical Chemistry,</u> 626, 197-200.

# APPENDICES

## APPENDIX A  Synthesized Polycarbazole by Interfacial Polymerization Method
### A1.  Preparation of Polycarbazol (PCB) by Interfacial Polymerization Method

The synthesizing conditions of PCB by interfacial polymerization method with various concentrations and types of surfactant are shown in Table A1 and the proposed mechanism of synthesized PCB is shown in Figure A1.

**Table A1**   The synthesizing conditions of PCB by interfacial polymerization with various types and concentrations of surfactant at polymerization time of 24 h

| Surfactant Types | Monomer : Surfactant (Mole Ratio) | Remark |
|---|---|---|
| None | 1:0 | PCB |
| Tween 20 (nonionic) | 1:0.0034 | PCB_TW20 (1:0.0034) |
| | 1:0.0068 | PCB_TW20 (1:0.0068) |
| | 1:0.0136 | PCB_TW20 (1:0.0136) |
| | 1:0.0272 | - |
| CTAB (cationic) | 1:0.0034 | PCB_CTAB (1:0.0034) |
| | 1:0.0068 | PCB_CTAB (1:0.0068) |
| | 1:0.0126 | - |
| SDS (anionic) | 1:0.0034 | PCB_SDS (1:0.0034) |
| | 1:0.0068 | PCB_SDS (1:0.0068) |
| | 1:0.0126 | PCB_SDS (1:0.0126) |
| | 1:0.0272 | PCB_SDS (1:0.0272) |
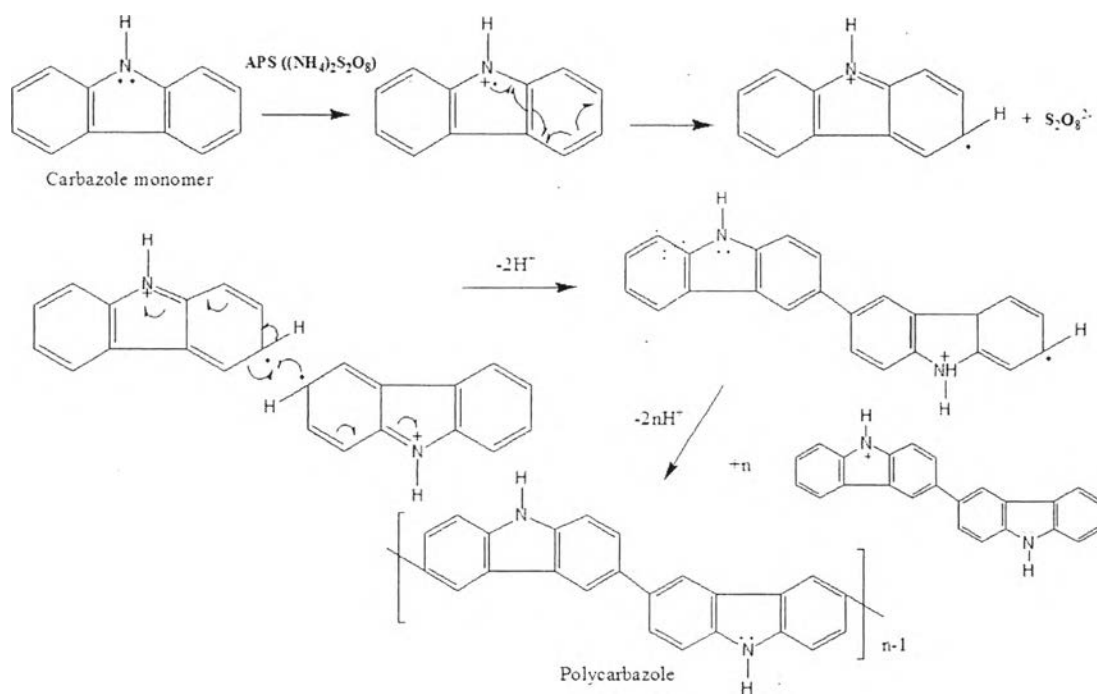
**Figure A1** Proposed mechanistic scheme for the polymerization of PCB.

## A2. Fourier Transform Infrared Spectroscopy

Polycarbazole (PCB) was synthesized via the interfacial polymerization of carbazole monomer. This polymerization was performed at 30 °C (room temperature) with and without adding surfactant. The FT-IR characteristic peaks of synthesized PCB are shown in Figure A2.
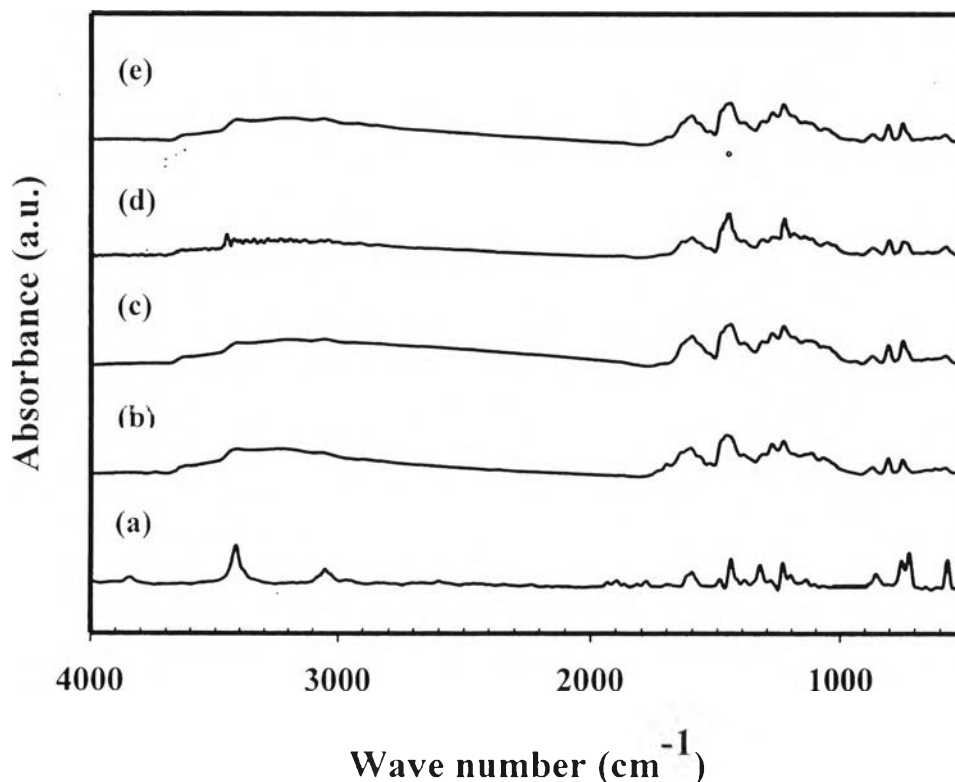
**Figure A2** The FTIR spectra of PCB with interfacial polymerization synthesized by various surfactant types: (a) PCB_monomer; (b) PCB; (c) PCB_TW20 (1 : 0.0068); (d) PCB_CTAB (1 : 0.0068); and (d) PCB_SDS (1 : 0.0068).

The spectra indicate the successfully synthesized PCB and all the systems show the same characteristic peaks. The absorbance peaks at 3400 cm$^{-1}$, 1600-1625 cm$^{-1}$, 1400-1489 cm$^{-1}$, 1200-1235 cm$^{-1}$, 800-875 cm$^{-1}$, and 700-750 cm$^{-1}$ correspond to the N-H stretching of hetero-aromatics, the C=C stretching of aromatic compound, the C-N stretching of substitutions, the C-H in plane bending, the C-H deformation of tri-substituted benzene ring, and the C-H out-of-plane bending, respectively (Macit *et al.*, 2005, Gupta *et al.*, 2010, and Raj *et al.*, 2010). From this result, it can be claimed that the synthesized PCB is not contaminated with any residual surfactant.

## A3. Thermal Gravimetric Analyzer (TGA)

The thermal property of PCB, PCB_TW20 (1:0.0068), PCB_CTAB (1:0.0068), and PCB_SDS (1:0.0068) was investigated using TGA to obtain the onset decomposition temperature ($T_{d,onset}$) of polymer as shown in Figure A3.
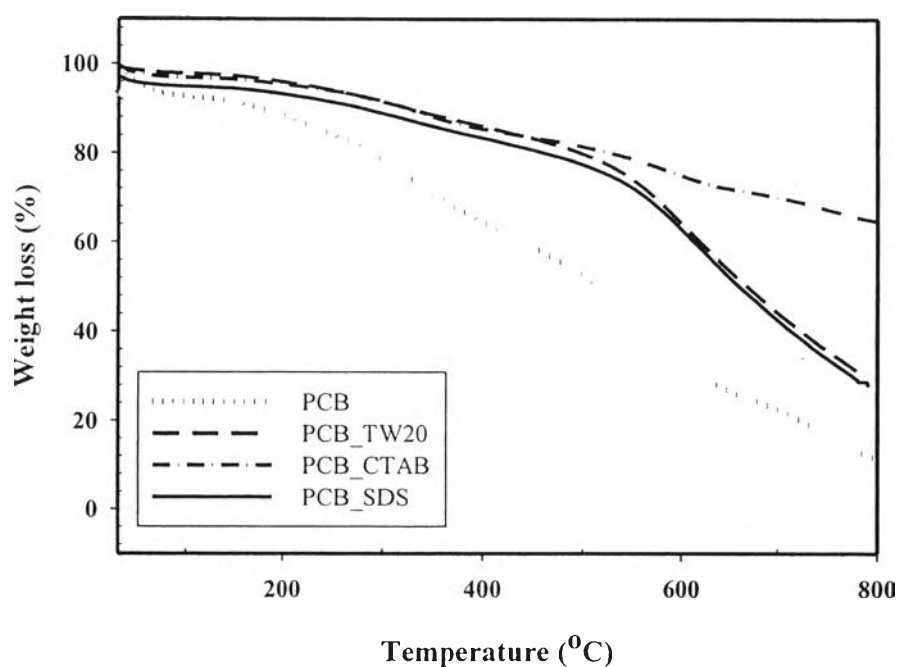


**Figure A3** TGA thermograms of PCB with interfacial polymerization synthesized by various surfactant types.

PCB, PCB_TW20 (1:0.0068), PCB_CTAB (1:0.0068), and PCB_SDS (1:0.0068) show two transition temperatures. In the first transition at 400-600 °C ($T_{d,onset}$: 471.69, 485.34, 534.68, and 472.73 °C, respectively) can be assigned to the elimination of PCB small molecule. The second transition at 400 - 800 °C ($T_{d,onset}$: 731.62, 746.86, 767.08, and 740.34 °C, respectively) can be referred to the decomposition of the polymeric chain (Abthagir et al., 2004). This result indicated that $T_{d,onset}$ of both step increase after adding surfactant. $T_{d,onset}$ of PCB_SDS (1:0.0068) is higher than PCB due to decreasing of the particle size.

$T_{d,onset}$ of PCB_TW20 (1 : 0.0068) is higher than PCB_SDS (1:0.0068) because of the changing of shape hollow sphere to macroporous honeycomb structure that is reduced surface area for thermal attachive. $T_{d,onset}$ of PCB_CTAB (1:0.0068) is the highest because its shape is a connected hollow microsphere that is the highest packing of hollow spheres (Figure A4). Moreover, The char yield increases with increasing $T_{d,onset}$ because the higher $T_{d,onset}$ provides less time for decomposition and char formation (Paradee *et al.*, 2013). The char yields at $T_{d,onset}$ of the polymeric chain are 18.51, 35.27, 60.85, and 27.47, respectively.

## A4 Morphological Structure

SEM images with a magnification of 6000 times were used to examine the morphological structure of the synthesized PCB with various concentrations and types of surfactant using three surfactants (nonionic as TW20, cationic as CTAB, and anionic as SDS), as illustrated in Figure A4.
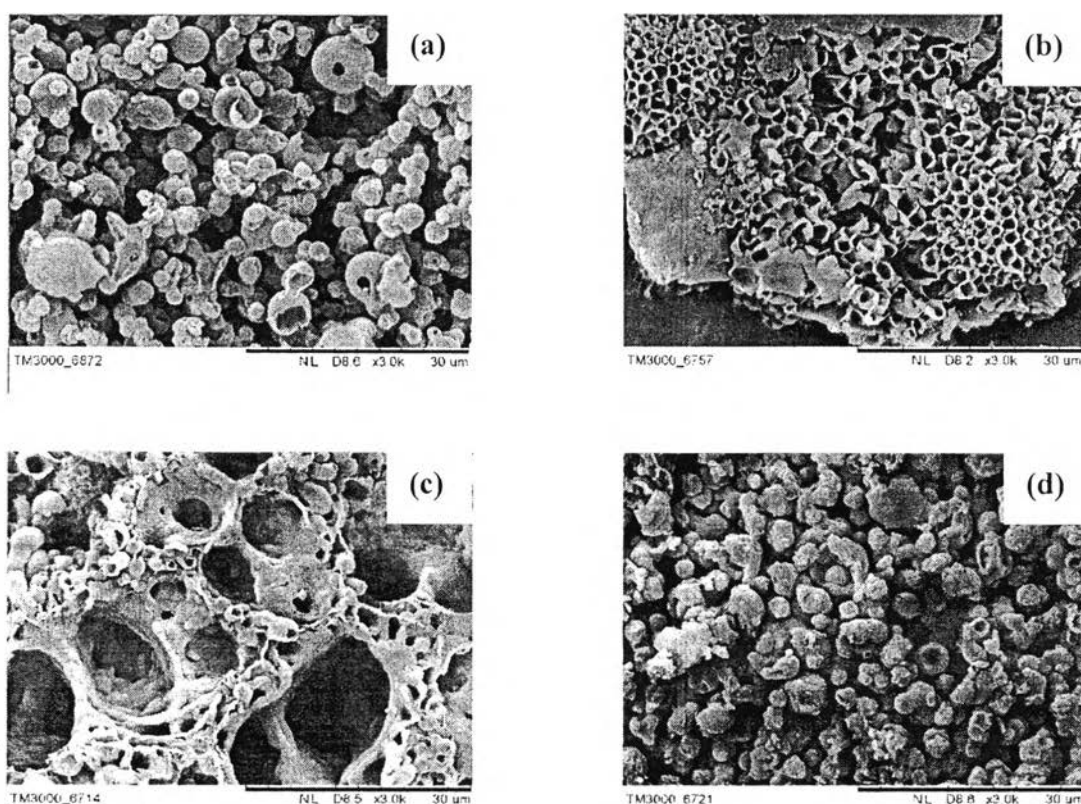
**Figure A4** SEM photographs of PCB synthesized by interfacial polymerization with different surfactant types: (a) PCB; (b) PCB_TW20 (1:0.0068); (c) PCB_CTAB (1:0.0068); and (d) PCB_SDS (1:0.0068) at 24 h).

Figure A4 shows the morphology of the synthesized PCB and the synthesized PCB of various types of surfactant fixed (monomer:surfactant mole ratios of 1:0.0068). The system of no adding surfactant, the particle shapes as the hollow sphere structure (Figure A4 (a)). The system of adding TW20, CTAB, and SDS reveal a porous structure (Figure A4 (b)), a connected hollow sphere structure (Figure A4 (c)), and a small hollow sphere structure (Figure A4 (d)), respectively. For the PCB synthesized without surfactant, the formation of the spherical PCB as polymerized by the interfacial polymerization occurs similar to the vesicle micelle forming mechanism (Gupta *et al.*, 2010). Radical monomer cations are formed by the oxidation of the monomers near the interface between HCl and DCM where polymerization takes place initially within the CB micelles (Gupta *et al.*, 2010). The

shapes of PCB are change with type of surfactant types. For the PCB synthesized with TW20, it produces a porous structure duce to hexagonally packed cylinders formation of micelle. For the PCB synthesized with CTAB, it produces a connected hollow sphere structure because the reverse micelles generate pore spaces within the system and prodcues a fusion and aggregation of the hollow spheres. For the PCB synthesized with SDS, it produces a small hollow sphere due to vesicle forming of CB micelle. SDS as anionic surfactant neutralizes the charges of CB micelle to reduce the size of PCB.
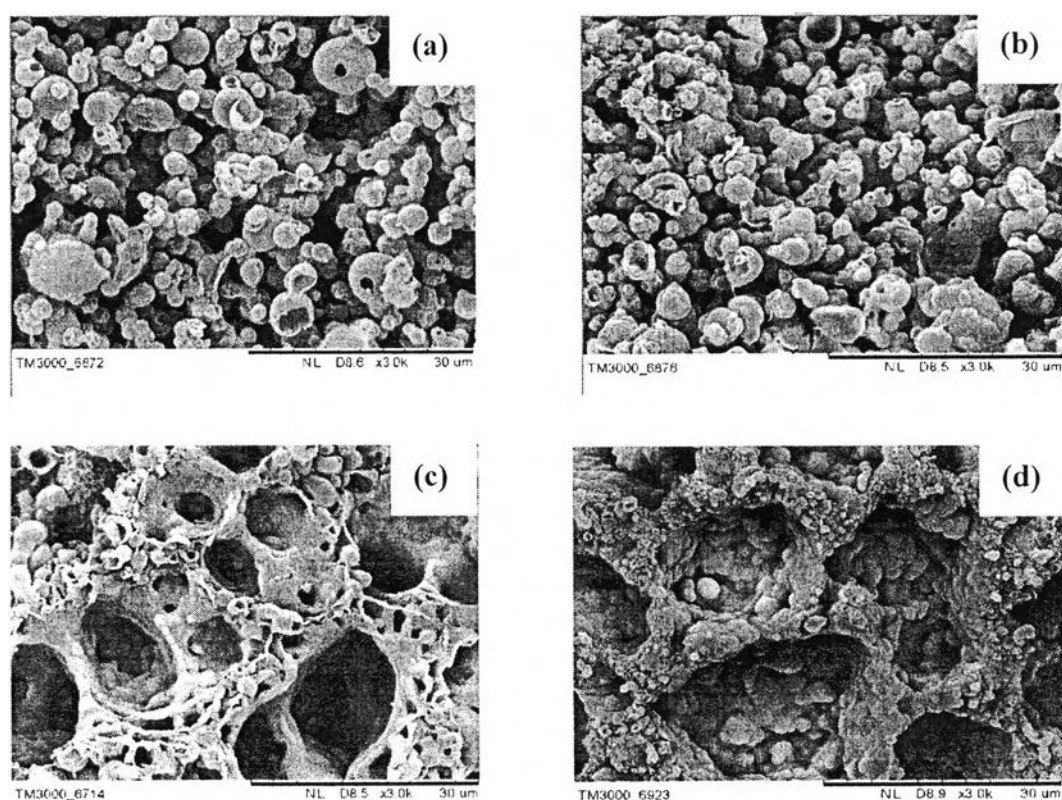


**Figure A5** SEM photographs of PCB synthesized by interfacial polymerization at various monomer: CTAB mole ratios: (a) PCB:CTAB (1:0), (without CTAB); (b) PCB:CTAB (1: 0.0034), ( less than CMC; (c) PCB:CTAB (1:0.0068), (at CMC); and (d) PCB:CTAB (1:0.0126), (more than 2 x CMC) at 24 h.

The morphology of the synthesized PCB (Figure A5 (a)) and the synthesized PCB of various surfactant concentrations (CTAB) (Figure A5 (b) – A5 (d)) reveal the particle shapes as the hollow spheres structure and a connected closed-hollow spheres structure, respectively. For the PCB synthesized without CTAB, the formation of the spherical PCB as polymerized by the interfacial polymerization occurs similar to the micelle forming mechanism (Gupta *et al.*, 2010). Radical monomer cations are formed by the oxidation of the monomers near the interface between APS and DCM where polymerization takes place initially within the PCB micelles (Gupta *et al.*, 2010). For the system with CTAB at concentration less than CMC (monomer: CTAB mole ratio of 1 : 0.0034) , it produces a closed-hollow spheres PCB structure similar to the case without CTAB added (Figure A5 (b)). At a CTAB concentration lower than CMC, micelle is not generated and it has no effect on the packing of PCB. In a system with CTAB concentration equal to CMC (monomer: CTAB mole ratio of 1:0.0068), the CTAB molecules form the reverse micelles (Preni *et al.*, 1993). The formation of the spherical PCB occurs outside the reverse micelles. The mechanism is however the same as the system without CTAB. So, the reverse micelles generate pore spaces within the system and prodcues a fusion and aggregation of the closed-hollow spheres (Figure A5 (c)). For the system with CTAB concentration at more than 2 x CMC (monomer:CTAB mole ratio of 1:0.0126), it produces even a higher packing of connected closed-hollow sphere structures (Figure A5 (d)) when compared with the system synthesized at CMC (Figure A5 (c)). The size of micelle increases with increasing CTAB concentration thus a higher packing of the closed-hollow spherical structures can be expected. Furthermore the polymerization of PCB does not occur at a CTAB concentration more than 2 x CMC.
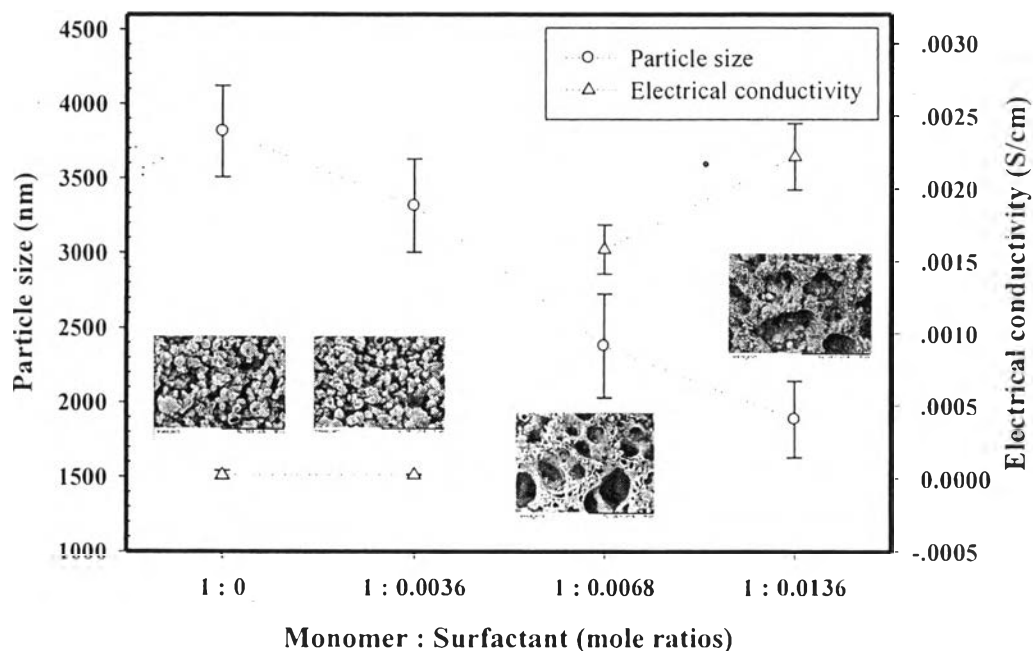
**Figure A6** The particle size and electrical conductivity of PCB with interfacial polymerization synthesized by various CTAB concentrations.

Figure A6 shows particle size and electrical conductivity under the effect of CTAB concentrations. When the concentration of CTAB is increased from 1 : 0 to 1 : 0.0036 mole ratio, the particle size is decreased, but the electrical conductivity is slightly increased. When the concentration of CTAB is increased from 1 : 0.0036 to 1 : 0.0068 and from 1 : 0.0068 to 1 : 0.0136 mole ratio, the particle size is continuously decreased, but the electrical conductivity is greatly increased because the smaller size and higher packing of particle corresponds to the higher surface area for electron transfer (Paradee *et al.*, 2013).

The electrical conduction of both PCB_TW20 and PCB_SDS are 1.72E-04 ± 5.80E-06 and 2.62E-03 ± 7.88E-04 S/cm, respectively, which lower than PCB_CTAB (2.62E-03 ± 7.88E-04) because they have a lower particle packing that correspond to the lower surface area for electron transfer. However, PCB_TW20 shows higher electrical conductivity because it has a lower particle packing that

corresponds to the lower surface area for electron transfer (Table A2). Moreover, the electrical conductivity of the all systems of PCB is increased after doped by $HClO_4$. The concentration of $HClO_4$ affects to the electrical conductivity that is polymer : $HClO_4$ ratio of 1 : 50 mole shown the highest electrical conductivity (Table A2) because this condition is appropriated for doped acting as an electron withdrawing group. It pulls an electron out of the polymer backbone. Then, the polymer backbone contains a hole and an electron from a neighboring bond jumps to fill the bond (Permpool *et al.*, 2013). However, PCB_CTAB has the highest electrical conductivity after doped with the polymer:$HClO_4$ ratio of 1:50 mole that the electrical conductivity is increased four orders of magnitude relative to the undoped PCB_CTAB and three orders of magnitude higher than doped PCB.
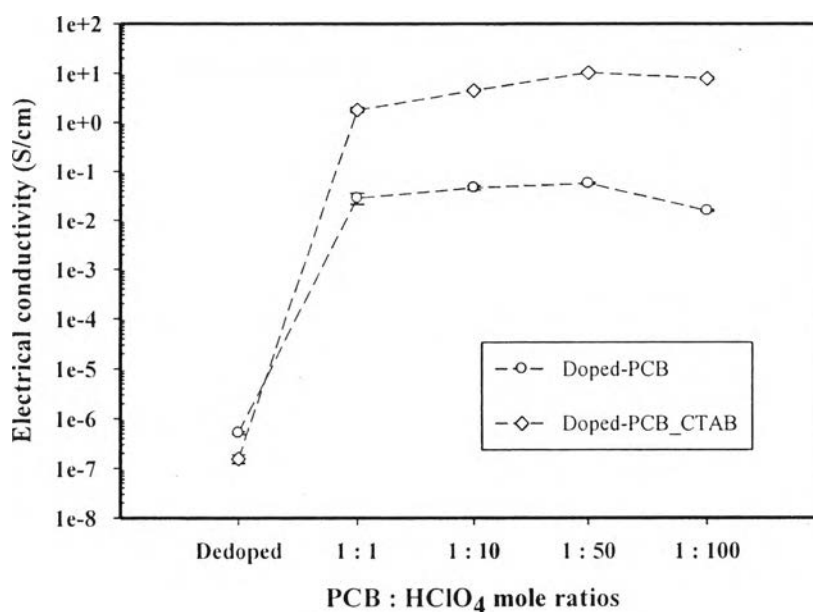


**Figure A7** The electrical conductivity of PCB after doped with various mole ratios of PCB:$HClO_4$.

**Table A2** Particle size and electrical conductivity of PCB with various surfactant types

| Samples | Particle Size (nm) | Electrical Conductivity (S/cm) | |
|---|---|---|---|
| | | Undoped | Doped |
| PCB | $3213 \pm 944$ | $2.72E-06 \pm 3.16E-07$ | $5.59E-02 \pm 2.69E-03$ |
| PCB_TW20 (1:0.0136) | $1182 \pm 327$ | $1.72E-04 \pm 5.80E-06$ | $7.67E-01 \pm 3.70E-02$ |
| PCB_CTAB (1:0.0136) | $2068 \pm 455$ | $2.62E-03 \pm 7.88E-04$ | $1.13E+01 \pm 3.61E-01$ |
| PCB_SDS (1:0.0136) | $2841 \pm 835$ | $2.16E-05 \pm 1.79E-05$ | $4.49E-02 \pm 3.32E-03$ |

## A5 Critical Micelle Concentration of Surfactant

The critical micelle concentration (CMC) of the three surfactants were determined by measuring the surface tension of the pure surfactant with a tensiometer (Kruss/Easydyne tensiomeyer, K20) using the plate method. The three surfactants were dissolved in dichlomethan at various concentrations at 25 °C. Surface tension was recorded eight times and averaged for each sample.
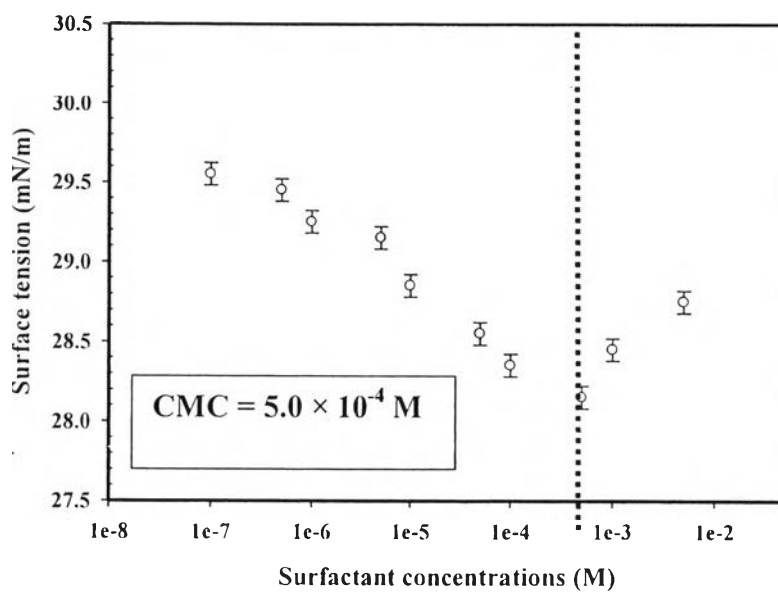
**Figure A8** The critical micelle concentration (CMC) of CTAB in dichloromethane at 25 °C.
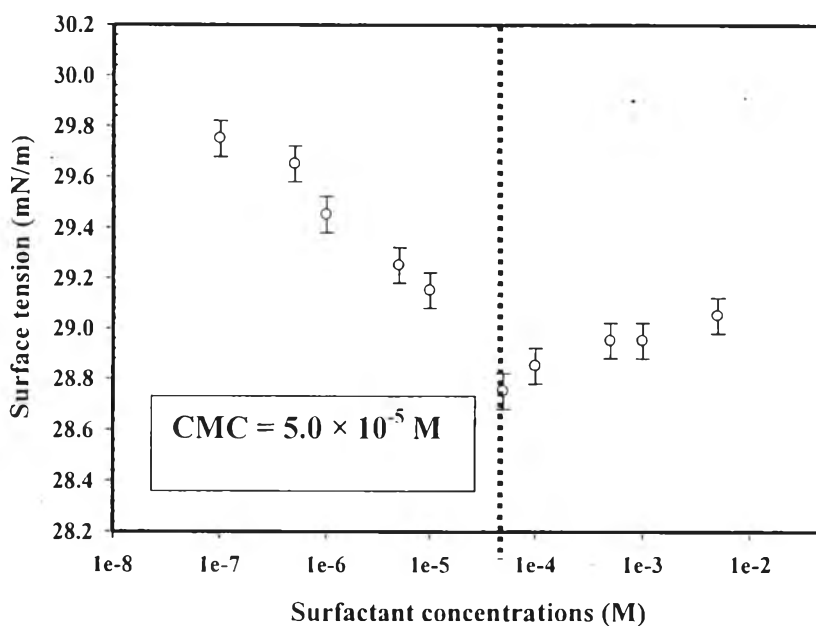


**Figure A9** The critical micelle concentration (CMC) of TW20 in dichloromethane at 25 °C.
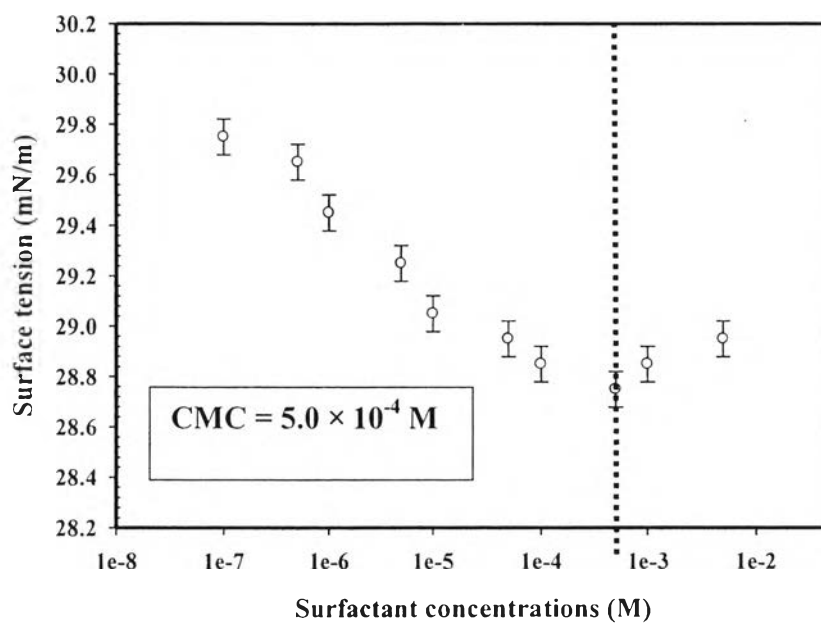
**Figure A10** The critical micelle concentration (CMC) of SDS in dichloromethane at 25 °C.

## A6  Density of PCB after Doped with $HClO_4$

Density of PCB was analyzed by Ultrapycnometer 100 (version 2.4).

**Table A3**  Density of PCB after doped with $HClO_4$

| Run | Density (g/cm$^3$) |
|:---:|:---:|
| 1 | 2.1266 |
| 2 | 2.1210 |
| 3 | 2.1224 |
| 4 | 2.1231 |
| 5 | 2.1222 |
| 6 | 2.1255 |
| 7 | 2.1297 |
| 8 | 2.1266 |
| 9 | 2.1272 |
| 10 | 2.1274 |
| **Average Density** | **2.1252** |
| **Deviation Achieved** | **0.0028** |

## APPENDIX B  Characterization of Sodium Alginate Hydrogels (SA)
## B1  Crosslinking Density of SA Hydrogel

The alginate hydrogels were analyzed by swelling studies immediately after crosslinking, according to the method of Gudeman and Peppas (1995). A sample of the hydrogel (1 cm$^2$ square) was cut and weighed in air and heptane (a non-solvent). The sample was placed in a stainless steel mesh basket which was suspended in heptane to obtain accurate weight measurements in heptane.  The sample was then placed in a buffer solution at 37 °C for 5 days to allow it to swell towards equilibrium, and then was weighed in air and heptane again. Before weighting, the sample was blotted with tissue paper to remove surface water. Finally, the sample was dried at 25 °C in a vacuum for 5 days. Once again it was weighed in air and heptane. The crosslinking density was calculated using equation B1.

$$\frac{1}{\overline{M}_c} = \frac{1}{\overline{M}_n} - \frac{\dfrac{\overline{v}}{\overline{V}_1}\left[\ln\left(1 - v_{2,s}\right) + v_{2,s} + \chi v_{2,s}^2\right]}{v_{2,r}\left[\left(\dfrac{v_{2,s}}{v_{2,r}}\right)^{1/3} - \dfrac{1}{2}\left(\dfrac{v_{2,s}}{v_{2,r}}\right)\right]}$$

(B1)

Where:

$\overline{M}_n$ = the number-average molecular weight of the polymer before cross-linking

$\overline{v}$ = the specific volume of alginate

$\overline{V}_1$ = the molar volume of water (18.1 cm3/mol)

$\chi$ = the Flory interaction parameter of alginate and the dissociation constant is pKa = 4.7

## B1.1 Crosslinking Density of SA Hydrogel with Ionic Crosslinking (CaCl$_2$)

**Table B1** Weight loss (%) and crosslinking density (mol/cm$^3$) of SA hydrogels of various CaCl$_2$ concentrations

| SA Hydrogel Types | CaCl$_2$ Concentrations (%v/v) | Weight Loss (%) | Crosslinking Density (mol/cm$^3$)×10$^6$ |
|---|---|---|---|
| 1%v/v High molecular weight (1%v/v HSA) | 0.0050 | 61.40 ± 2.05 | 10.36 ± 2.33 |
| | 0.0100 | 49.67 ± 7.50 | 14.70 ± 6.28 |
| | 0.0150 | 40.57 ± 5.40 | 18.50 ± 8.87 |
| | 0.0200 | 28.39 ± 5.91 | 19.80 ± 7.31 |
| 1%v/v Medium molecular weight (1%v/v MSA) | 0.0050 | 75.73 ± 1.62 | 11.47 ± 0.58 |
| | 0.0100 | 75.28 ± 2.25 | 12.06 ± 0.04 |
| | 0.0150 | 50.34 ±7.30 | 16.71 ± 1.20 |
| | 0.0200 | 42.50 ± 1.02 | 21.01 ± 2.00 |
| 1%v/v Low molecular weight (1%v/v LSA) | 0.0050 | 81.51 ± 3.33 | 12.66 ± 0.21 |
| | 0.0100 | 80.38 ± 6.91 | 14.43 ± 0.72 |
| | 0.0150 | 58.98 ± 2.30 | 22.31 ± 9.46 |
| | 0.0200 | 37.15 ± 2.26 | 38.78 ± 0.24 |

## B1.2 Crosslinking Density of SA Hydrogels with Covalent Crosslinking (Citric Acid:CA)

**Table B2** Weight loss (%) and crosslinking density (mol/cm$^3$) of SA hydrogel of various CA concentrations

| SA Hydrogel Types | CA Concentrations (%v/v) | Weight Loss (%) | Crosslinking Density (mol/cm$^3$)×10$^6$ |
|---|---|---|---|
| 1%v/v High molecular weight (1%v/v HSA) | 0.25 | - | - |
| | 0.50 | 78.42 ± 1.36 | 19.79 ± 8.78 |
| | 0.75 | 75.43±4.57 | 74.34 ± 12.65 |
| | 1.00 | 73.58 ± 0.52 | 165.8 ± 14.26 |
| 1%v/v Medium molecular weight (1%v/v MSA) | 0.25 | - | - |
| | 0.50 | 78.92 ± 2.07 | 15.60 ± 2.77 |
| | 0.75 | 74.56 ± 1.34 | 63.82 ±8.16 |
| | 1.00 | 71.42 ± 1.24 | 156.23 ± 28.32 |
| 1%v/v Low molecular weight (1%v/v LSA) | 0.25 | - | - |
| | 0.50 | 85.22 ± 5.35 | 20.82 ± 9.78 |
| | 0.75 | 80.23 ± 2.18 | 60.23 ± 9.64 |
| | 1.00 | 72.43 ± 1.35 | 132.76 ± 26.54 |

## B2 Fourier Transform Infrared Spectroscopy

Sodium alginate (SA) hydrogels were prepared by the crosslinkings through either ionic crosslinking $(CaCl_2)$ or covalent crosslinking (citric acid; CA). Both of SA hydrogels were first characterized for the functional groups by the Fourier transform infrared spectrometer (Thermo Nicolet, Nexus 670) in the absorbance mode with 64 scans at a resolution of $4\ cm^{-1}$.
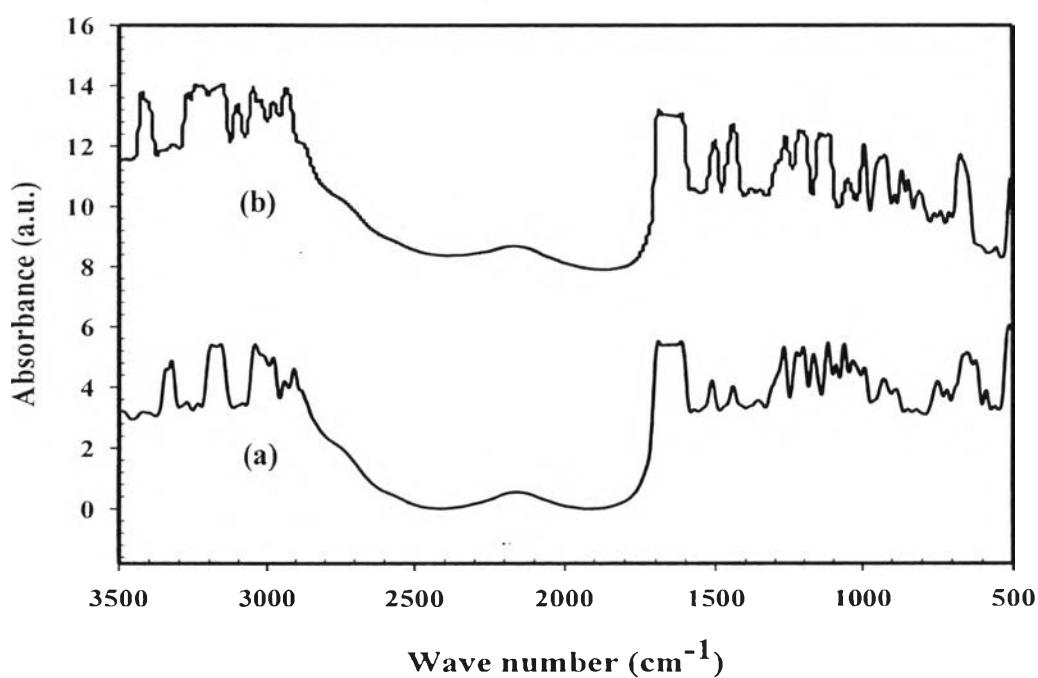


(A)

**Figure B1** FTIR spectra of SA hydrogels: (A) ionic crosslinking method; (B) covalent crosslinking (B); (a) pristine 1%v/v HSA; (b) 1%v/v HSA + 0.015%v/v $CaCl_2$; and (c) 1%v/v HAS + 0.50%v/v $CaCl_2$.
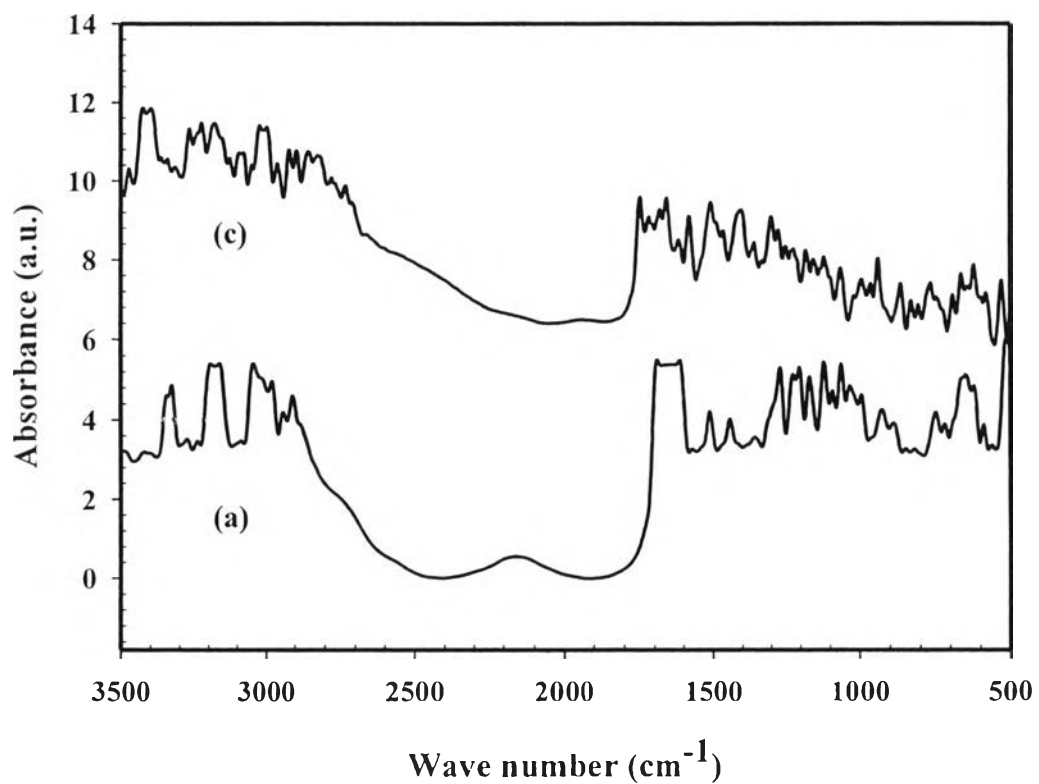
**(B)**

**Figure B1** FTIR spectra of SA hydrogels: (A) ionic crosslinking method; (B) covalent crosslinking (B); (a) pristine 1%v/v HSA; (b) 1%v/v HSA + 0.015%vlv CaCl₂; and (c) 1%v/v HAS + 0.50%vlv CaCl₂. (Cont.)

**Table B3** FTIR assignments of SA hydrogels

| Wavenumber ($cm^{-1}$) | Assignment Peaks | References |
|---|---|---|
| 3265 | O-H stretching | Saarai et al., 2013 |
| 1590-1587 | -COO- | Saarai et al., 2013 |
| 1071 | C-C and C-O stretching | Saarai et al., 2013 |
| 1200-1235 | C-H in plane bending | Saarai et al., 2013 |
| 1025 | C-C stretching | Saarai et al., 2013 |
| 800-875 | C-H stretching | Saarai et al., 2013 |

## B3 Thermal Gravimetric Analyzer

A thermal gravimetric analyzer (DuPont, TGA 2950) was used to characterize the thermal behavior and the water content of SA hydrogels. They were investigated by weighting example of 5-10 mg and placed it in platinum pan, and then heating it under nitrogen flow with the heating rate 10°C/min from 30-800°C.
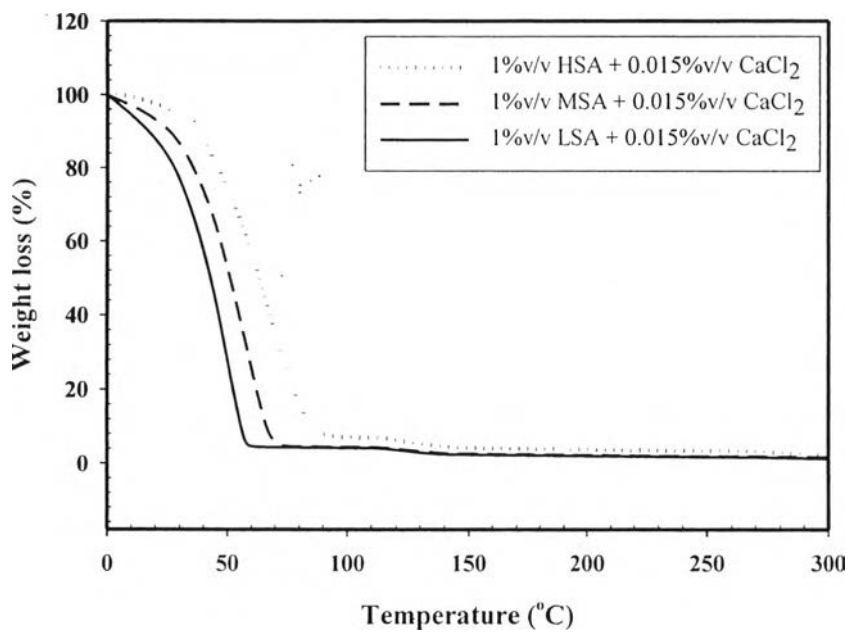
**(A)**
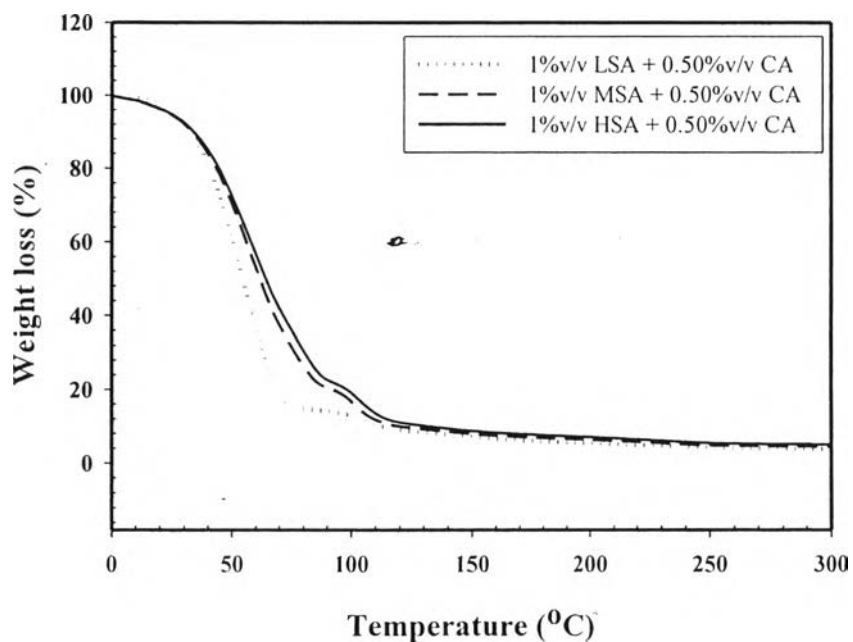


**(B)**

**Figure B2** TGA thermogram of SA hydrogels: (A) ionic crosslinking method, (B) covalent crosslinking.

## B4 X-ray Diffraction

X-ray diffraction (Gupta *et al.*, 2010) was used to investigate the amount of crystalline in SA hydrogels in a based powder form. The diffractometer was operated in the Bragg-Brentano geometry and fitted with a graphite monochromator in the diffracted beam with 5°/min scan rate.
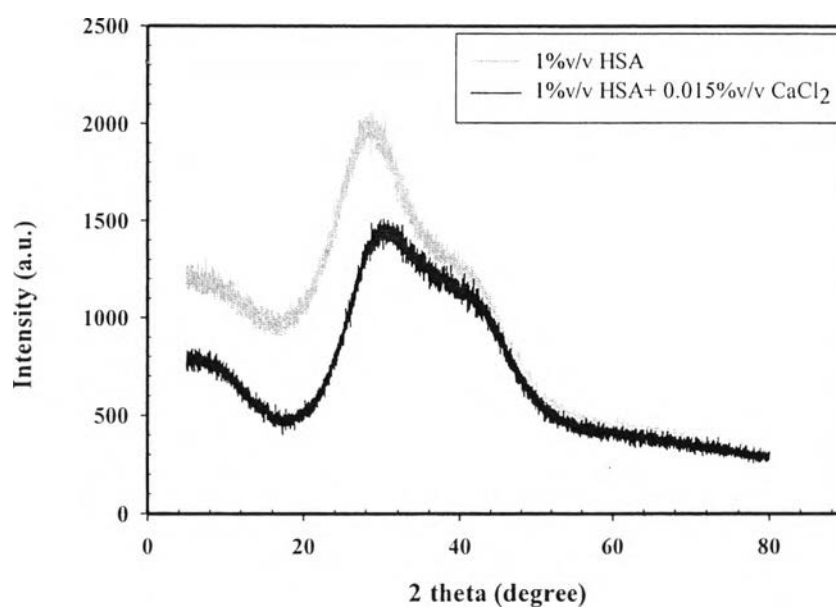


(A)

**Figure B3** XRD measurement of SA hydrogels: (A) ionic crosslinking method, (B) covalent crosslinking method.
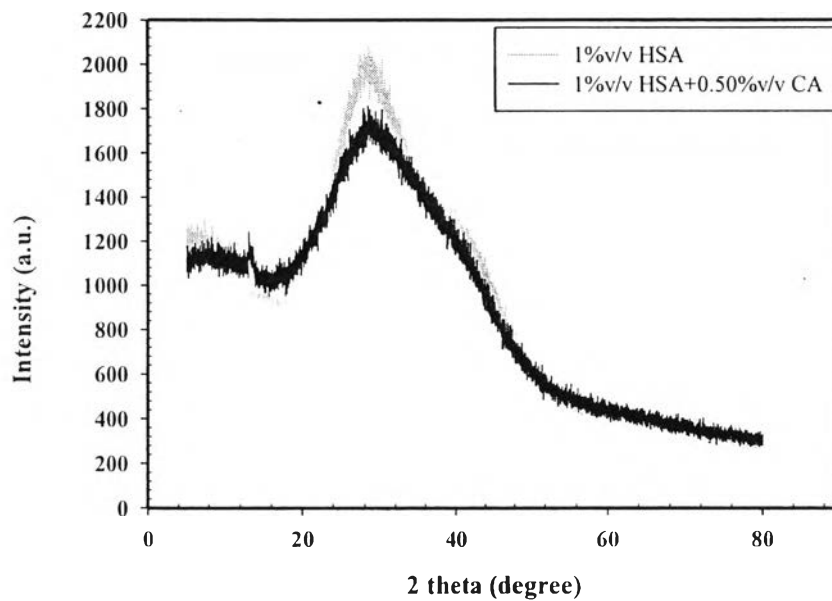
**(B)**

**Figure B3** XRD measurement of SA hydrogels: (A) ionic crosslinking method, (B) covalent crosslinking method. (Cont.)

**B5 Atomic Force Microscopy (AFM)**

AFM (CSPM 400) images were taken with a scanning electron microscope to determine the topology of the hydrogels at crosslinking types by using a scan rate 0.5 Hz and a scan sized of $2.5\mu m \times 2.5\mu m^2$.
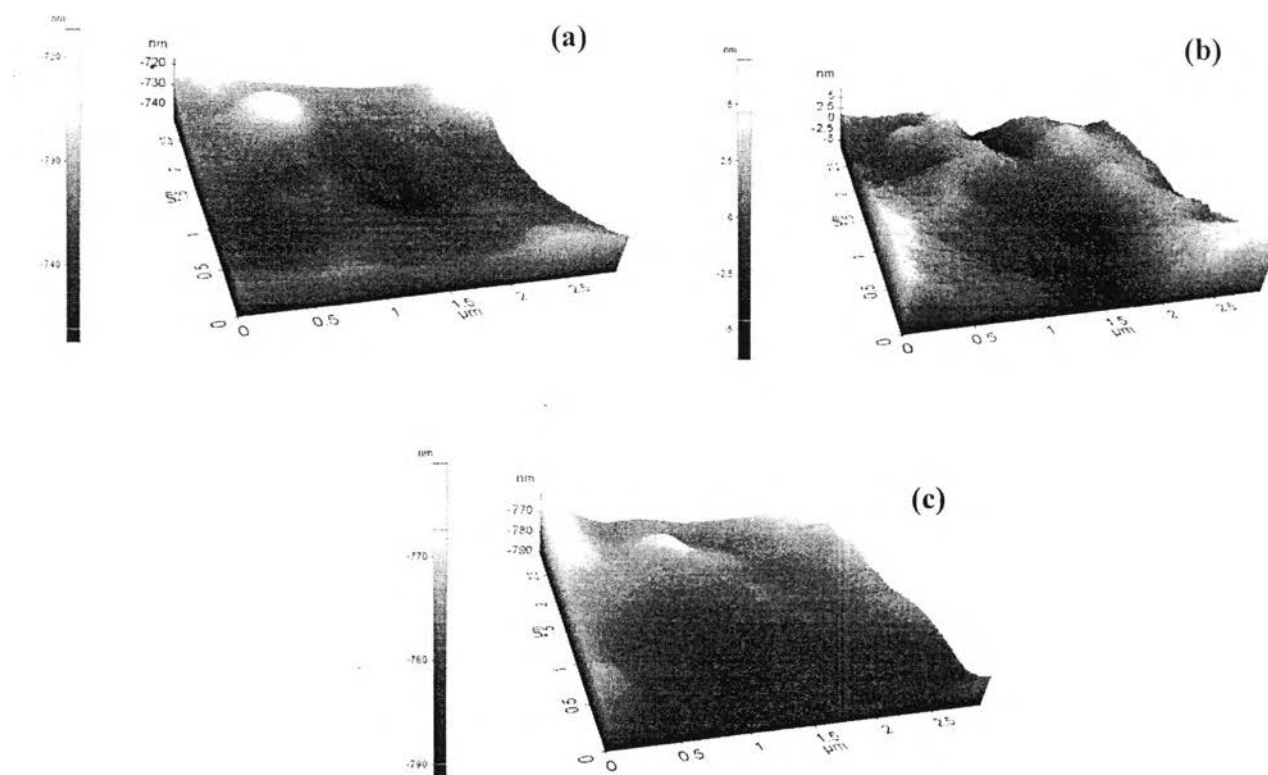
**Figure B4**  AFM micrographs: (a) HSA without crosslinking; (b) HSA by ionic crosslinking; and (c) HSA by covalent crosslinking.

## APPENDIX C  Electromechanical Properties Measurements of Sodium Alginate (SA) Hydrogels

### C1  Sodium alginate hydrogels crosslinked with ionic crosslinking ($CaCl_2$)

**Table C1**  The storage modulus of sodium alginate hydrogels with fixed 0.015%v/v $CaCl_2$ under applied electric field strength (fixed frequency =100 and %strain = 0.1)

| Electric Field Strength (V/mm) | The Storage Modulus (Pa) | | |
|---|---|---|---|
| | High Molecular Weight Alginate | Medium Molecular Weight alginate | Low Molecular Weight Alginate |
| 0 | 1.09E+05 ± 1.49E+04 | 8.58E+04 ± 3.07E+03 | 5.75E+04 ± 2.15E+03 |
| 25 | 1.16E+05 ± 9.26E+03 | 9.68E+04 ± 3.62E+03 | 7.01E+04 ± 2.62E+03 |
| 50 | 2.06E+05 ± 4.99E+03 | 9.90E+04 ± 3.70E+03 | 8.31E+04 ± 3.11E+03 |
| 100 | 3.12E+05 ± 2.04E+04 | 1.20E+05 ± 4.49E+03 | 8.77E+04 ± 3.28E+03 |
| 200 | 4.53E+05 ± 2.07E+04 | 1.42E+05 ± 5.30E+03 | 9.54E+04 ± 3.57E+03 |
| 300 | 5.77E+05 ± 2.64E+04 | 2.05E+05 ± 7.65E+03 | 9.79E+04 ± 3.66E+03 |
| 400 | 6.39E+05 ± 2.92E+04 | 2.47E+05 ± 9.25E+03 | 1.08E+05 ± 4.03E+03 |
| 500 | 7.37E+05 ± 3.44E+04 | 2.78E+05 ± 1.04E+04 | 1.46E+05 ± 5.45E+03 |
| 600 | 7.85E+05 ± 4.40E+04 | 3.84E+05 ± 1.44E+04 | 1.83E+05 ± 6.84E+03 |
| 700 | 8.02E+05 ± 4.49E+04 | 4.62E+05 ± 1.73E+04 | 2.12E+05 ± 7.93E+03 |
| 800 | 8.16E+05 ± 3.81E+04 | 5.35E+05 ± 2.41E+04 | 2.51E+05 ± 9.38E+03 |

**Table C2**  The storage modulus sensitivity of sodium alginate hydrogels with 0.015%v/v $CaCl_2$ under applied electric field strength (fixed frequency =100 and %strain =0.1)

| Electric Field Strength (V/mm) | The storage modulus sensitivity | | |
|---|---|---|---|
| | High Molecular Weight Alginate | Medium Molecular Weight Alginate | Low Molecular Weight Alginate |
| 25 | $0.06 \pm 0.05$ | $0.13 \pm 0.01$ | $0.22 \pm 0.07$ |
| 50 | $0.89 \pm 0.05$ | $0.16 \pm 0.04$ | $0.45 \pm 0.08$ |
| 100 | $1.86 \pm 0.14$ | $0.43 \pm 0.05$ | $0.53 \pm 0.11$ |
| 200 | $3.15 \pm 0.08$ | $0.68 \pm 0.06$ | $0.66 \pm 0.12$ |
| 300 | $4.39 \pm 0.17$ | $1.43 \pm 0.09$ | $0.70 \pm 0.13$ |
| 400 | $4.86 \pm 0.07$ | $1.94 \pm 0.11$ | $0.88 \pm 0.06$ |
| 500 | $5.76 \pm 0.08$ | $2.30 \pm 0.12$ | $1.54 \pm 0.09$ |
| 600 | $6.19 \pm 0.17$ | $3.56 \pm 0.17$ | $2.19 \pm 0.02$ |
| 700 | $6.56 \pm 0.46$ | $4.49 \pm 0.20$ | $2.69 \pm 0.27$ |
| 800 | $7.66 \pm 0.35$ | $6.20 \pm 0.28$ | $3.37 \pm 0.33$ |
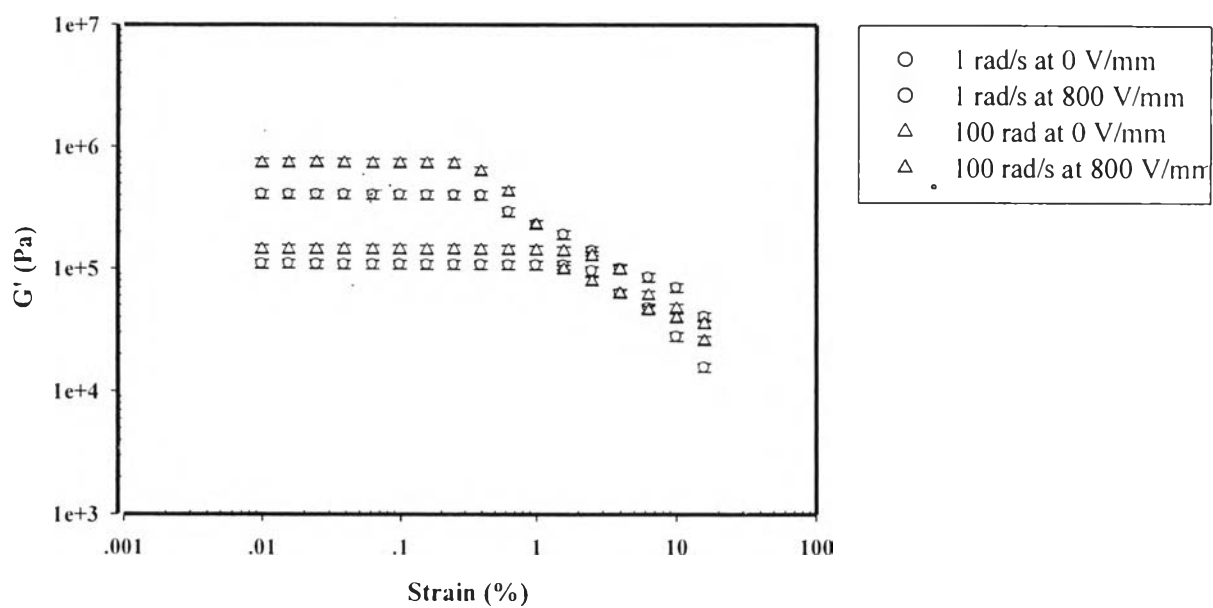
(a)
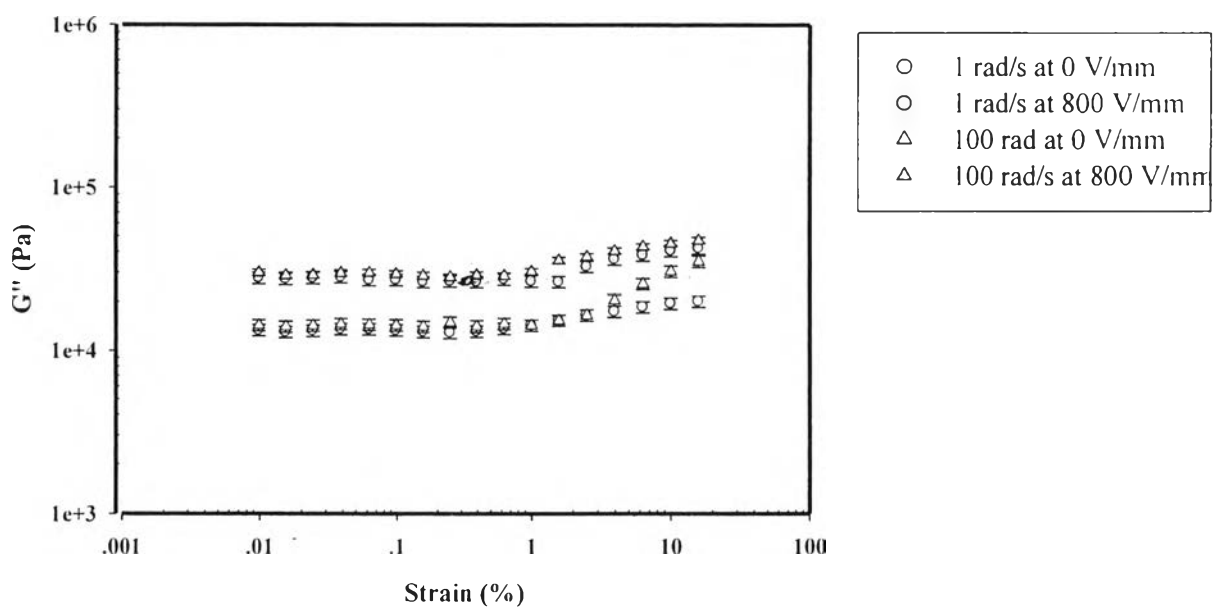


(b)

**Figure C1** Strain sweep test: (a) storage modulus and (b) loss modulus of 1%v/v HSA hydrogel with 0.015%v/v $CaCl_2$ at frequency 1 rad/s and 100 rad/s, electric field strength 0 V/mm and 800 V/mm, sample thickness 1.65 mm, 300 K.
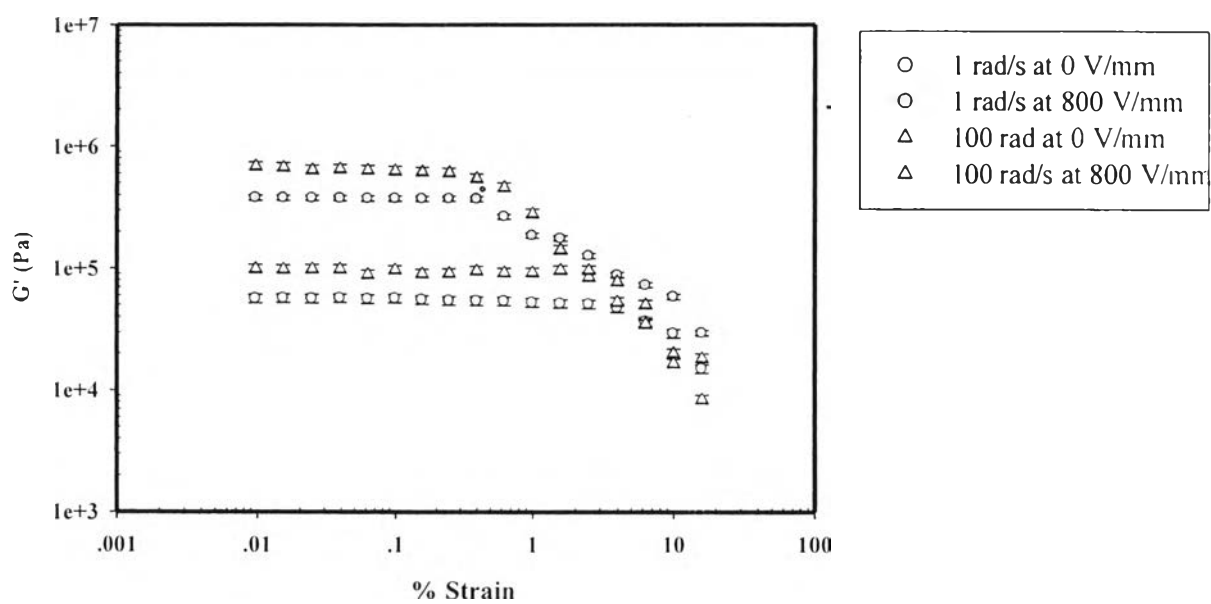
(a)
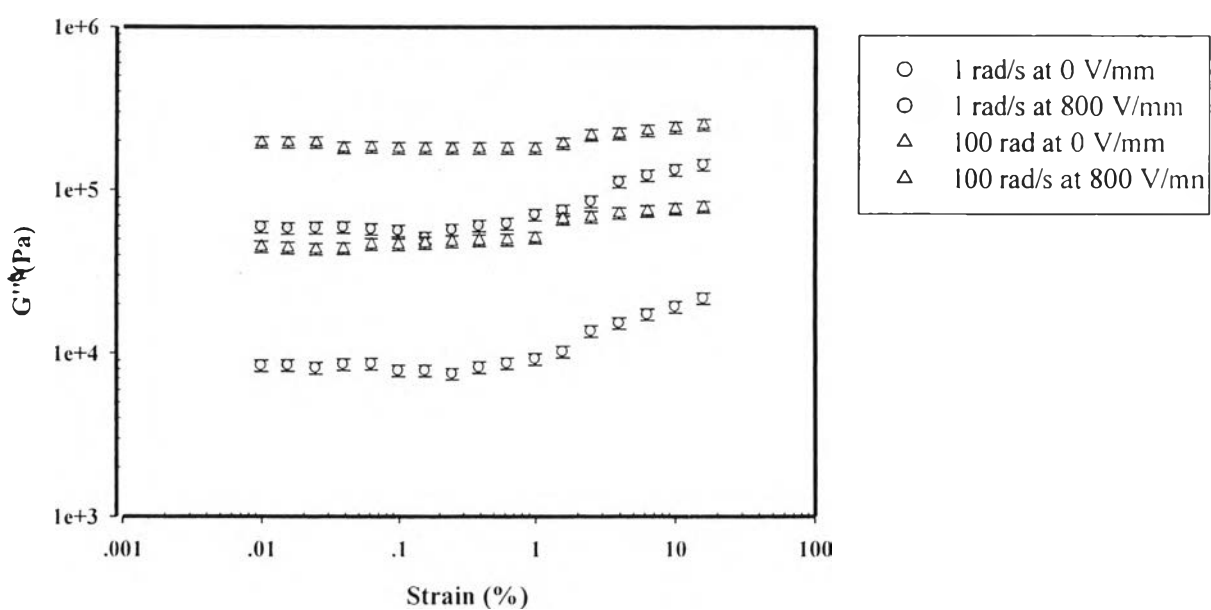


(b)

**Figure C2** Strain sweep test: (a) storage modulus and (b) loss modulus of 1%v/v MSA hydrogel with 0.015%v/v $CaCl_2$ at frequency 1 rad/s and 100 rad/s, electric field strength 0 V/mm and 800 V/mm, sample thickness 1.69 mm, 300 K.
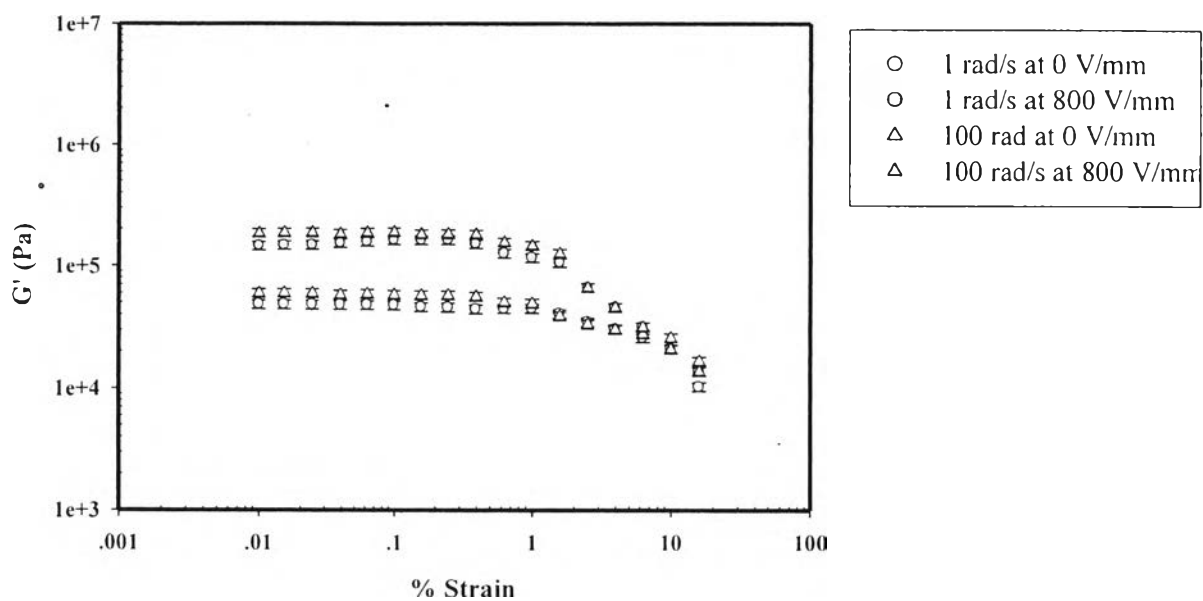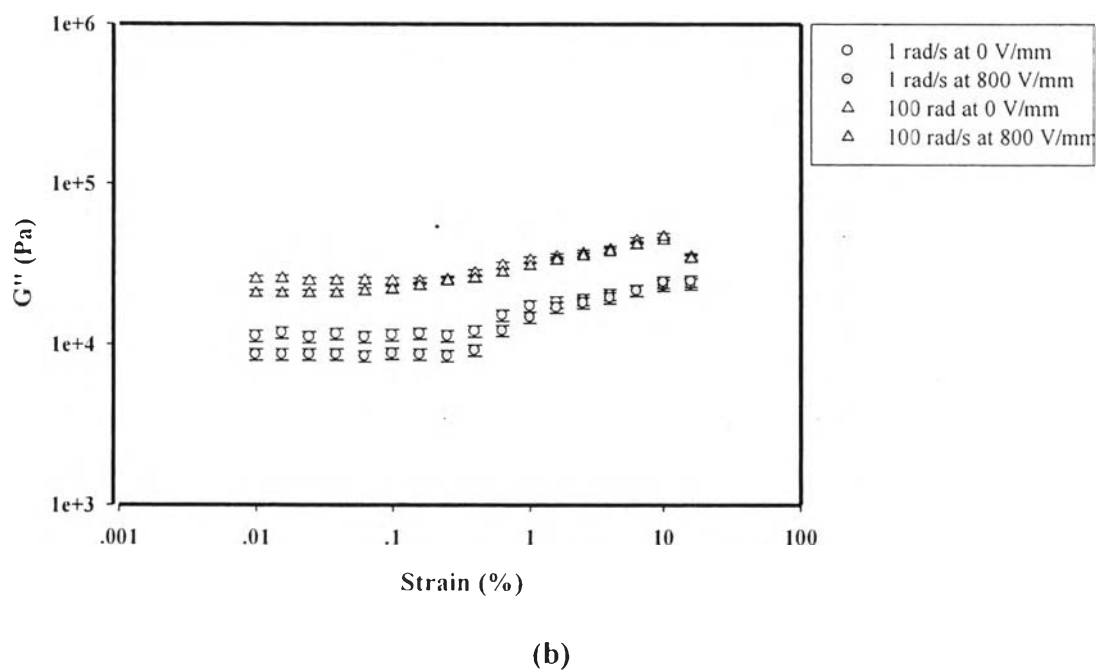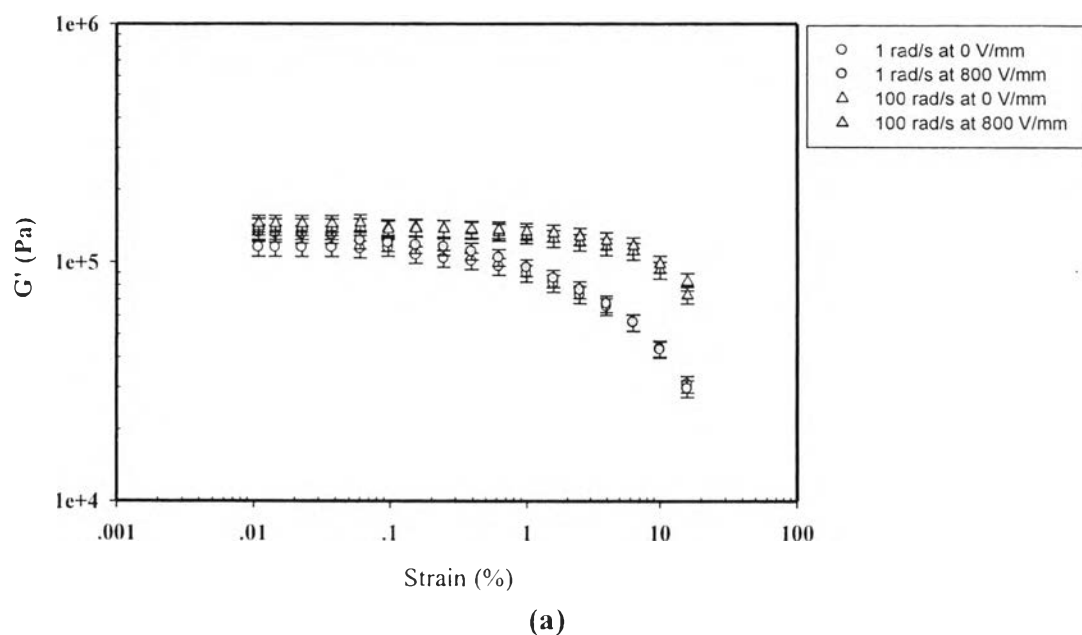
**(a)**
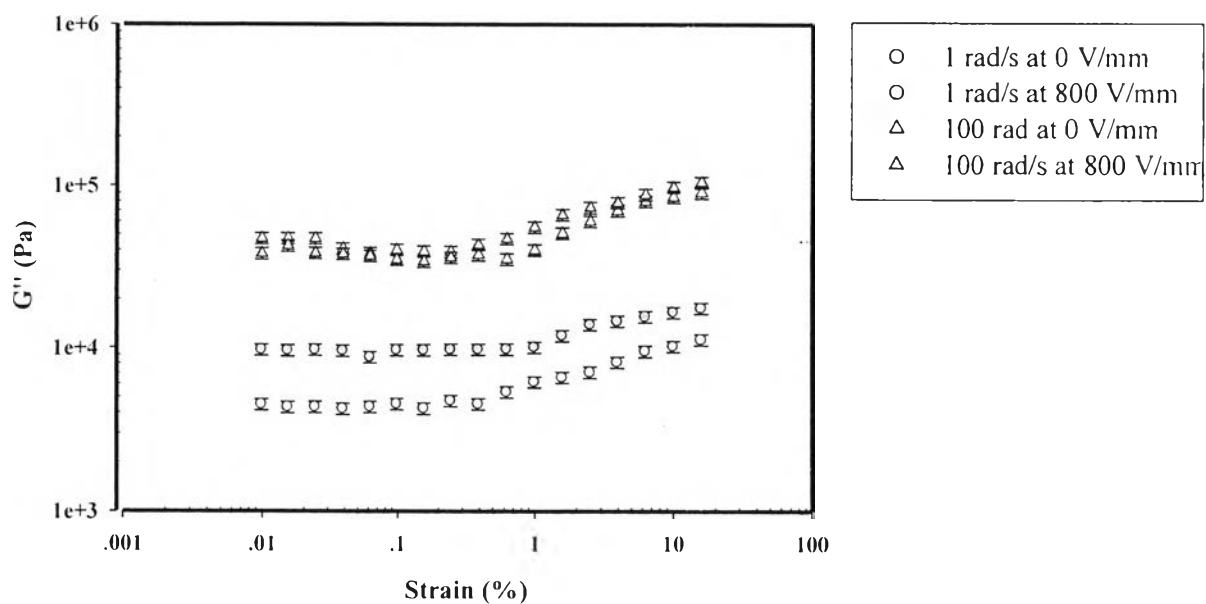


**(b)**
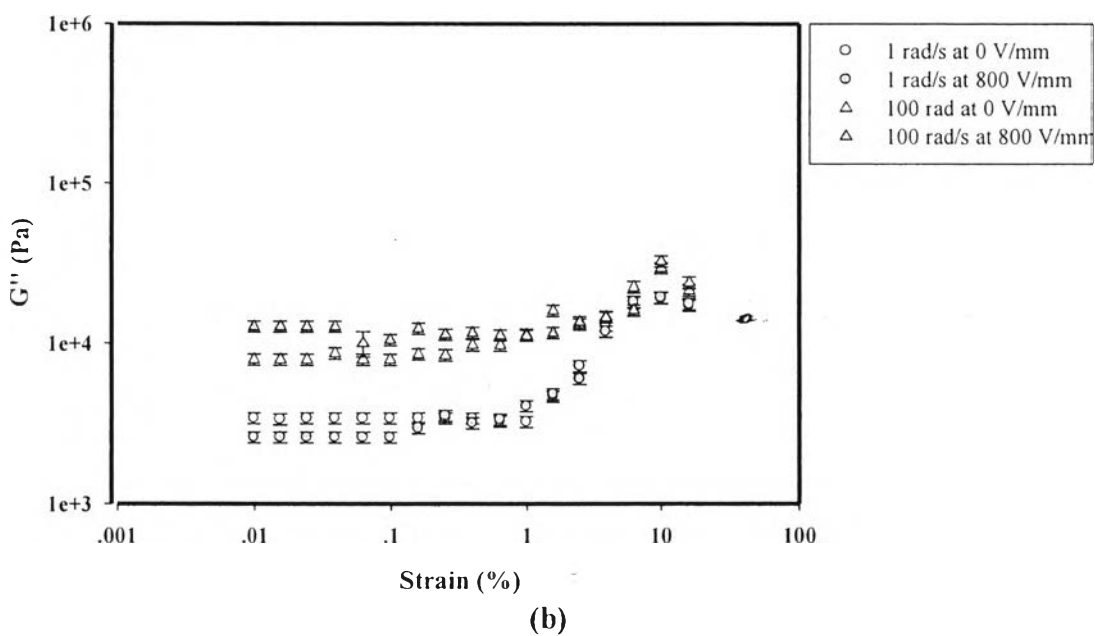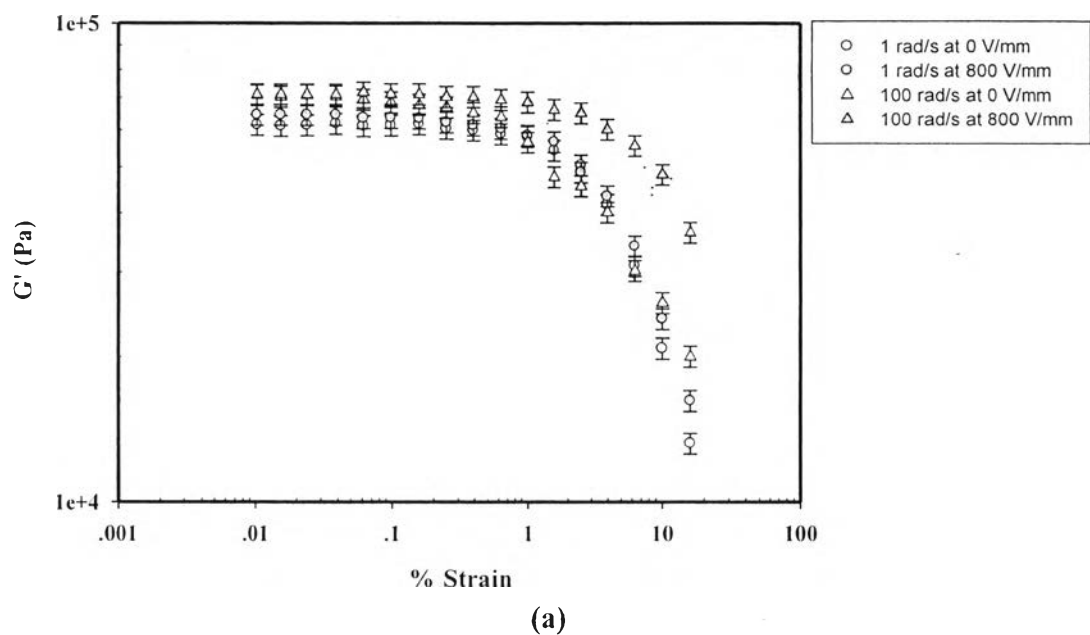
**Figure C3** Strain sweep test: (a) storage modulus and (b) loss modulus of 1%v/v LSA hydrogel with 0.015%v/v CaCl₂ at frequency 1 rad/s and 100 rad/s, electric field 0 V/mm and 800 V/mm, sample thickness 1.63 mm, 300 K.
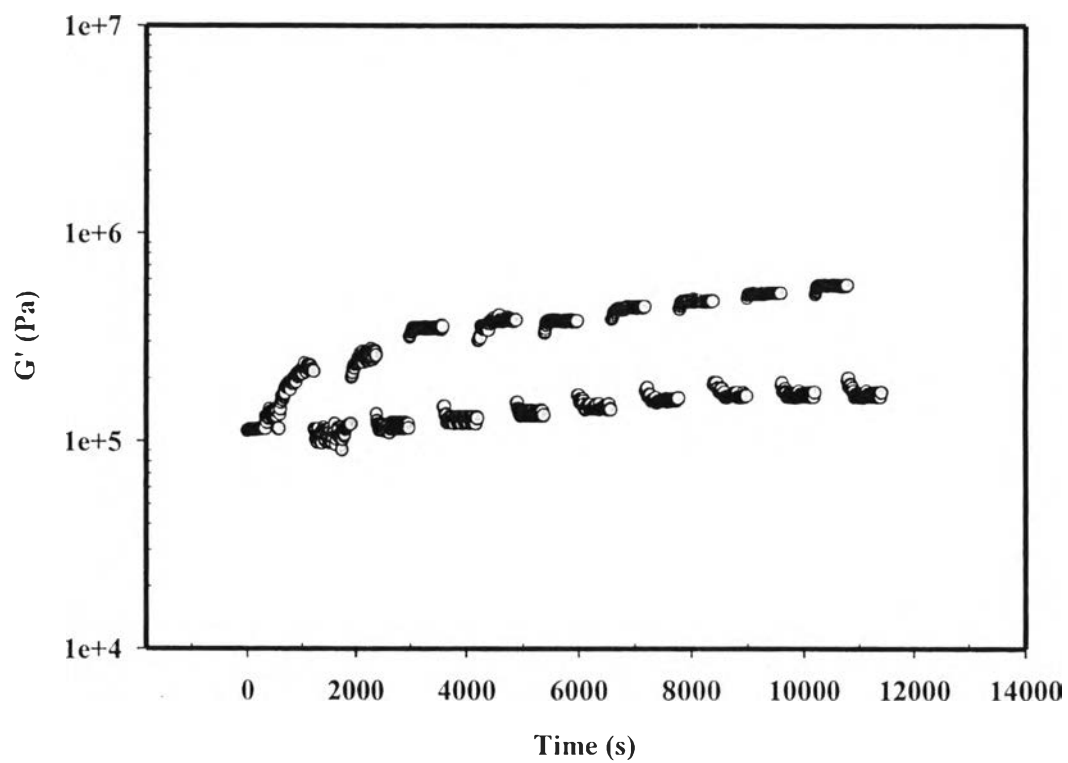
**Figure C4** Temporal response test of 1%v/v HSA hydrogel with 0.015%v/v CaCl$_2$ at frequency 100 rad/s, electric field strength 800 V/mm, sample thickness 1.65 mm, 300 K.
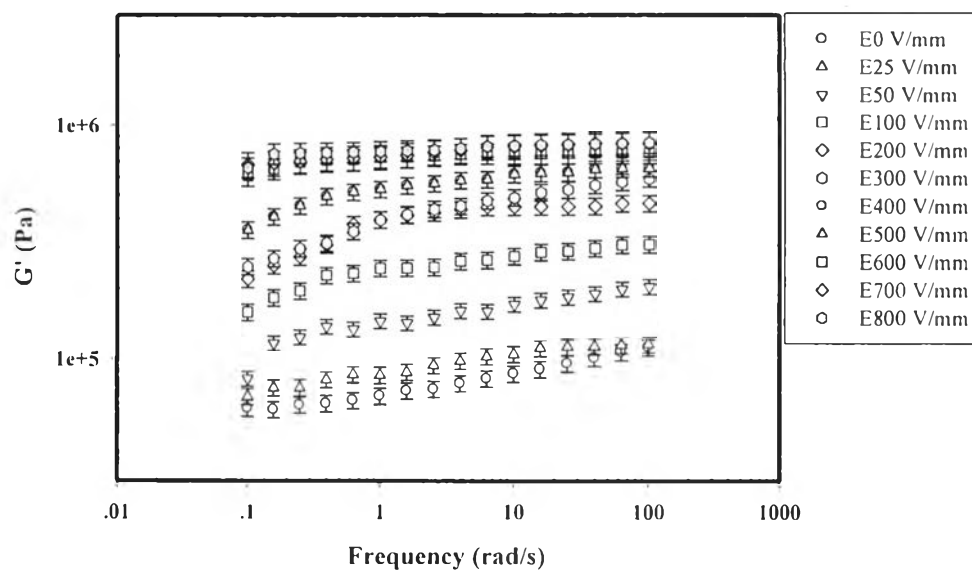
**(a)**
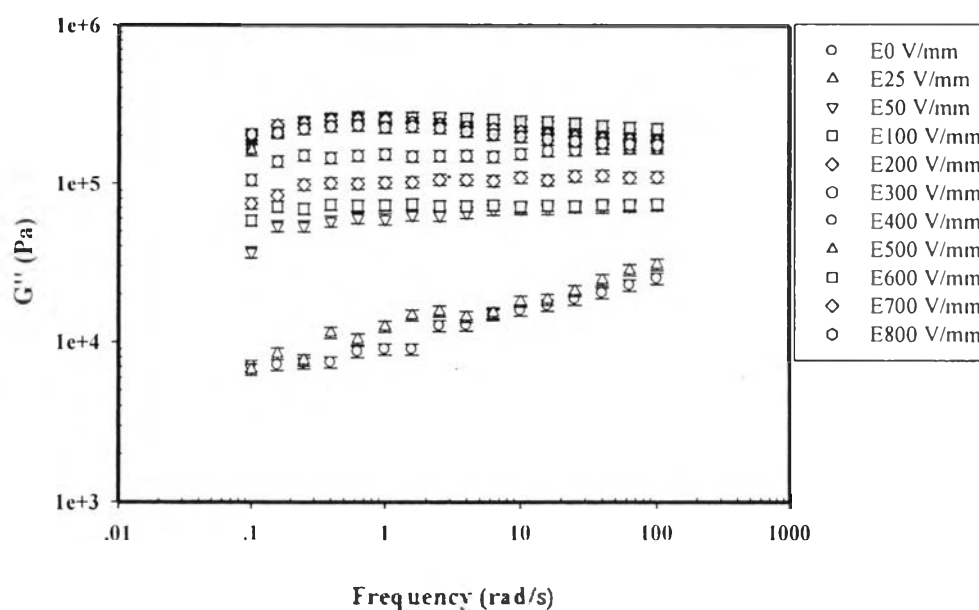


**(b)**
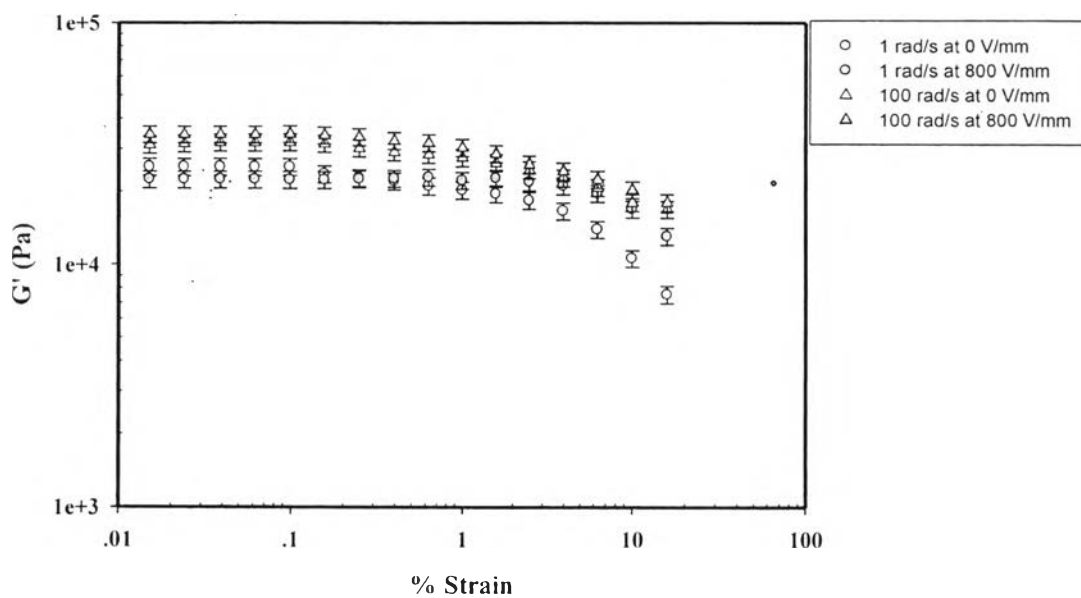
**Figure C5** Frequency sweep test: (a) storage modulus and (b) loss modulus of 1%v/v HSA hydrogel with 0.015%v/v $CaCl_2$ at strain 0.1%, sample thickness 1.65 mm, temperature 300 K.
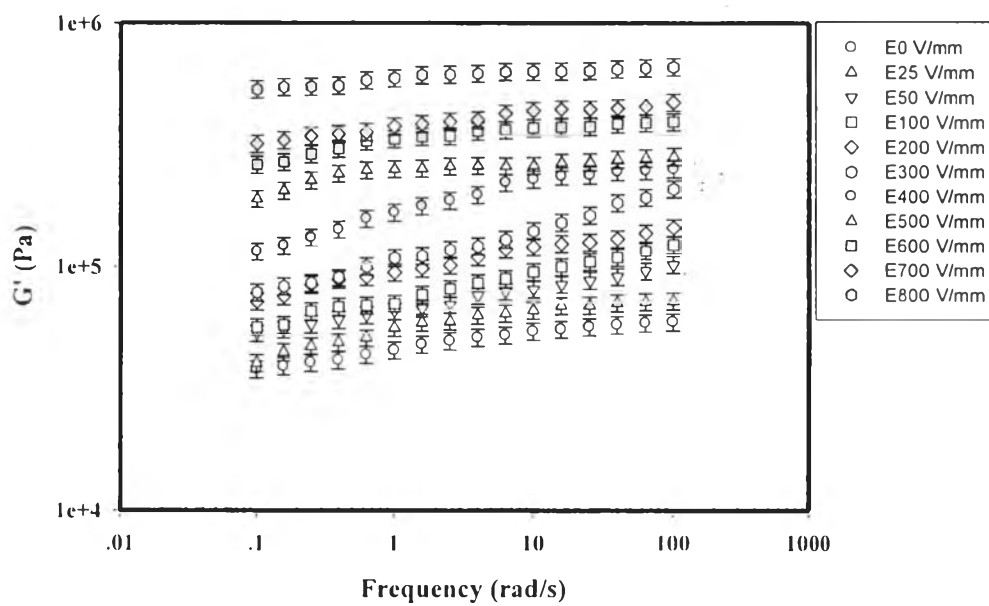
(a)
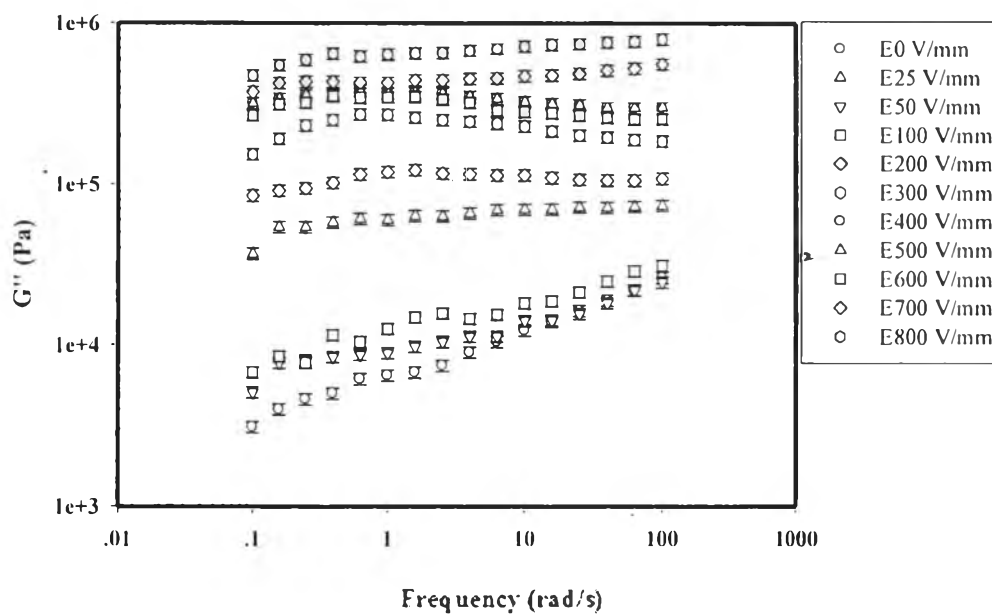


(b)

**Figure C6** Frequency sweep test: (a) storage modulus and (b) loss modulus of 1%v/v MSA hydrogel with 0.015%v/v $CaCl_2$ at strain 0.1%, sample thickness 1.69 mm, temperature 300 K.
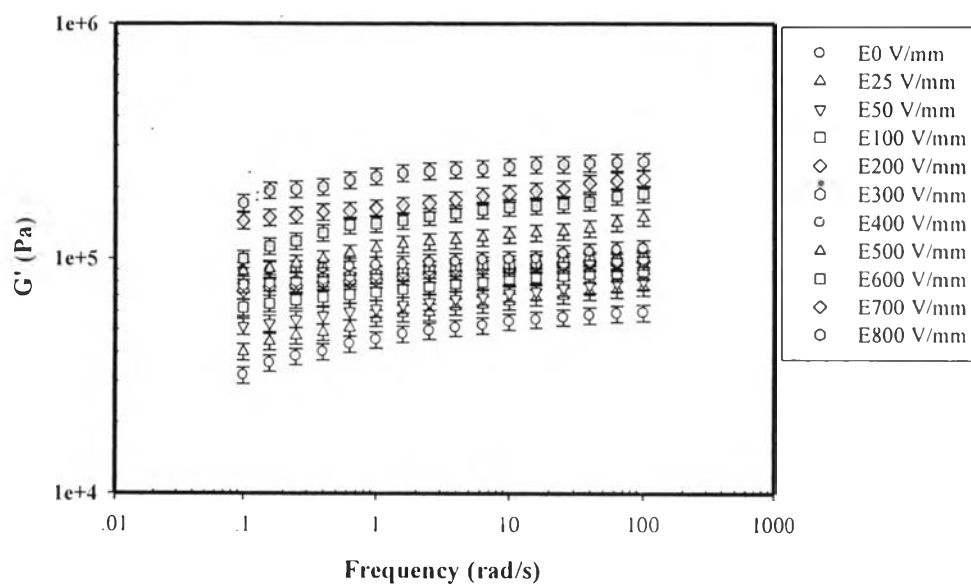
(a)
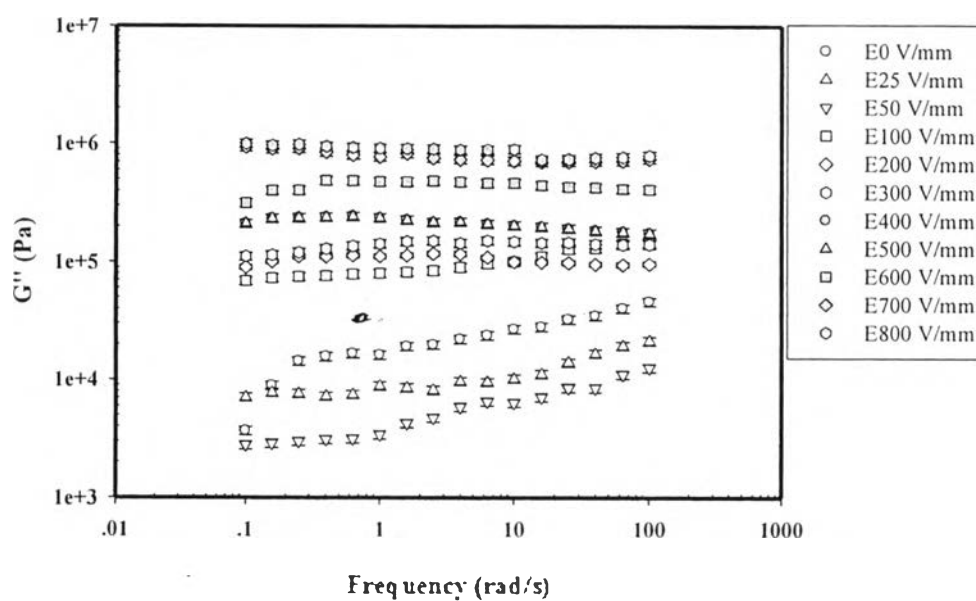


(b)

**Figure C7**  Frequency sweep test: (a) storage modulus and (b) loss modulus of 1%v/v LSA hydrogel with 0.015%v/v $CaCl_2$ at strain 0.1%, sample thickness 1.63 mm, temperature300K.
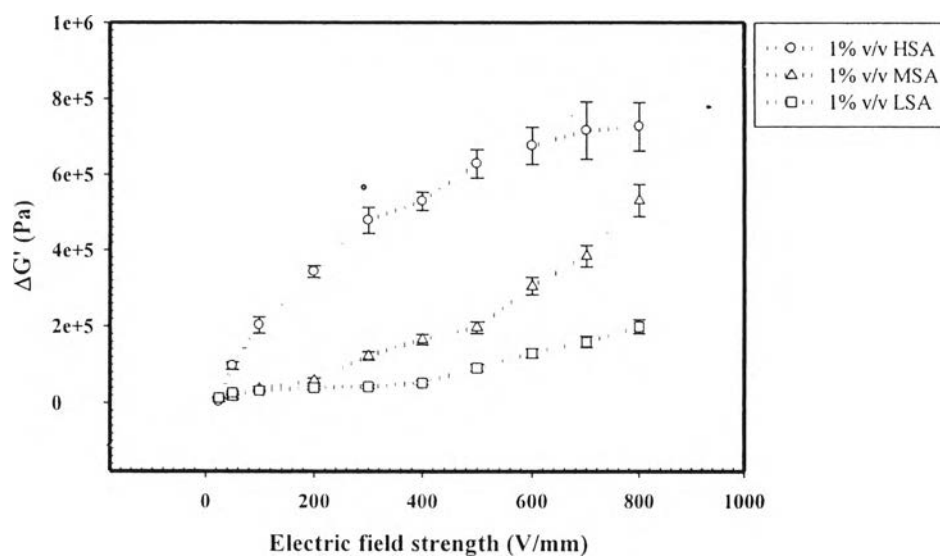
**Figure C8** The storage modulus response ($\Delta G'$) versus electric field strength of alginate hydrogels crosslinked with 0.015%v/v $CaCl_2$ at strain 0.1%, frequency 100 rad/s, temperature 300 K.
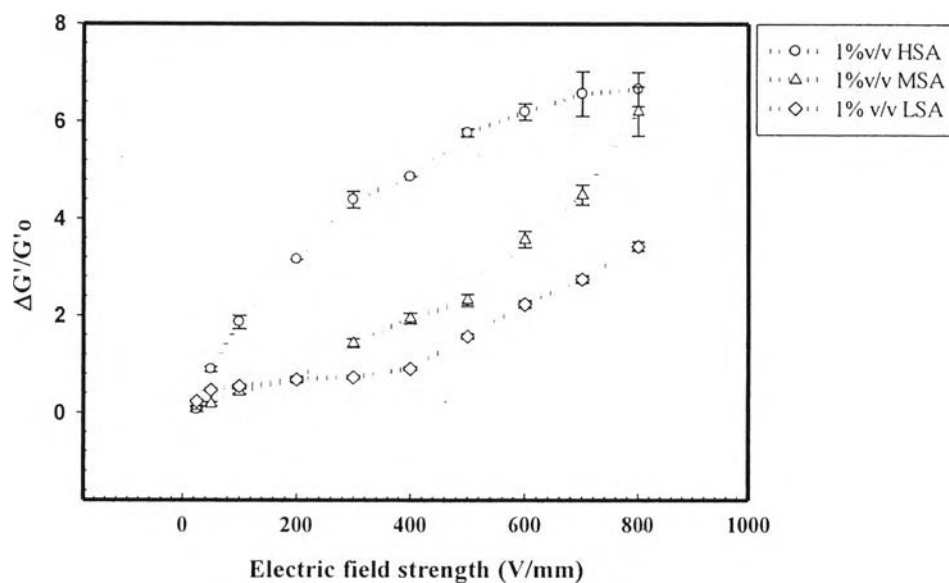


**Figure C9** The storage modulus sensitivity ($\Delta G'/G'_0$) versus electric field strength of alginate hydrogels crosslinked with 0.015%v/v $CaCl_2$ at strain 0.1%, frequency 100 rad/s, temperature 300 K.

## C2 Sodium Alginate Hydrogels Crosslinked with Ionic Crosslinking (Citric Acid; CA)

**Table C3** The storage modulus of sodium alginate hydrogels with fixed 0.050%v/v CA under applied electric field strength. (fixed frequency =100 rad/s and % strain = 0.1)

| Electric Field Strength (V/mm) | The Storage Modulus (Pa) | | |
|---|---|---|---|
| | High Molecular Weight Alginate | Medium Molecular Weight Alginate | Low Molecular Weight Alginate |
| 0 | 1.10E+05 ± 6.69E+03 | 9.50E+04 ± 7.60E+03 | 9.76E+04 ± 7.81E+03 |
| 25 | 1.29E+05 ± 6.06E+03 | 1.21E+05 ± 9.65E+03 | 1.33E+05 ± 1.07E+04 |
| 50 | 1.61E+05 ± 1.29E+04 | 1.70E+05 ± 1.36E+04 | 1.52E+05 ± 1.22E+04 |
| 100 | 2.24E+05 ± 1.79E+04 | 2.26E+05 ± 1.80E+04 | 1.70E+05 ± 1.36E+04 |
| 200 | 2.89E+05 ± 2.31E+04 | 2.62E+05 ± 2.10E+04 | 1.91E+05 ± 1.53E+04 |
| 300 | 3.58E+05 ± 2.86E+04 | 3.12E+05 ± 2.49E+04 | 2.12E+05 ± 3.66E+03 |
| 400 | 4.25E+05 ± 3.40E+04 | 3.66E+05 ± 2.93E+04 | 2.24E+05 ± 1.89E+04 |
| 500 | 5.03E+05 ± 4.02E+04 | 4.23E+05 ± 3.39E+04 | 2.36E+05 ± 5.45E+03 |
| 600 | 5.87E+05 ± 4.70E+04 | 4.81E+05 ± 3.85E+04 | 2.45E+05 ± 6.84E+03 |
| 700 | 6.38E+05 ± 5.11E+04 | 5.26E+05 ± 4.21E+04 | 2.80E+05 ± 7.93E+03 |
| 800 | 6.89E+05 ± 5.51E+04 | 6.10E+05 ± 4.88E+04 | 3.06E+05 ± 9.38E+03 |

**Table C4** The storage modulus sensitivity of sodium alginate hydrogels with fixed 0.50%v/v CA under applied electric field strength. (fixed frequency =100 rad/s and %strain = 0.1)

| Electric Field Strength (V/mm) | The storage Modulus Sensitivity | | |
|---|---|---|---|
| | High Molecular Weight Alginate | Medium Molecular Weight Alginate | Low Molecular Weight Alginate |
| 25 | 0.18 ± 0.01 | 0.25 ± 0.02 | 0.35± 0.03 |
| 50 | 0.57 ± 0.04 | 0.77 ± 0.06 | 0.55 ± 0.04 |
| 100 | 1.20 ± 0.10 | 1.37 ± 0.11 | 0.73 ± 0.06 |
| 200 | 1.85 ± 0.15 | 1.76 ± 0.14 | 0.94 ± 0.08 |
| 300 | 2.53 ± 0.20 | 2.29 ± 0.18 | 1.02 ± 0.08 |
| 400 | 3.20 ± 0.26 | 2.87 ± 0.23 | 1.32 ± 0.11 |
| 500 | 3.97 ± 0.32 | 3.49 ± 0.28 | 1.40 ± 0.11 |
| 600 | 4.75 ± 0.38 | 4.11 ± 0.33 | 1.50 ± 0.12 |
| 700 | 5.16 ± 0.41 | 4.58 ± 0.37 | 1.86 ± 0.15 |
| 800 | 5.36± 0.43 | 5.02 ± 0.40 | 2.12 ± 0.17 |

**(a)**



**(b)**

**Figure C10** Strain sweep tests: (a) storage modulus and (b) loss modulus of 1%v/v HSA hydrogel with 0.50%v/v CA at frequency 1 rad/s and 100 rad/s, electric field strength 0 V/mm and 800 V/mm, sample thickness 1.65 mm, 300 K.

**Figure C11** Strain sweep tests: (a) storage modulus and (b) loss modulus of 1%v/v MSA hydrogel with 0.50%v/v CA at frequency 1 rad/s and 100 rad/s, electric field strength 0 V/mm and 800 V/mm, sample thickness 1.69 mm, 300 K.

(a)
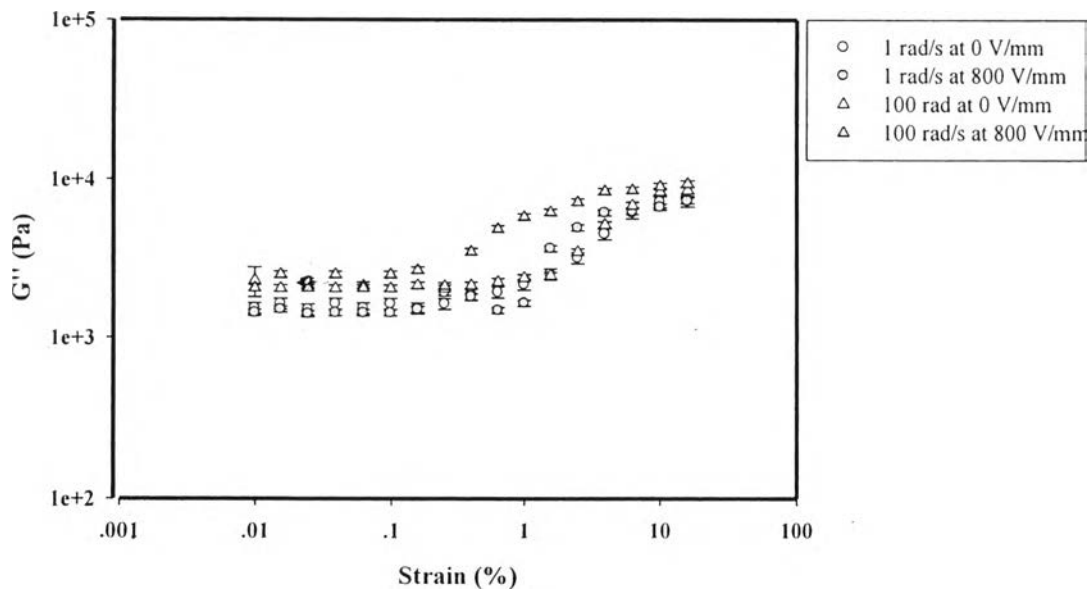


(b)

**Figure C12** Strain sweep tests: (a) storage modulus and (b) loss modulus of 1%v/v LSA hydrogel with 0.50 %v/v CA at frequency 1 rad/s and 100 rad/s, electric field 0 V/mm and 800 V/mm, sample thickness 1.63 mm, 300 K.
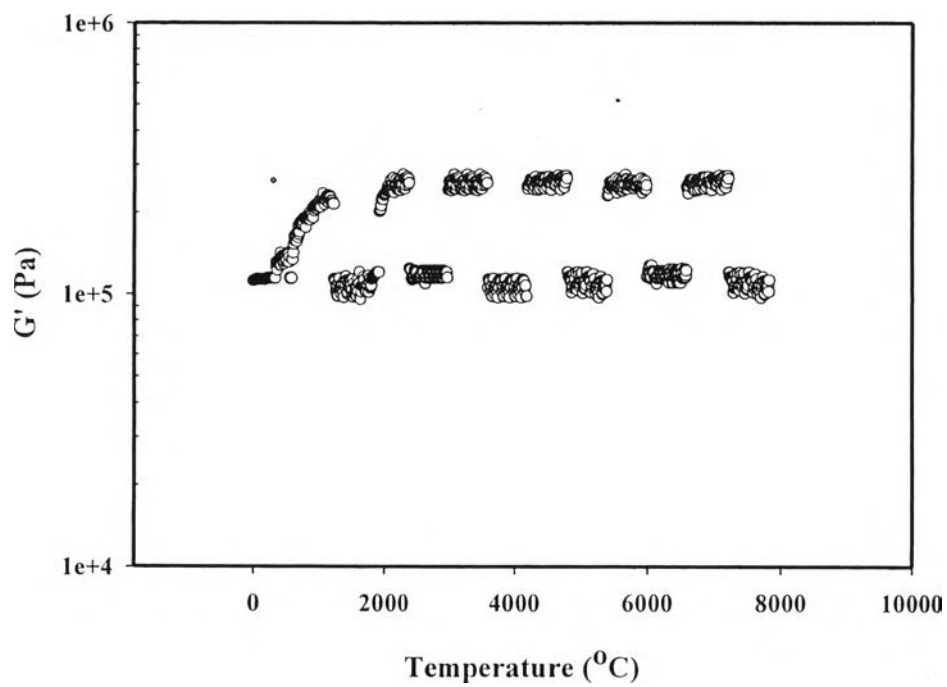
**Figure C13** Temporal response test of 1%v/v HSA hydrogel with 0.50%v/v CaCl$_2$ at frequency 100 rad/s, electric field strength 800 V/mm, sample thickness 1.65 mm, 300 K.

(a)
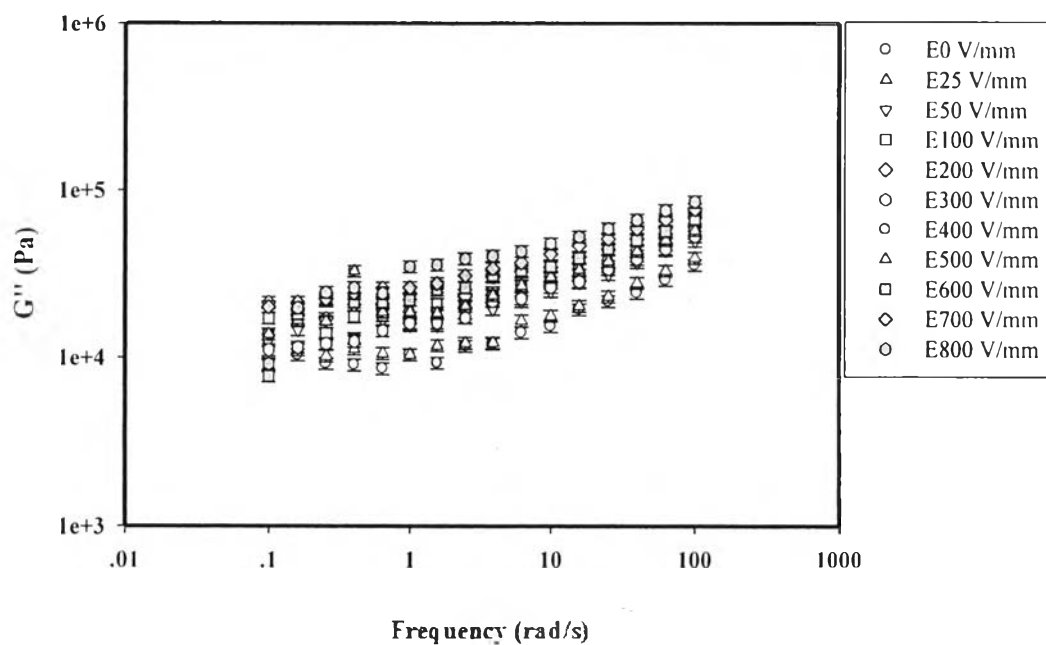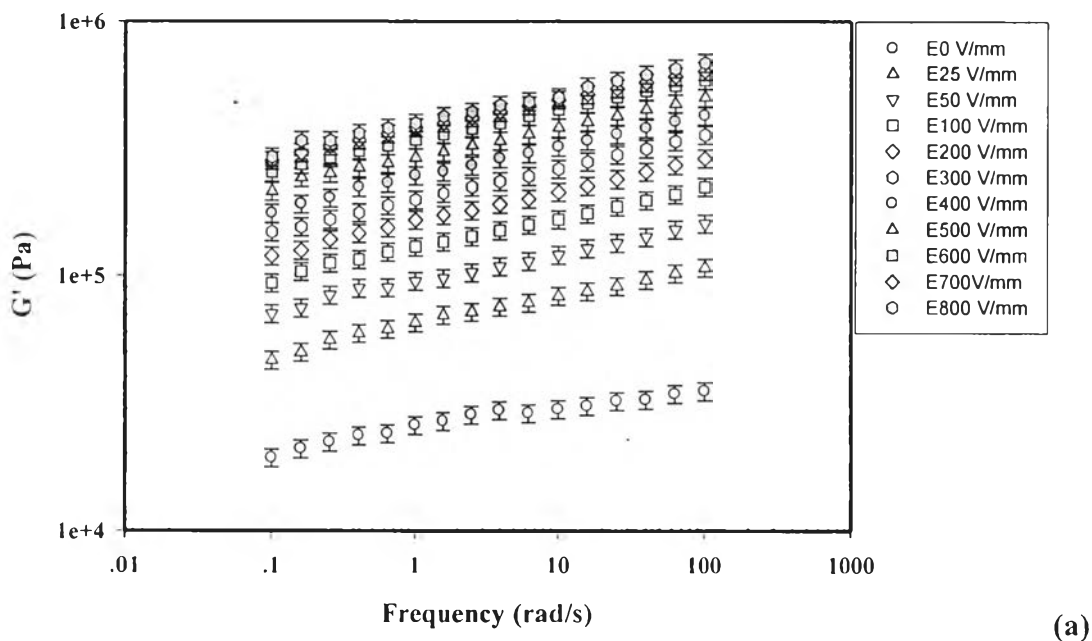


(b)

**Figure C14** Frequency sweep test of 1%v/v HSA hydrogel with 0.50%v/v CA at strain 0.1%, sample thickness 1.65 mm, temperature 300 K.
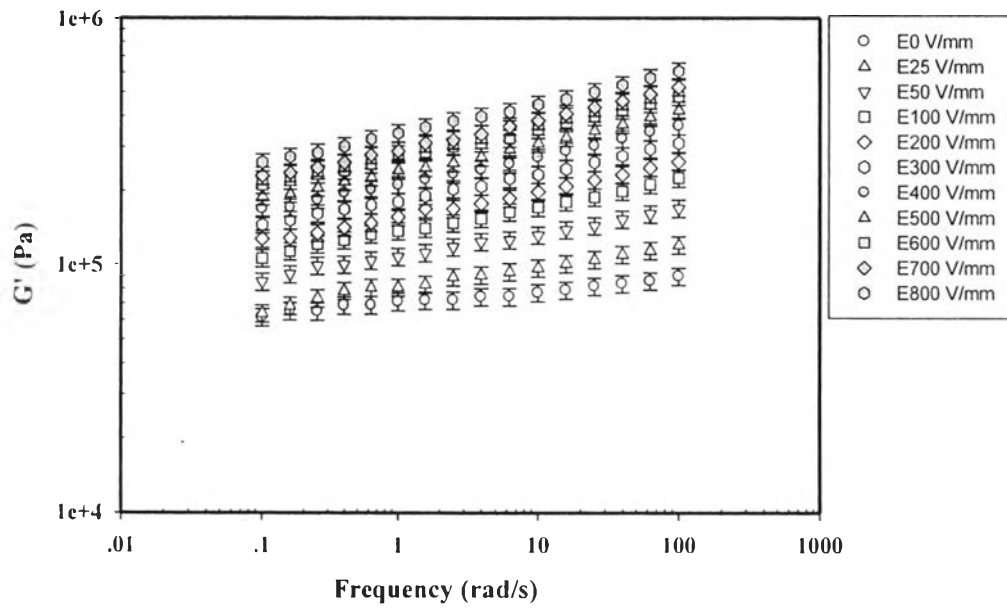
(a)
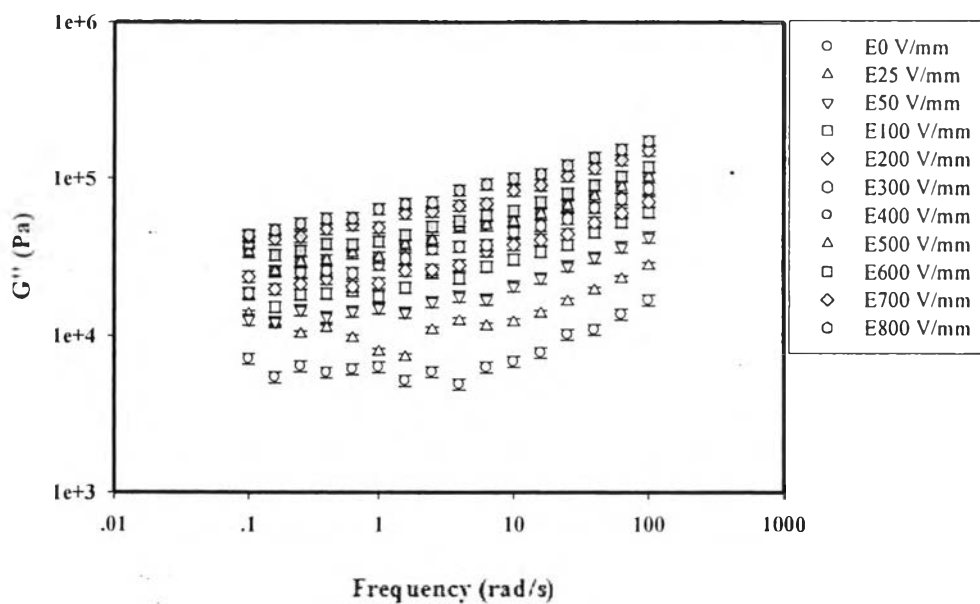


(b)

**Figure 15** Frequency sweep tests: (a) storage modulus and (b) loss modulus of 1%v/v MSA hydrogel with 0.50%v/v CA at strain 0.1%, sample thickness 1.69 mm, temperature 300 K.
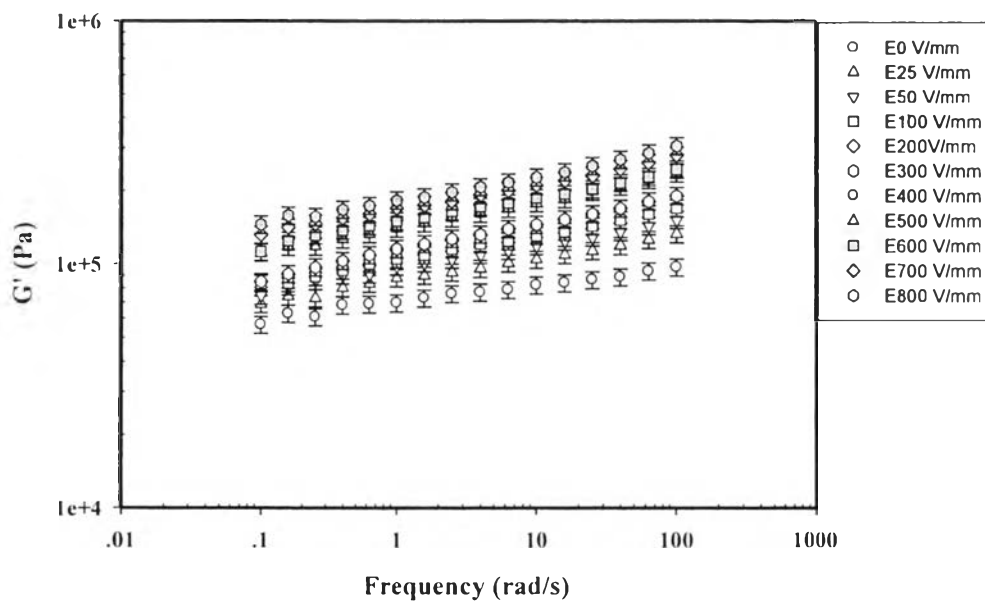
(a)
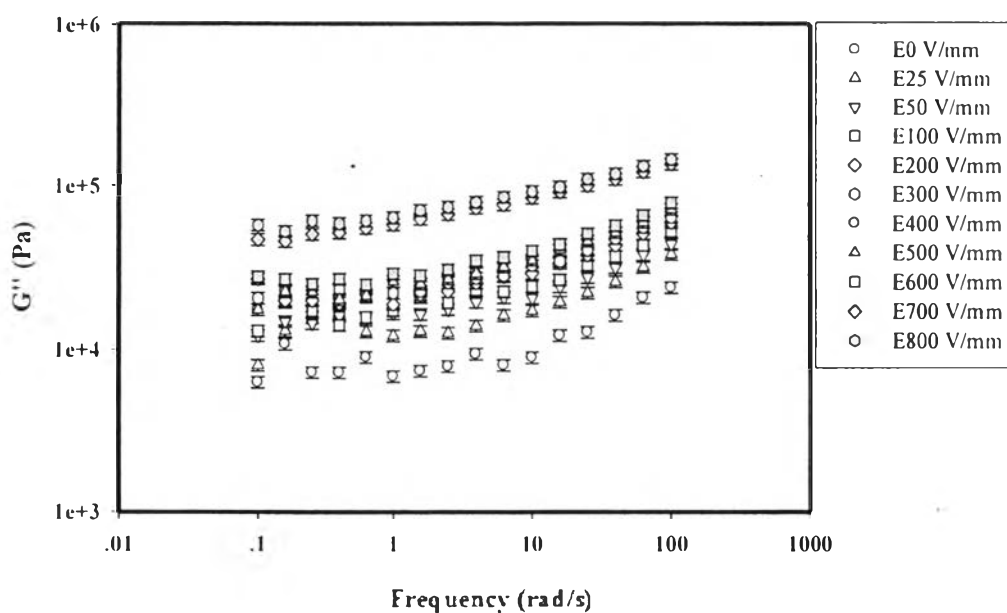


(b)

**Figure C16** Frequency sweep tests: (a) storage modulus and (b) loss modulus of 1%v/v LSA hydrogel with 0.50 %v/v CA at strain 0.1%, sample thickness 1.63 mm, temperature 300 K.
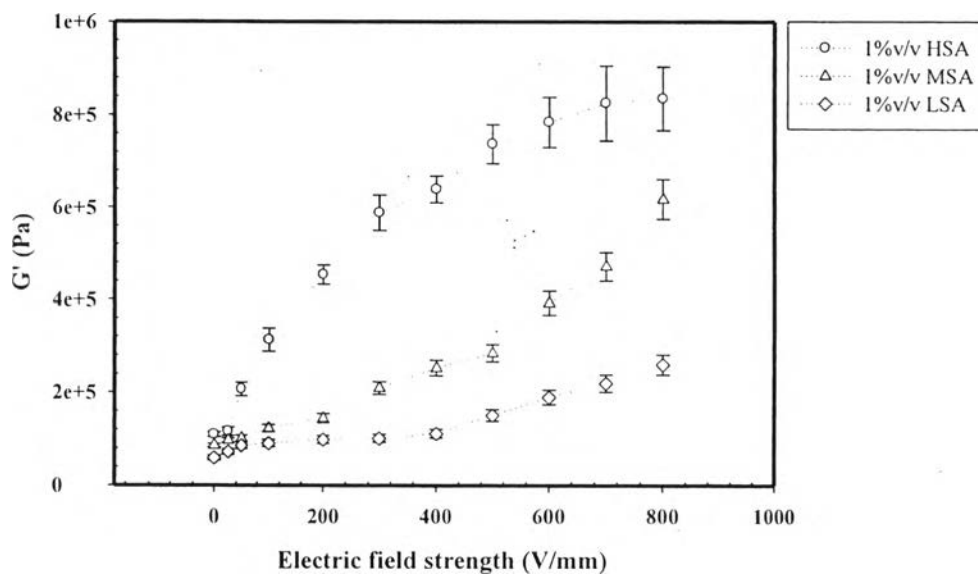
**Figure C17** The storage modulus (G') versus electric field strength of alginate hydrogels crosslinked with 0.50%v/v CA at strain 0.1 %, frequency 100 rad/s, temperature 300 K.
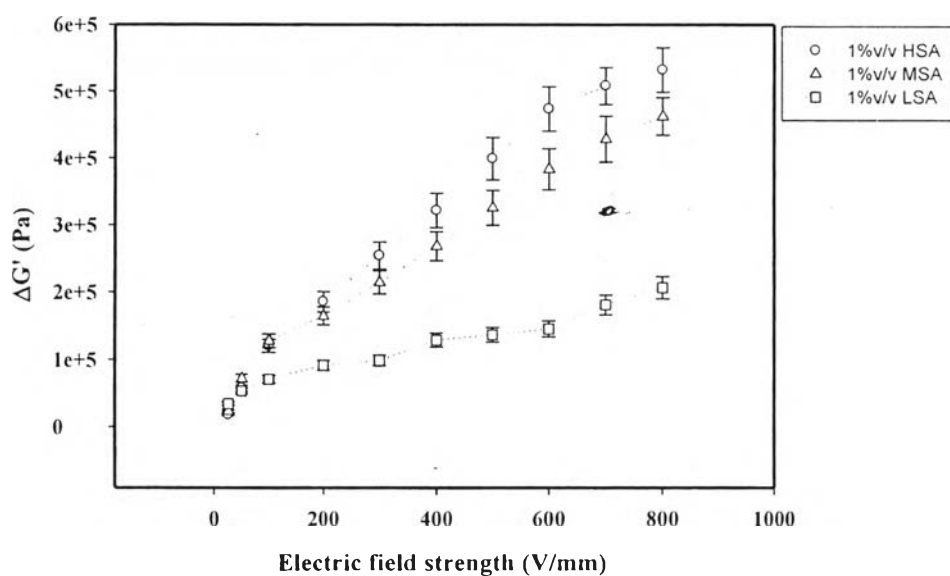


**Figure C18** The storage modulus response ($\Delta$G') versus electric field strength of alginate hydrogels crosslinked with 0.50%v/v CA at strain 0.1 %, frequency 100 rad/s, temperature 300 K.
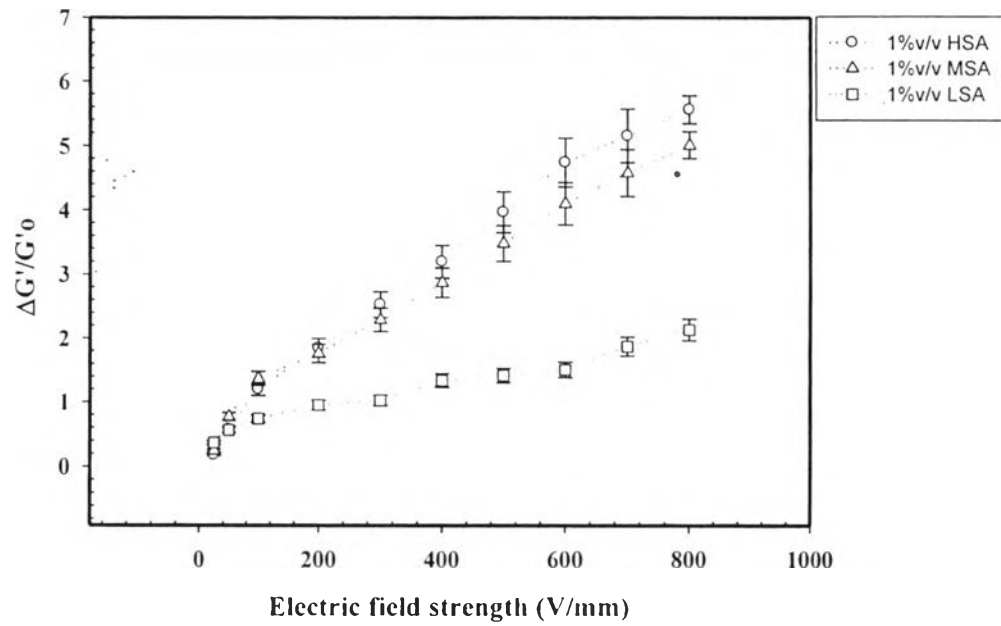
**Figure C19** The storage modulus sensitivity ($\Delta G'/G'_0$) versus electric field strength of alginate hydrogels crosslinked with 0.50%v/v CA at strain 0.1 %, frequency 100 rad/s, temperature 300 K.

## C3 Comparison of Crosslinking Method Affected to Electromechanical Properties.
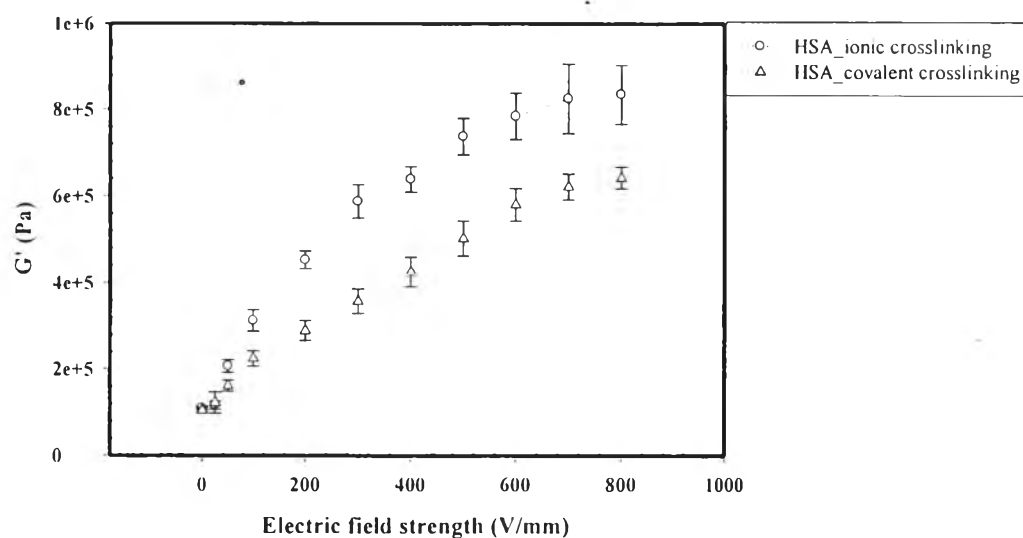


**Figure C20** The storage modulus (G') versus electric field strength of 1%v/v HSA at strain 0.1 %, frequency 100 rad/s, temperature 300 K.
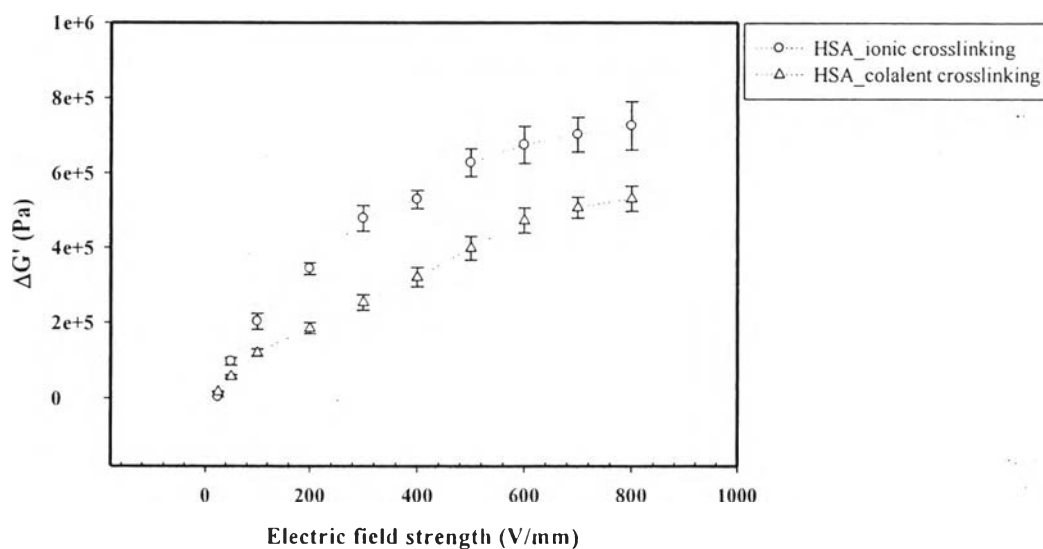


**Figure C21** The storage modulus response (ΔG') versus electric field strength of 1%v/v HSA at strain 0.1 %, frequency 100 rad/s, temperature 300 K.
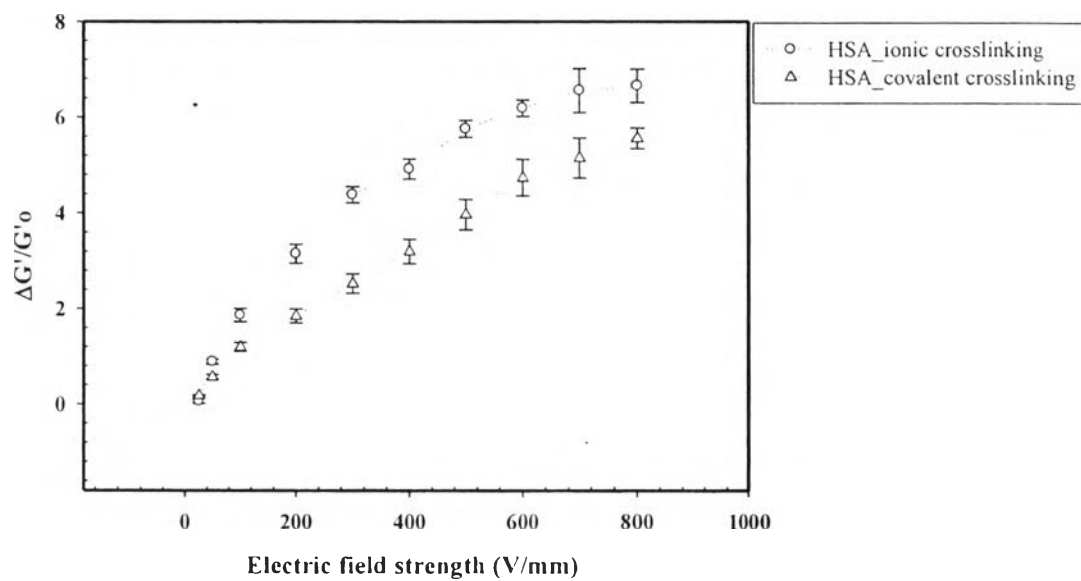
**Figure C22** The storage modulus sensitivity ($\Delta G'/G'_0$) versus electric field strength of 1%v/v HSA at strain 0.1 %, frequency 100 rad/s, temperature 300 K.

## C4 Deflection Responses of Pristine High Molecular Weight Sodium Alginate Hydrogel with Crosslinked by Ionic Crosslinking ($CaCl_2$) and Ionic Crosslinking (CA)

**Table C5** Deflection angle ($\theta$) and dielectrophoresis force ($F_d$) versus electric field strength of pristine HSA hydrogel with crosslinked by ionic crosslinking ($CaCl_2$) (sample width 3 mm, sample thickness 1.25 mm, sample weight 0.0812 g)

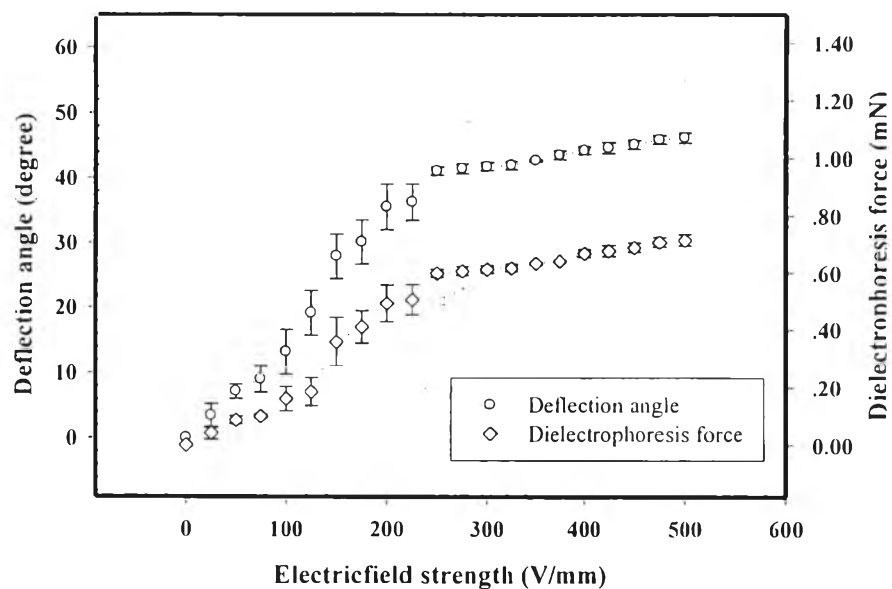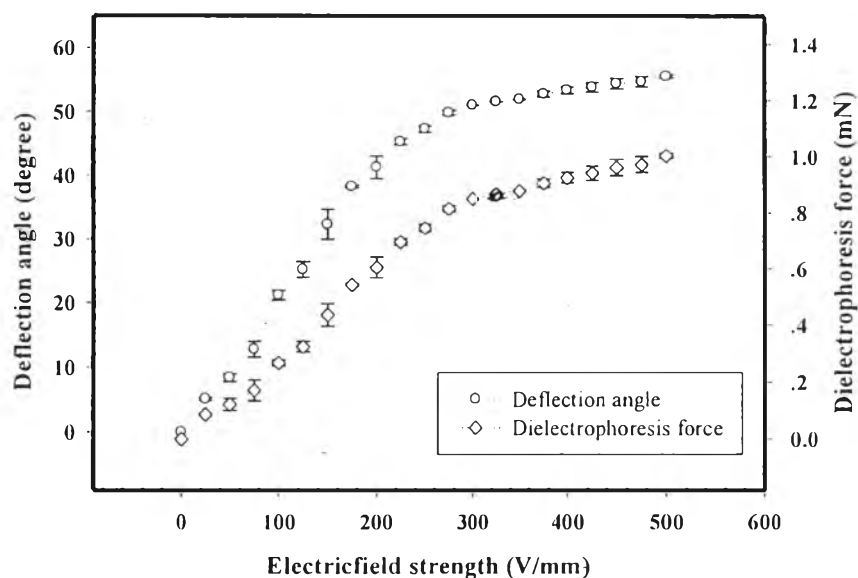| Electric Field Strength (V/mm) | Deflection Angle (Degree) | Deflection Distance (mm) | Dielectrophoresis Force (mN) |
|---|---|---|---|
| 0 | 0 | 0 | 0 |
| 25 | 7.13 ± 0.11 | 1.55 ± 0.01 | 8.60E-02 ± 2.75E-03 |
| 50 | 8.40 ± 0.29 | 1.83 ± 0.08 | 1.02E-01 ± 7.03E-03 |
| 75 | 10.77 ± 0.80 | 2.36 ± 0.30 | 1.31E-01 ± 1.98E-02 |
| 100 | 21.19 ± 0.80 | 4.81 ± 0.08 | 2.66E-01 ± 1.04E-02 |
| 125 | 25.22 ± 0.38 | 5.85 ± 0.46 | 3.24E-01 ± 1.81E-02 |
| 150 | 32.33 ± 0.62 | 7.87 ± 0.90 | 4.35E-01 ± 3.98E-02 |
| 175 | 38.30 ± 1.19 | 9.80 ± 0.29 | 5.43E-01 ± 3.64E-03 |
| 200 | 41.31 ± 0.09 | 10.90 ± 0.42 · | 6.05E-01 ± 3.74E-02 |
| 225 | 45.35 ± 0.88 | 12.55 ± 0.07 | 6.96E-01 ± 1.20E-02 |
| 250 | 47.33 ± 0.25 | 13.45 ± 0.07 | 7.46E-01 ± 1.32E-02 |
| 275 | 49.85 ± 0.25 | 14.70 ± 0.14 | 8.15E-01 ± 1.08E-02 |
| 300 | 51.07 ± 0.19 | 15.35 ± 0.35 | 8.51E-01 ± 1.11E-04 |
| 325 | 51.61 ± 0.01 | 15.65 ± 0.35 | 8.67E-01 ± 2.70E-04 |
| 350 | 51.96 ± 0.02 | 15.85 ± 0.35 | 8.79E-01 ± 5.23E-04 |
| 375 | 52.82 ± 0.01 | 16.35 ± 0.64 | 9.06E-01 ± 1.45E-02 |
| 400 | 53.40 ± 0.22 | 16.70 ± 0.71 | 9.25E-01 ± 1.80E-02 |
| 425 | 53.88 ± 0.27 | 17.00 ± 0.85 | 9.42E-01 ± 2.55E-02 |
| 450 | 54.43 ± 0.37 | 17.35 ± 0.92 | 9.61E-01 ± 2.89E-02 |
| 475 | 54.74 ± 0.41 | 17.55 ± 0.92 | 9.72E-01 ± 2.87E-02 |
| 500 | 55.58 ± 0.40 | 18.10 ± 0.57 | 1.00E+00 ± 8.38E-03 |

**Table C6** Deflection angle (θ) and dielectrophoresis force ($F_d$) versus electric field strength of pristine sodium alginate hydrogel with crosslinked by covalent crosslinking (CA) (sample width 3 mm, sample thickness 1.25 mm, sample weight 0.1112 g)
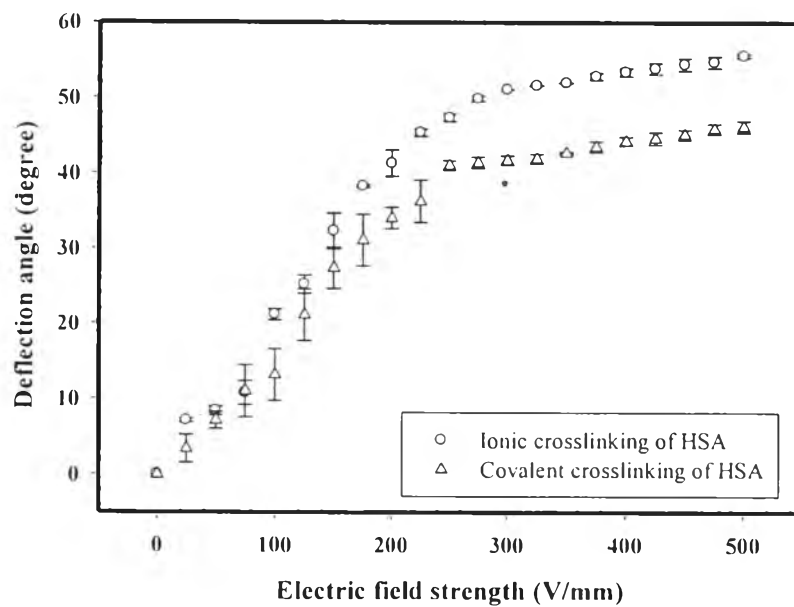
| Electric Field Strength (V/mm) | Deflection Angle (Degree) | Deflection Distance (mm) | Dielectrophoresis Force (mN) |
|---|---|---|---|
| 0 | 0 | 0 | 0 |
| 25 | 3.40 ± 0.92 | 0.88 ± 0.47 | 4.09E-02 ± 0.02 |
| 50 | 7.15 ± 0.56 | 1.85 ± 0.29 | 8.62E-02 ± 0.01 |
| 75 | 9.01 ± 3.13 | 2.35 ± 1.65 | 1.10E-01 ± 0.08 |
| 100 | 13.17 ± 1.71 | 3.45 ± 0.93 | 1.61E-01 ± 0.04 |
| 125 | 19.15 ± 3.14 | 5.14 ± 1.81 | 2.40E-01 ± 0.08 |
| 150 | 27.40 ± 2.78 | 7.67 ± 1.82 | 3.58E-01 ± 0.08 |
| 175 | 30.61 ± 3.48 | 8.79 ± 2.43 | 4.10E-01 ± 0.11 |
| 200 | 35.54 ± 1.77 | 10.53 ± 1.37 | 4.92E-01 ± 0.06 |
| 225 | 36.28 ± 1.41 | 10.81 ± 1.12 | 5.05E-01 ± 0.05 |
| 250 | ·41.04 ± 0.31 | 12.80 ± 0.28 | 5.98E-01 ± 0.01 |
| 275 | 41.41 ± 0.36 | 12.97 ± 0.33 | 6.06E-01 ± 0.02 |
| 300 | 41.70 ± 0.31 | 13.10 ± 0.28 | 6.12E-01 ± 0.01 |
| 325 | 41.92 ± 0.31 | 13.20 ± 0.28 | 6.17E-01 ± 0.01 |
| 350 | 42.67 ± 0.07 | 13.55 ± 0.07 | 6.33E-01 ± 0.02 |
| 375 | 42.98 ± 0.35 | 13.70 ± 0.07 | 6.41E-01 ± 0.03 |
| 400 | 44.21 ± 0.28 | 14.30 ± 0.28 | 6.68E-01 ± 0.01 |
| 425 | 44.60 ± 0.42 | 14.50 ± 0.42 | 6.78E-01 ± 0.02 |
| 450 | 45.09 ± 0.34 | 14.75 ± 0.35 | 6.89E-01 ± 0.02 |
| 475 | 45.86 ± 0.33 | 15.15 ± 0.35 | 7.08E-01 ± 0.02 |
| 500 | 46.15 ± 0.39 | 15.31 ± 0.42 | 7.15E-01 ± 0.02 |

**Figure C23** Deflection angle (θ) and dielectrophoresis force (F_d) versus electric field strength of pristine sodium alginate hydrogel with crosslinked by ionic crosslinking (CaCl_2) (sample width 3 mm, sample thickness 1.25 mm, sample weight 0.11g).



**Figure C24** Deflection angle (θ) and dielectrophoresis force (F_d) versus electric field strength of pristine sodium alginate hydrogel with crosslinked by covalent crosslinking (CA) (sample width 3 mm, sample thickness 1.25 mm, sample weight 0.13 g).

**Figure C25** Deflection angle (θ) versus electric field strength of pristine sodium alginate hydrogel.
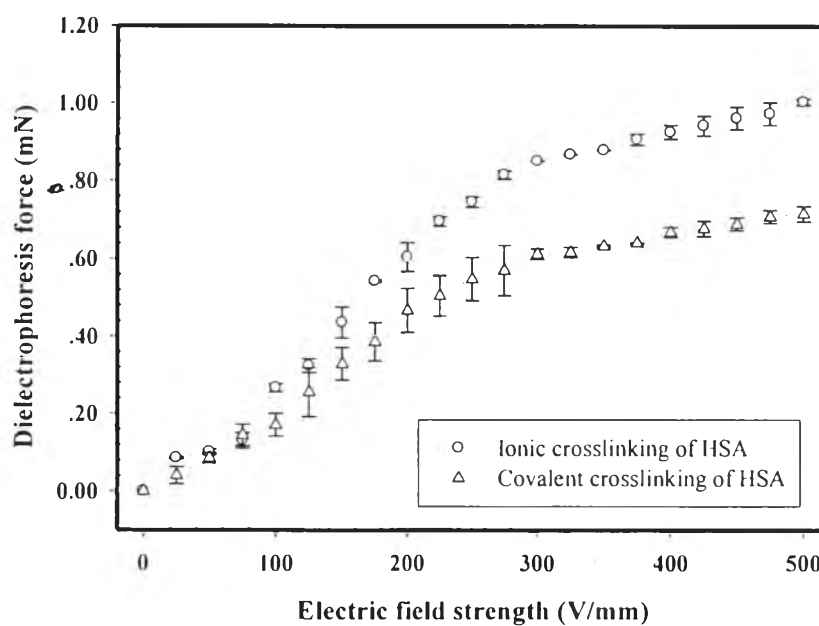


**Figure C26** Dielectrophoresis force ($F_d$) versus electric field strength of of pristine sodium alginate hydrogel.
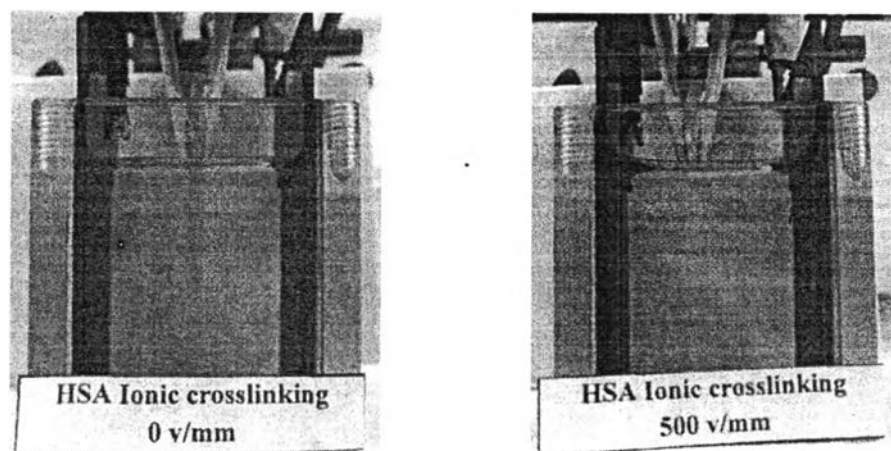
Figure C27 Bending of pristine HSA hydrogel at electric field strength 0 and 500 v/mm.
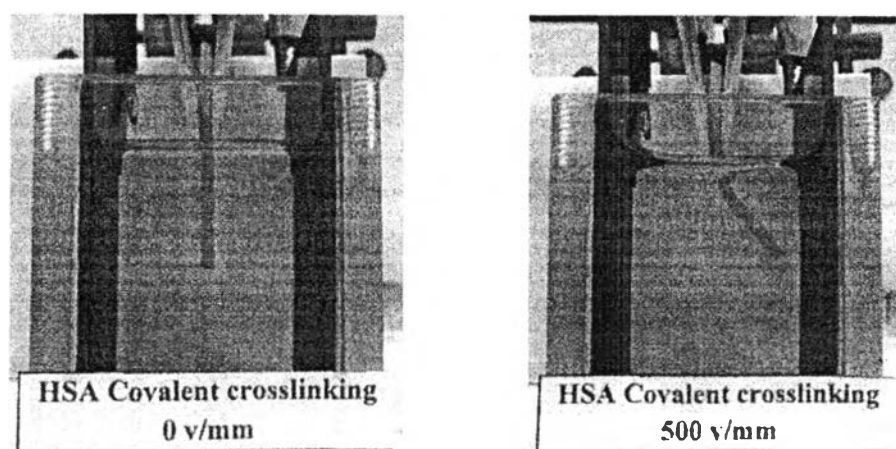


Figure C28 Bending of pristine HSA hydrogel at electric field strength 0 and 500 v/mm.

**APPENDIX D  Characterization of Polycarbazole/Sodium Alginate Hydrogel Blends (PCB/HSA)**

**D1  Thermal Gravimetric Analyzer**

A thermal gravimetric analyzer (DuPont, TGA 2950) was used to characterize the thermal behavior and the water content of PCB/HSA hydrogel blends. They were investigated by weighting example of 5-10 mg and placed in platinum pan, and then heating under nitrogen flow with the heating rate of 10°C/min in the temperature range of 30-800°C.
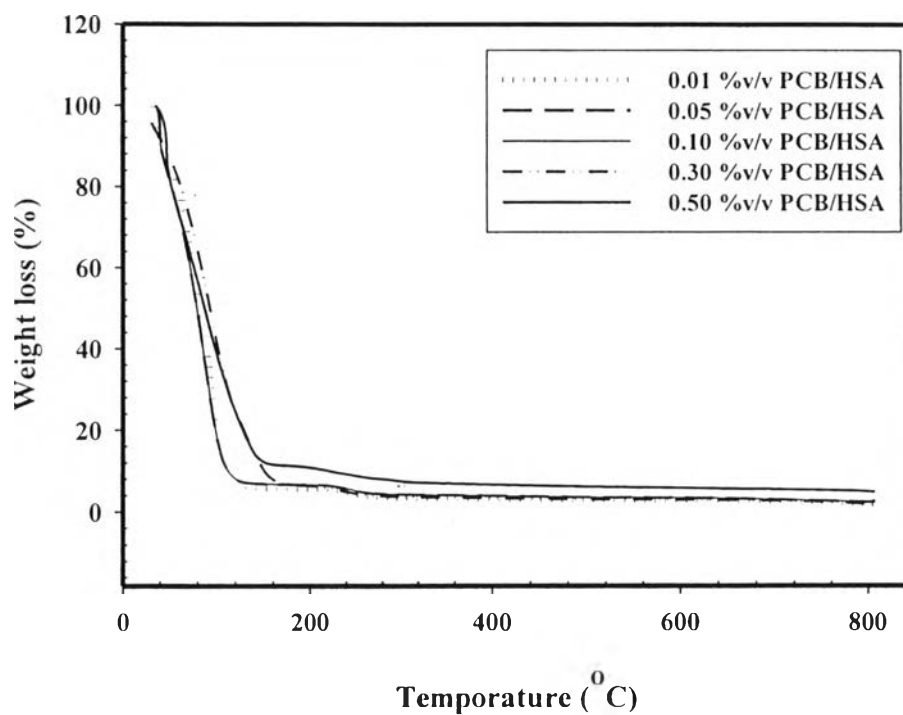


**Figure D1**  TGA thermogram of PCB/HSA hydrogel blends with various PCB concentrations.

**Table D1** The summary of degradation temperature and percent weight loss in TGA thermograms of pristine HSA hydrogel and HSA hydrogel blends with various PCB concentrations.

| Sample | Water Content (%) | $T_d$ (°C) | Weight Loss (%) |
|---|---|---|---|
| Pristine 1%v/v HSA | 93.15 | 132 | 95.23 |
| 0.01%v/v PCB/HSA | 93.45 | 239 | 92.07 |
| 0.05%v/v PCB/HSA | 92.93 | 248 | 88.43 |
| 0.10%v/v PCB/HSA | 92.40 | 250 | 88.07 |
| 0.30%v/v PCB/HSA | 92.13 | 252 | 87.66 |
| 0.50%v/v PCB/HSA | 89.82 | 257 | 83.74 |

## D2 X-ray Diffractionometer

X-ray diffraction (Gupta *et al.*, 2010) was used to investigate the amount of crystallinity in PCB/HSA hydrogel blends in hydrogel form. The diffractometer was operated in the Bragg-Brentano geometry and fitted with a graphite monochromator in the diffracted beam with scan rate of 5°/min scan rate.
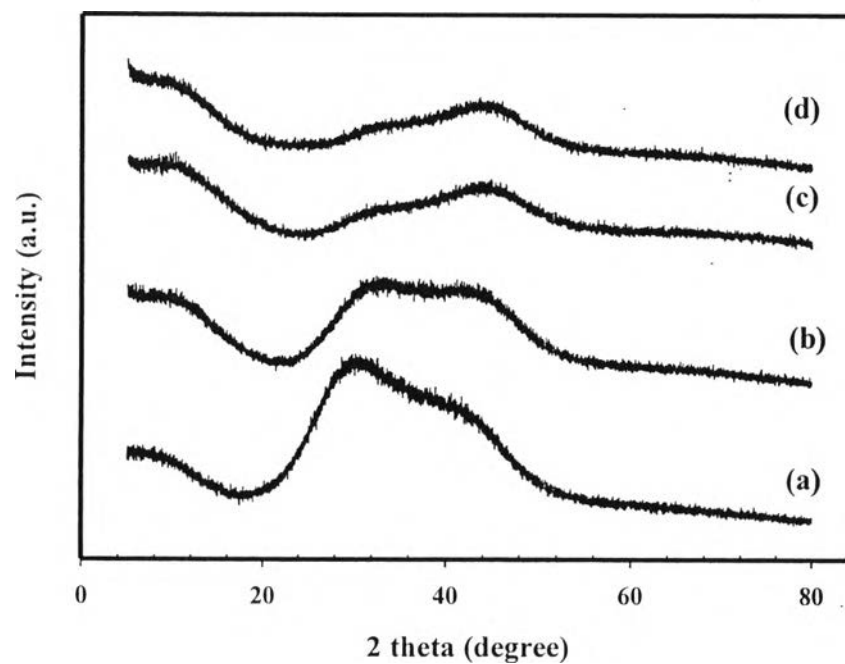
**Figure D2** XRD diffraction peaks of PCB/HSA hydrogel blends with various PCB concentrations: (a) pristine HAS; (b) 0.01 %v/v PCB; (c) 0.05 %v/v PCB; and (d) 0.10 %v/v PCB.

**Table D2** The summary of XRD diffraction of pristine HSA hydrogel and HSA hydrogel blends with various PCB concentrations.

| Sample | 2 Theta (Degree) |
| --- | --- |
| Pristine 1%v/v HSA | 29 |
| 0.01%v/v PCB/HSA | 29, 45 |
| 0.05%v/v PCB/HSA | 29, 45 |
| 0.10%v/v PCB/HSA | 29, 45 |

## D3 Scanning Electron Microscope (SEM)

Scanning electron microscope (Hitachi, S4800) was used to determine the morphological structure. The SEM images were captured at the magnification of 250 times with acceleration voltage of 10 kV.
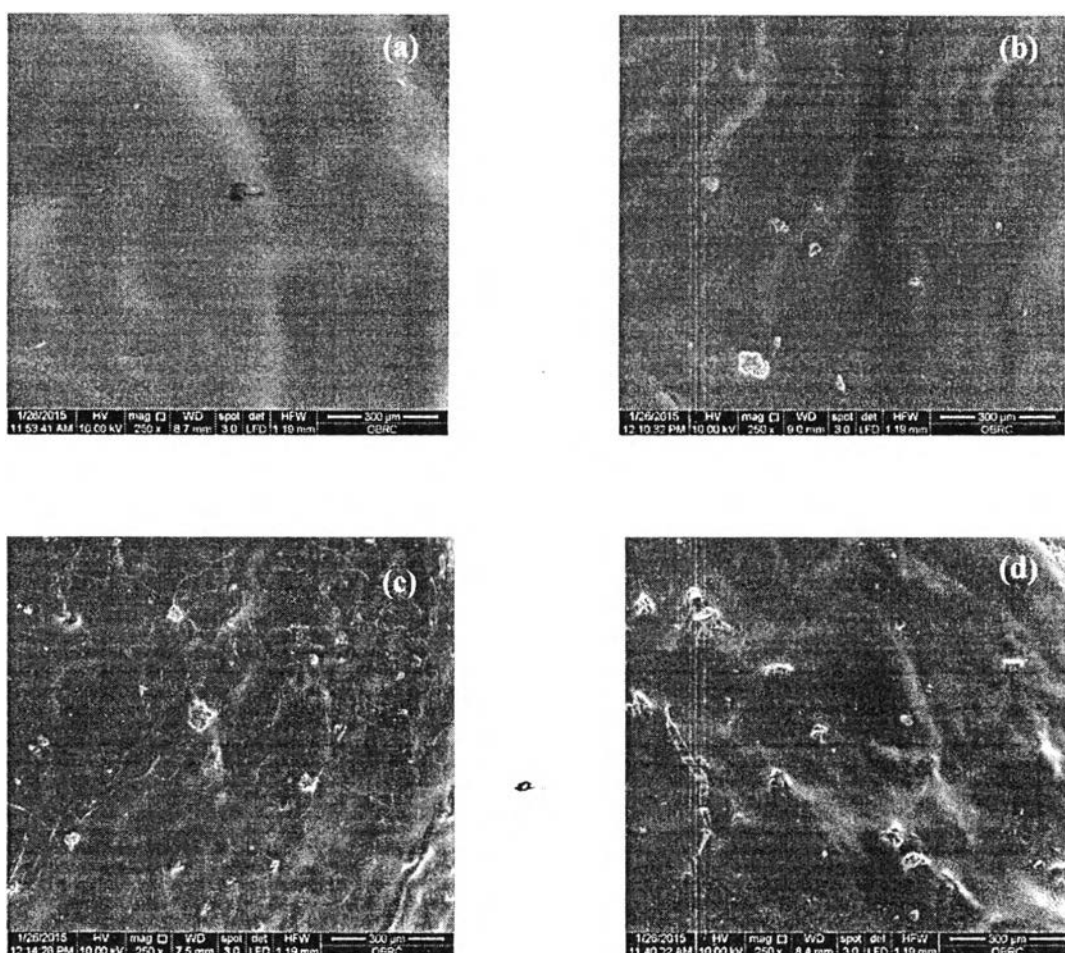


**Figure D3** SEM photographs of PCB/HAS hydrogel blends with various PCB concentrations: (a) 0.01%v/v PCB, (b) 0.05%v/v PCB, 0.10%v/v, 0.30%v/v PCB, and 0.50%v/v PCB
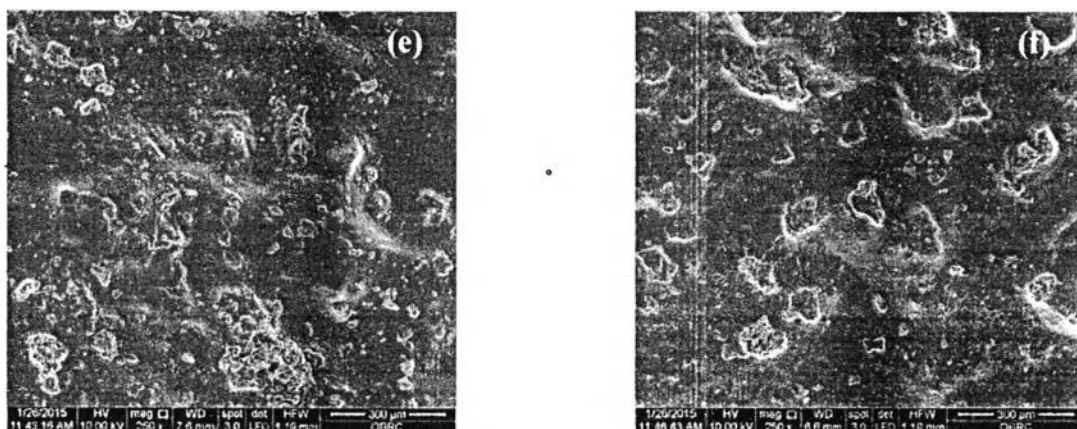
**Figure D3** SEM photographs of PCB/HAS hydrogel blends with various PCB concentrations: (a) 0.01%v/v PCB, (b) 0.05%v/v PCB, 0.10%v/v, 0.30%v/v PCB, and 0.50%v/v PCB. (Cont.)

## D5 Atomic Force Microscopy (AFM)

AFM (CSPM 400) images were taken with a scanning electron microscope to determine the topology of PCB/HSA hydrogel blends by using a scan rate 0.5 Hz and a scan sized of 2.5µm × 2.5µm$^2$.
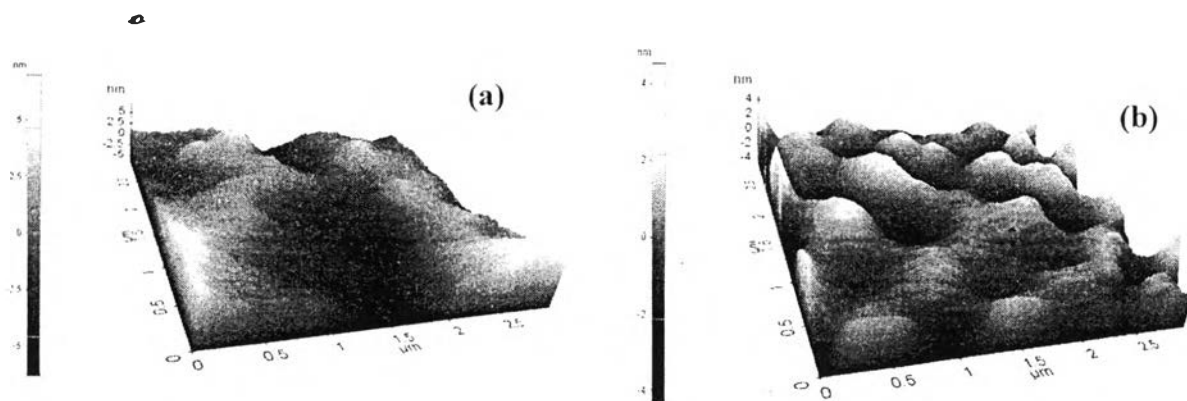


**Figure D4** AFM micrographs: (a) HSA by ionic crosslinking; and (b) 0.01%v/v PCB/HSA hydrogel blend by ionic crosslinking.

## APPENDIX E  Electromechanical Properties of Polycarbazole/Sodium Alginate (PCB/HSA) Hydrogel Blends

The electromechanical properties of the hydrogel blends were carried out by a melt rheometer (Rheometric Scientific, ARES). It was fitted with a costom-built copper parallel plate fixture, diameter 25 mm. A DC voltage was applied by DC power supply (Instek, GFG 8216A). A digital multimeter was used to monitor the voltage input. Dynamic strain sweep test was first carried out to find an appropriate strain by measuring G' and G" in the viscoelastic regime of the polycarbazole/sodium alginate hydrogel blends of various polycarbazole concentrations.

**Table E1** The storage modulus of sodium PCB/HSA hydrogel blends of various PCB concentrations under applied electric field strength. (fixed frequency =100 rad/s and %strain = 0.1)

| Electric Field Strength (V/mm) | Storage Modulus (Pa) | | | | | |
|---|---|---|---|---|---|---|
| | Pristine HSA | 0.01%v/v PCB | 0.05%v/v PCB | 0.1%v/v PCB | 0.3%v/v PCB | 0.5%v/v PCB |
| 0 | 1.02E+05 ± 1.38E+03 | 3.22E+04 ± 2.57E+03 | 3.25E+04 ± 2.60E+03 | 3.30E+04 ± 2.64E+03 | 3.32E+04 ± 2.66E+03 | 5.02E+04 ± 4.01E+03 |
| 25 | 1.17E+05 ± 1.15E+03 | 5.42E+04 ± 4.34E+03 | 4.36E+04 ± 3.48E+03 | 3.40E+04 ± 2.72E+03 | 5.37E+04 ± 4.E29+03 | 5.11E+04 ± 4.88E+03 |
| 50 | 2.06E+05 ± 1.49E+04 | 6.68E+04 ± 5.34E+03 | 4.50E+04 ± 3.60E+03 | 3.57E+04 ± 2.85E+03 | 5.55E+04 ± 4.44E+03 | 6.87E+04 ± 5.49E+03 |
| 100 | 3.12E+05 ± 2.50E+04 | 9.37E+04 ± 7.49E+03 | 7.27E+04 ± 5.82E+03 | 3.75E+04 ± 3.00E+03 | 6.05E+04 ± 4.84E+03 | 7.44E+04 ± 5.95E+03 |
| 200 | 4.53E+05 ± 2.07E+04 | 1.84E+04 ± 1.47E+04 | 1.86E+05 ± 1.49E+04 | 4.42E+04 ± 3.53E+03 | 7.65E+04 ± 6.12E+03 | 8.12E+04 ± 6.49E+03 |

**Table E1** The storage modulus of sodium PCB/HSA hydrogel blends of various PCB concentrations under applied electric field strength (fixed frequency =100 rad/s and %strain = 0.1)(Cont.)

| Electric Field Strength (V/mm) | Storage Modulus (Pa) | | | | | |
|---|---|---|---|---|---|---|
| | Pristine HSA | 0.01%v/v PCB | 0.05%v/v PCB | 0.1%v/v PCB | 0.3%v/v PCB | 0.5%v/v PCB |
| 300 | 5.88E+05 ± 3.86E+04 | 2.29E+05± 4.23E+04 | 2.61E+05 ± 2.09E+04 | 1.40E+05 ± 1.12E+04 | 1.26E+05 ± 1.01E+04 | 9.56E+04 ± 7.65E+03 |
| 400 | 6.39E+05 ± 2.92E+04 | 3.30E+05 ± 2.64E+04 | 3.19E+05 ± 2.55E+04 | 2.25E+05 ± 1.80E+04 | 2.26E+05 ± 1.81E+04 | 1.04E+05 ± 8.34E+03 |
| 500 | 7.37E+05 ± 4.22E+04 | 3.36E+05 ± 2.69E+04 | 4.05E+05 ± 3.24E+04 | 3.01E+05 ± 2.41E+04 | 2.80E+05 ± 2.24E+04 | 1.10E+05 ± 8.81E+03 |
| 600 | 7.85E+05 ± 5.38E+04 | 3.46E+05 ± 2.77E+04 | 4.35E+05 ± 3.48E+04 | 4.52E+05 ± 3.62E+04 | 3.17E+05 ± 2.54E+04 | 1.12E+05 ± 9.83E+03 |
| 700 | 8.25E+05 ± 8.06E+04 | 3.92E+05 ± 3.13E+04 | 4.96E+05 ± 3.97E+04 | 5.99E+05 ± 4.79E+04 | 3.93E+05 ± 3.14E+04 | 1.39E+05 ± 1.11E+04 |
| 800 | 8.36E+05 ± 6.83E+04 | 4.44E+05 ± 3.55E+04 | 5.27E+05 ± 4.22E+04 | 6.26E+05 ± 5.01E+04 | 4.21E+05 ± 3.37E+04 | 1.44E+05 ± 1.15E+04 |

**Table E2** The storage modulus sensitivity of PCB/HSA hydrogel blends of various PCB concentrations under applied electric field strength (fixed frequency =100 and %strain = 0.1)

| Electric Field Strength (V/mm) | Storage Modulus Sensitivity | | | | | |
|---|---|---|---|---|---|---|
| | Pristine HSA | 0.01%v/v PCB | 0.05%v/v PCB | 0.1%v/v PCB | 0.3%v/v PCB | 0.5%v/v PCB |
| 25 | 0.08 ± 0.05 | 0.68 ± 0.05 | 0.34 ± 0.23 | 0.06 ± 0.01 | 0.68 ± 0.05 | 0.89 ± 0.07 |
| 50 | 0.95 ±0.11 | 1.07 ± 0.09 | 0.38 ± 0.03 | 0.11 ± 0.01 | 0.73 ± 0.06 | 1.55 ± 0.12 |
| 100 | 1.99 ± 0.23 | 1.91 ± 0.15 | 1.24 ± 0.10 | 0.17 ± 0.02 | 0.89 ± 0.07 | 1.76 ± 0.14 |
| 200 | 3.37 ± 0.19 | 4.71 ± 0.38 | 4.71 ± 0.38 | 0.38 ± 0.27 | 1.39 ± 0.11 | 2.01 ± 0.16 |
| 300 | 4.69 ± 0.40 | 6.12 ± 0.49 | 7.04 ± 0.56 | 3.38 ± 0.27 | 2.93 ± 0.23 | 2.55 ± 0.20 |
| 400 | 5.19 ± 0.29 | 9.27 ± 0.74 | 8.81 ± 0.71 | 6.03 ± 0.48 | 6.05 ± 0.48 | 2.87 ± 0.23 |
| 500 | 6.16 ± 0.43 | 9.45 ± 0.76 | 11.47 ± 0.92 | 8.41 ± 0.67 | 7.75 ± 0.62 | 3.08 ± 0.25 |
| 600 | 6.62 ± 0.54 | 9.75 ± 0.78 | 12.39 ± 0.99 | 13.12 ± 1.05 | 8.90 ± 0.71 | 3.56 ± 0.28 |
| 700 | 7.03 ± 0.84 | 11.18 ± 0.89 | 14.25 ± 1.14 | 17.72 ± 1.42 | 11.26 ± 0.90 | 4.16 ± 0.33 |
| 800 | 7.13 ± 0.72 | 12.80 ± 1.02 | 15.21 ± 1.22 | 18.55 ± 1.48 | 12.15 ± 0.97 | 4.33 ± 0.35 |
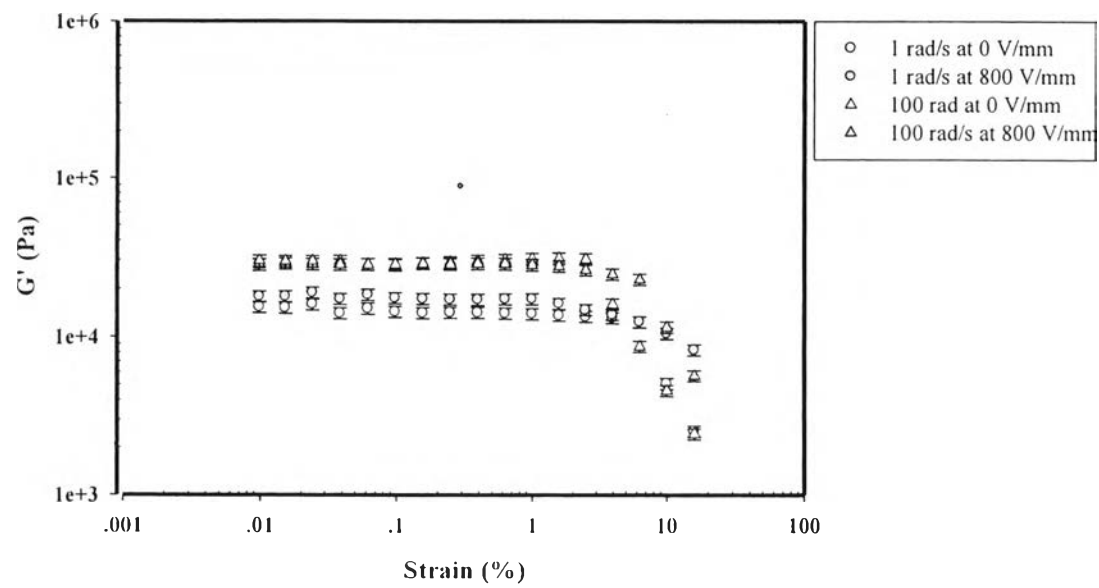
(a)
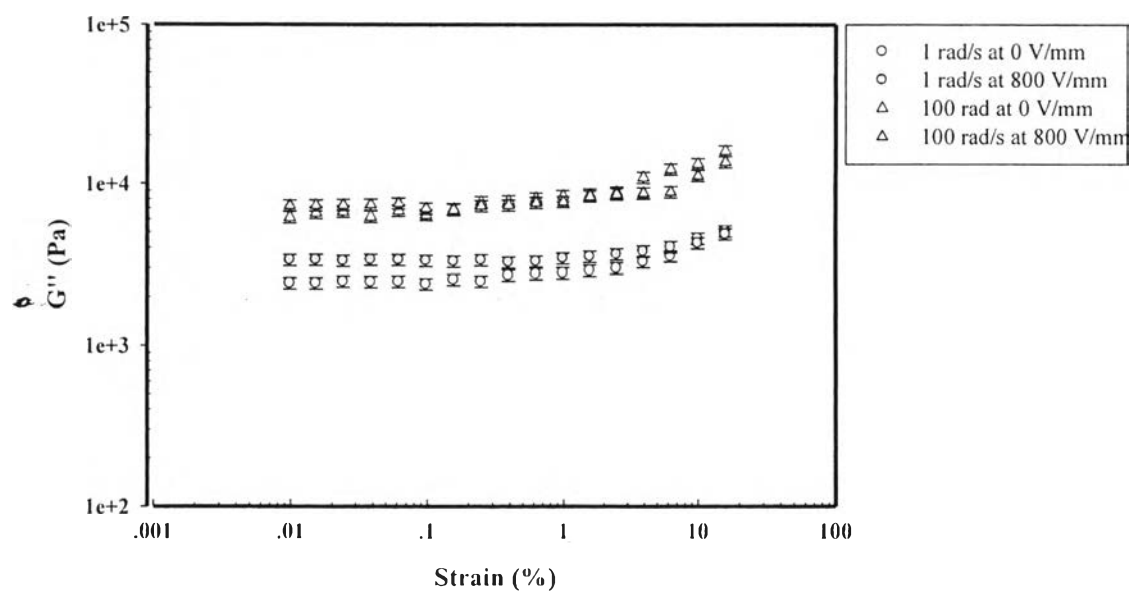


(b)

**Figure E1** Strain sweep test: (a) storage modulus; (b) loss modulus of 0.01%v/v PCB/HSA hydrogel blend with ionic crosslinking of 0.015%v/v CaCl$_2$ at frequency of 1 rad/s and 100 rad/s, electric field strength of 0 V/mm and 800 V/mm, sample thickness of 1.65 mm, 300 K.
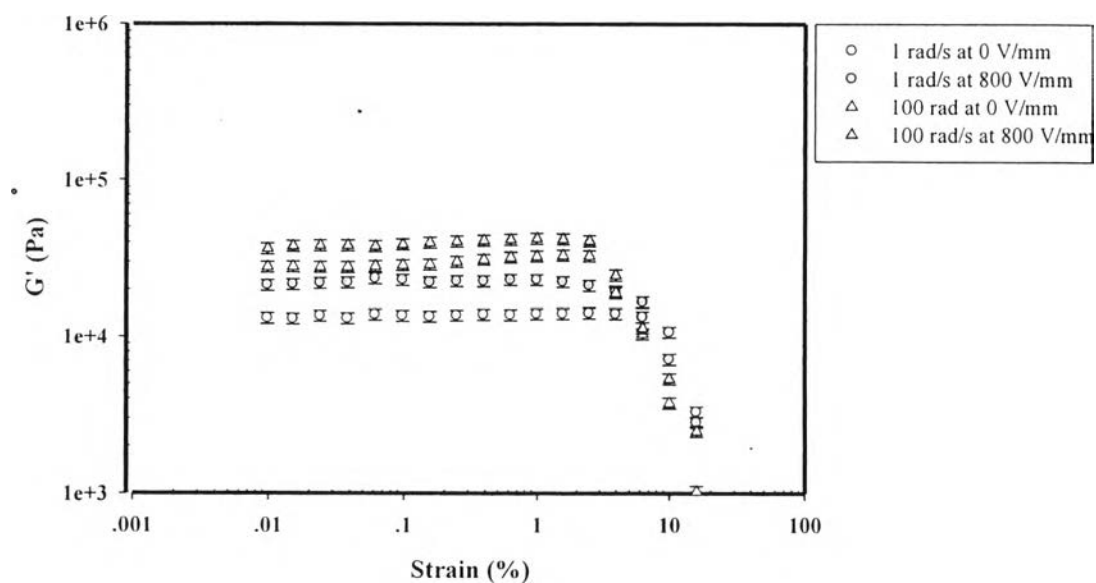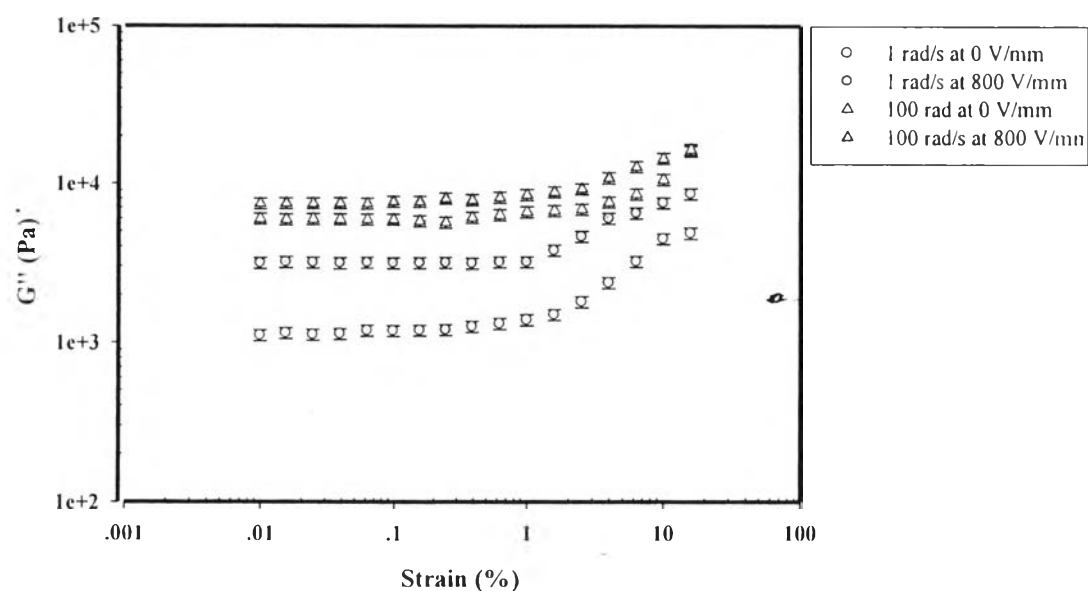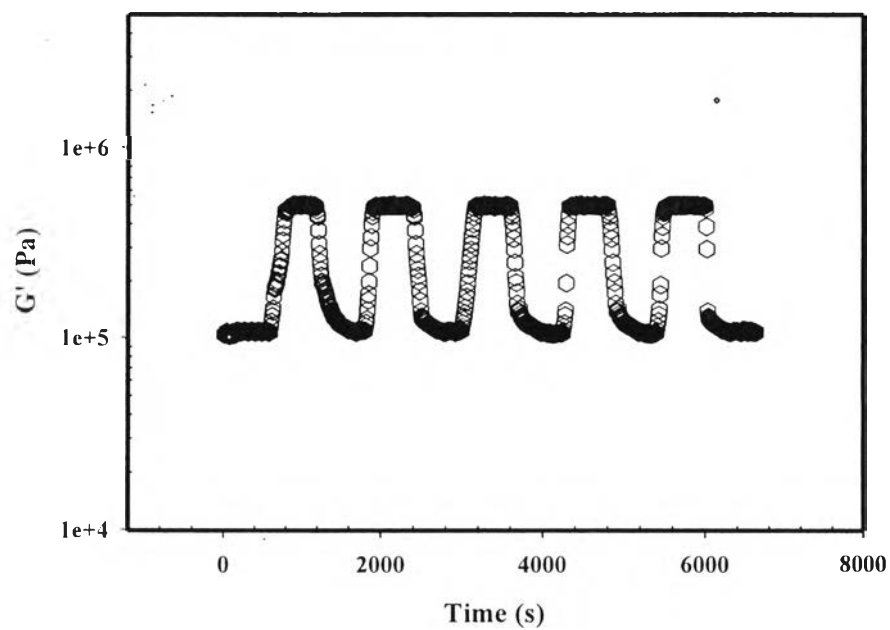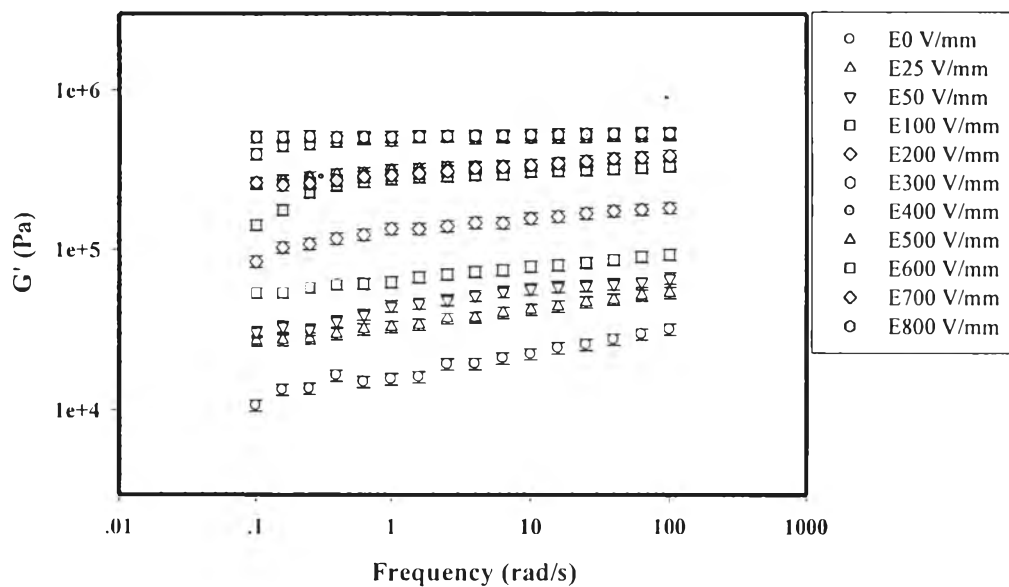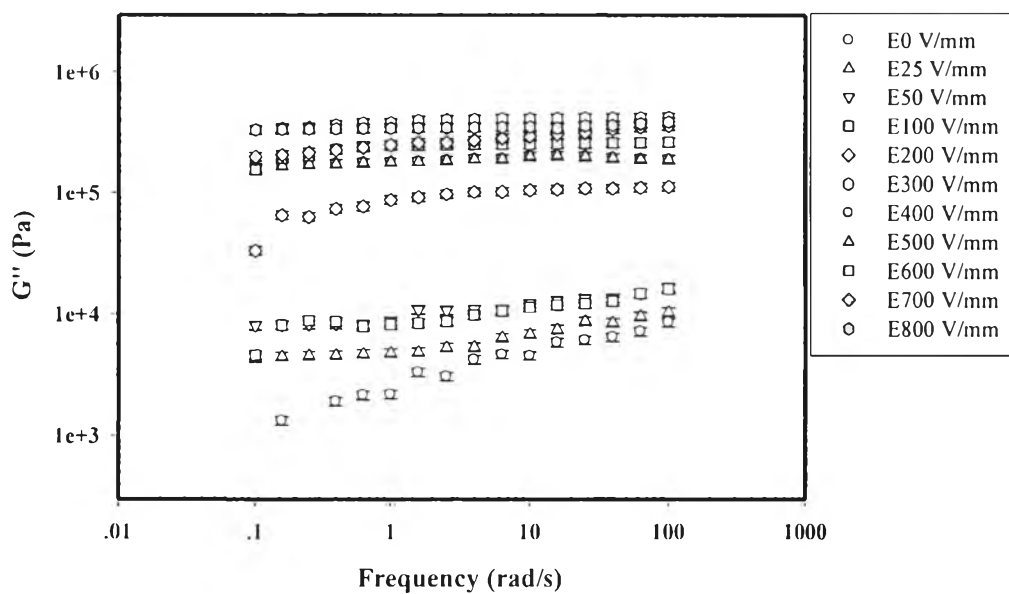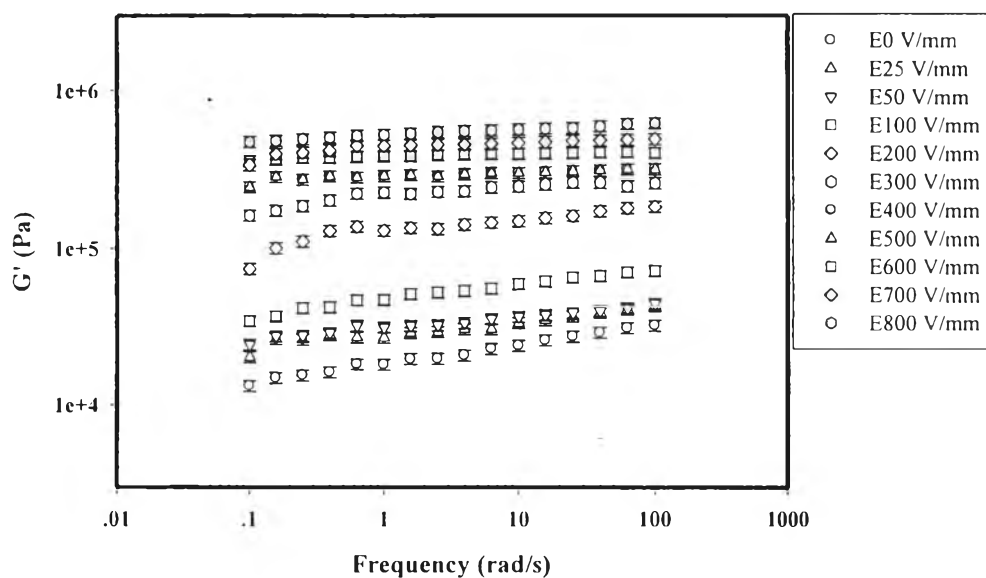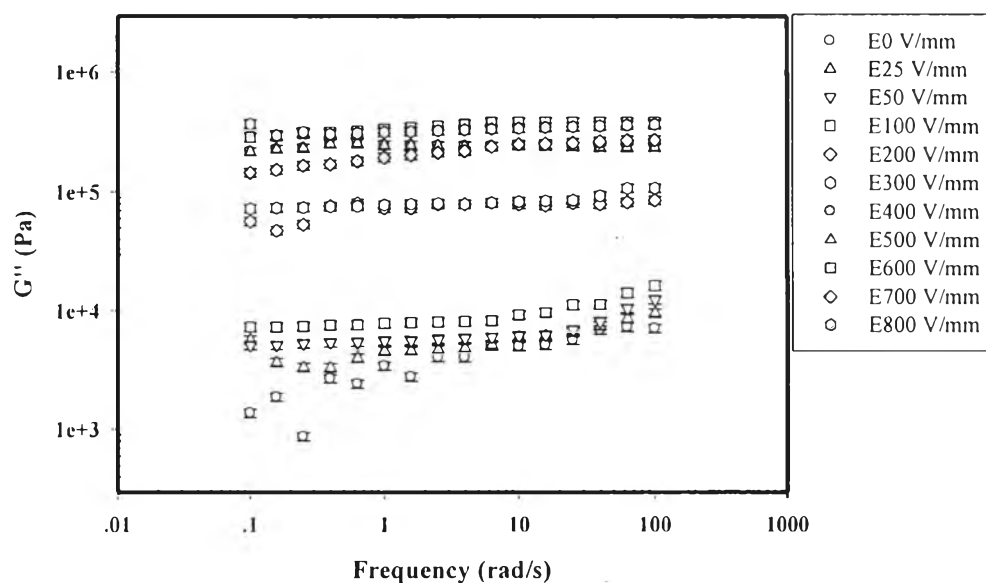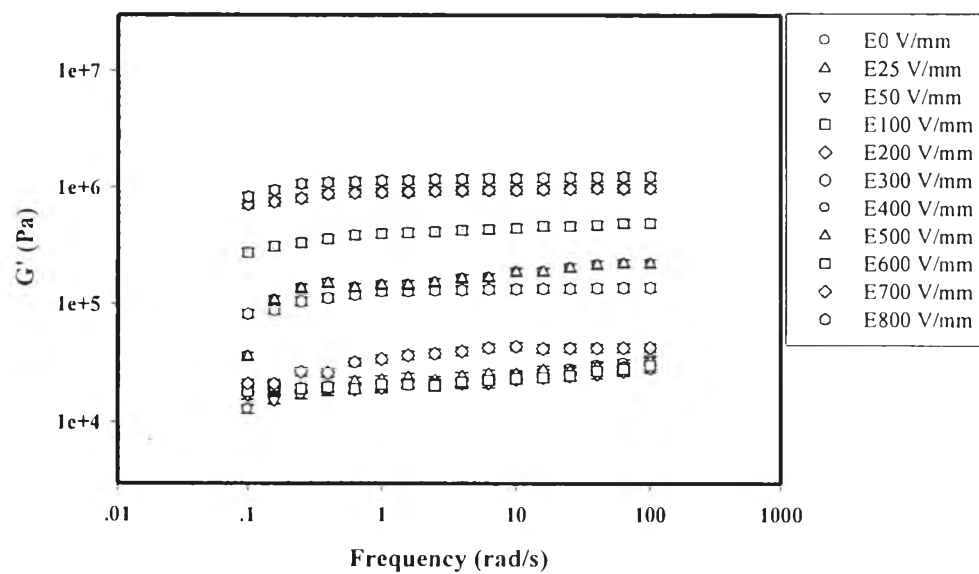
**(a)**
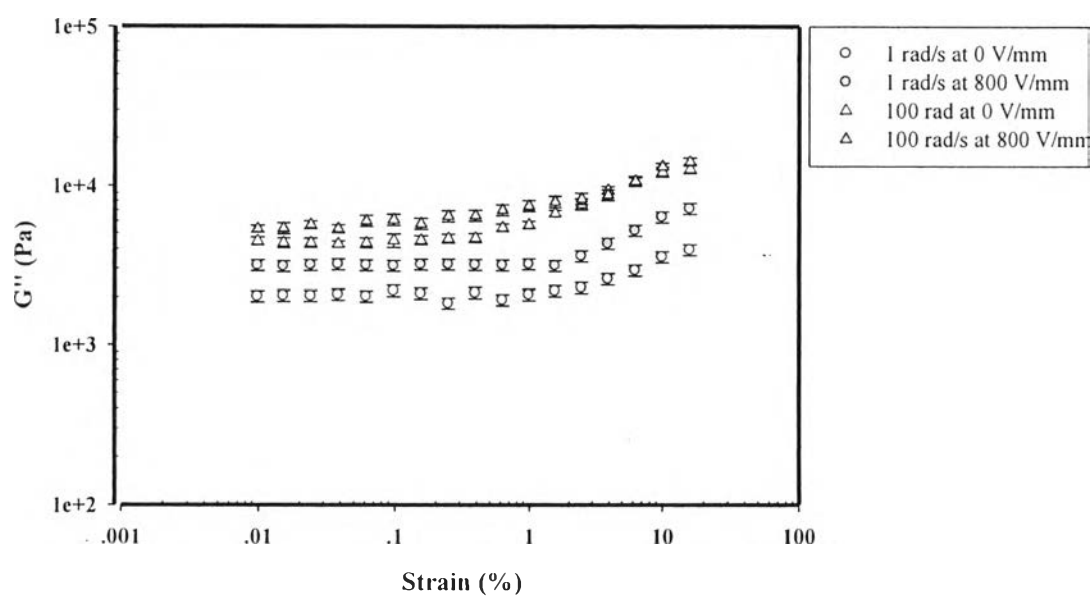


**(b)**

**Figure E2** Strain sweep test: (a) storage modulus; (b) loss modulus of 0.05%v/v PCB/HSA hydrogel blend with ionic crosslinking of 0.015%v/v CaCl$_2$ at frequency of 1 rad/s and 100 rad/s, electric field strength of 0 V/mm and 800 V/mm, sample thickness of 1.68 mm, 300 K.
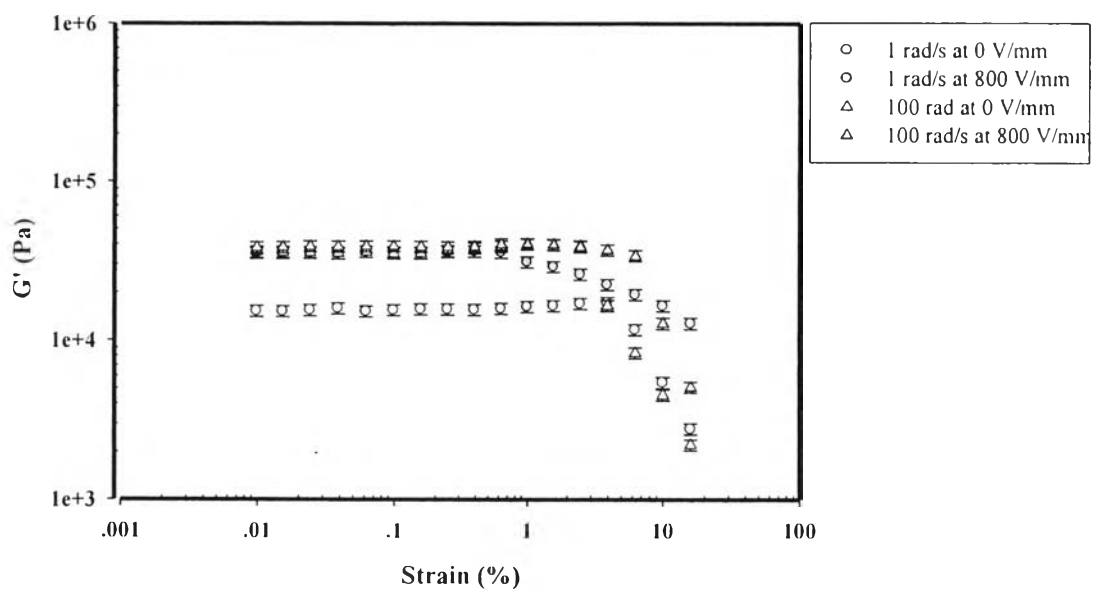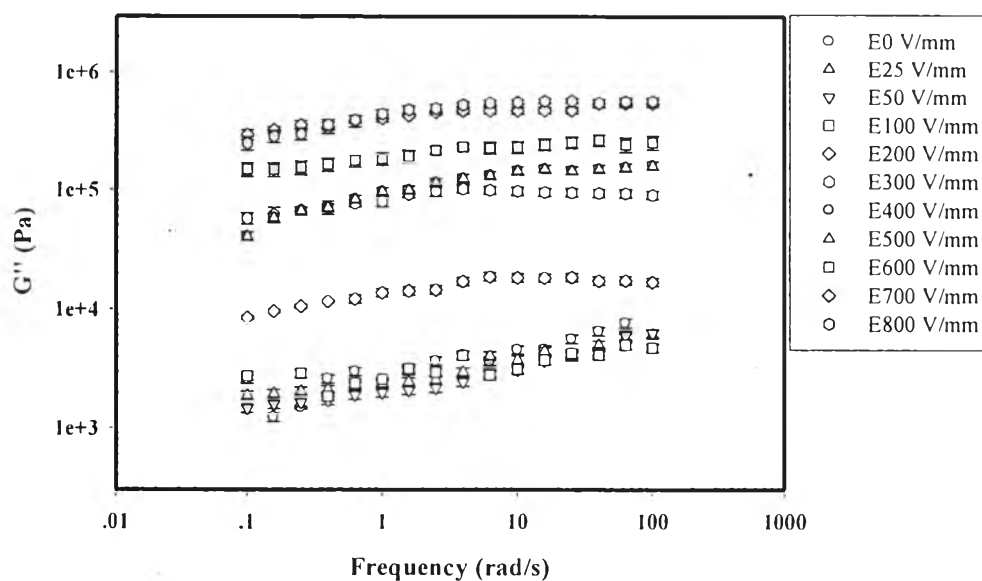
(a)
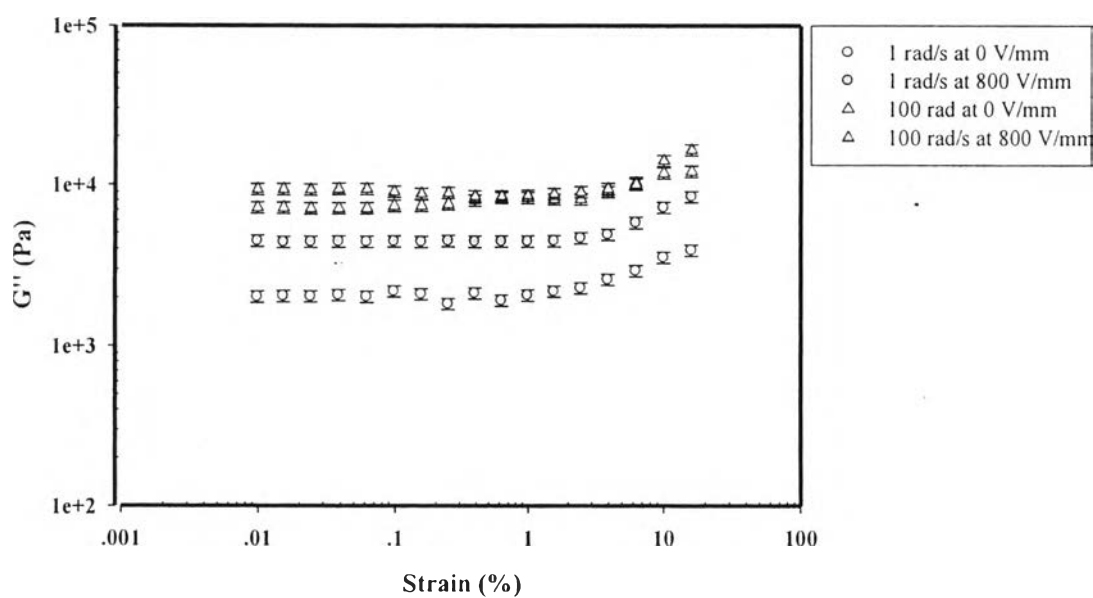


(b)

**Figure E3** Strain sweep test: (a) storage modulus; (b) loss modulus of 0.10%v/v PCB/HSA hydrogel blend with ionic crosslinking of 0.015%v/v $CaCl_2$ at frequency of 1 rad/s and 100 rad/s, electric field strength of 0 V/mm and 800 V/mm, sample thickness of 1.73 mm, 300 K.
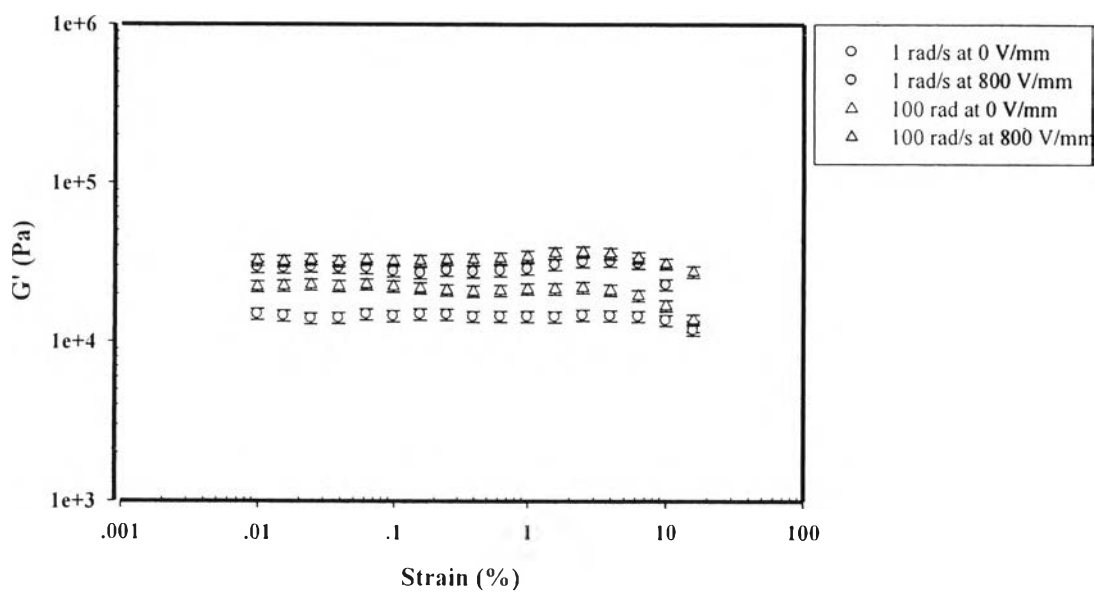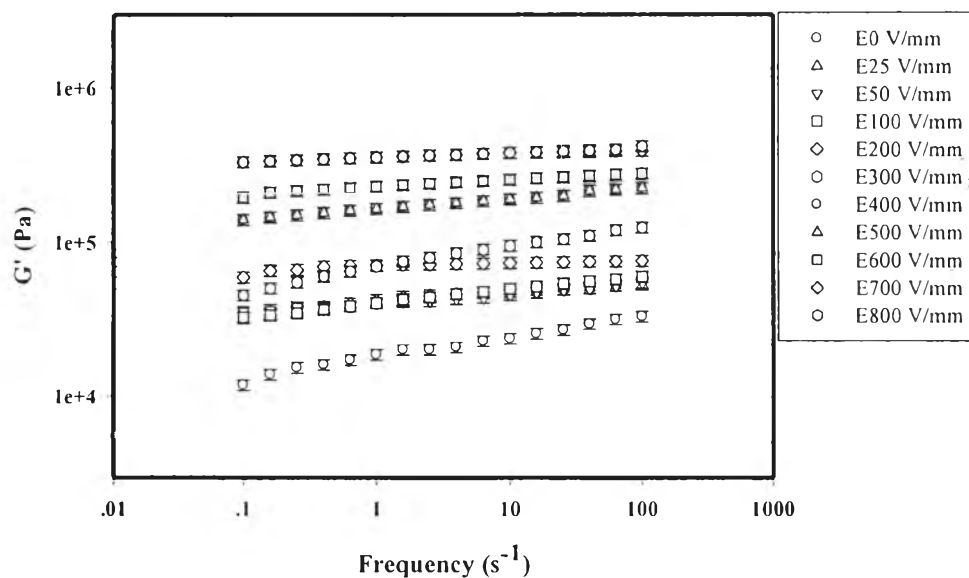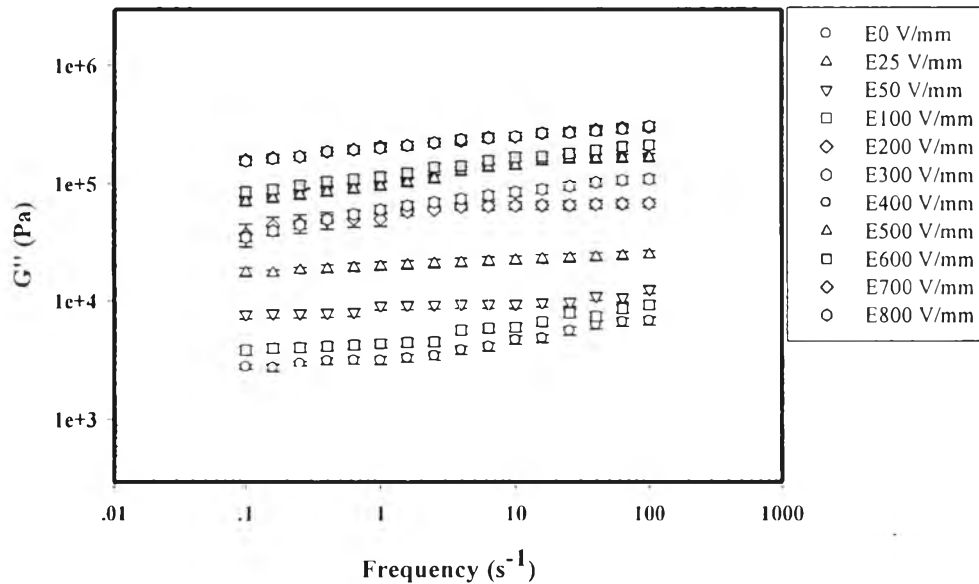
(a)
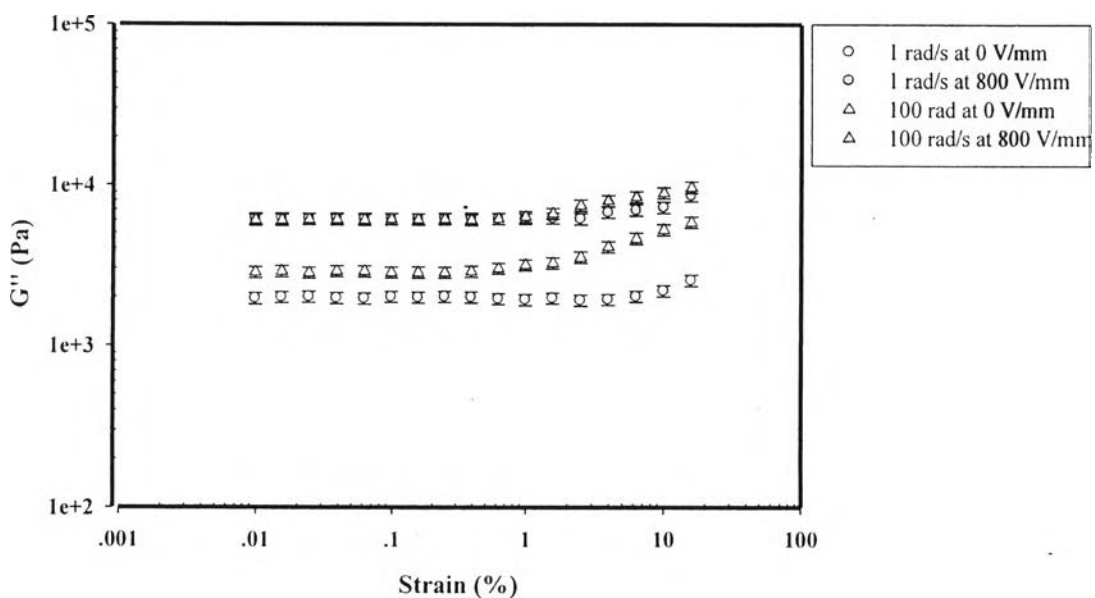


(b)

**Figure E4** Strain sweep test: (a) storage modulus; (b) loss modulus of 0.30%v/v PCB/HSA hydrogel blend with ionic crosslinking of 0.015%v/v $CaCl_2$ at frequency of 1 rad/s and 100 rad/s, electric field strength of 0 V/mm and 800 V/mm, sample thickness of 1.68 mm, 300 K.
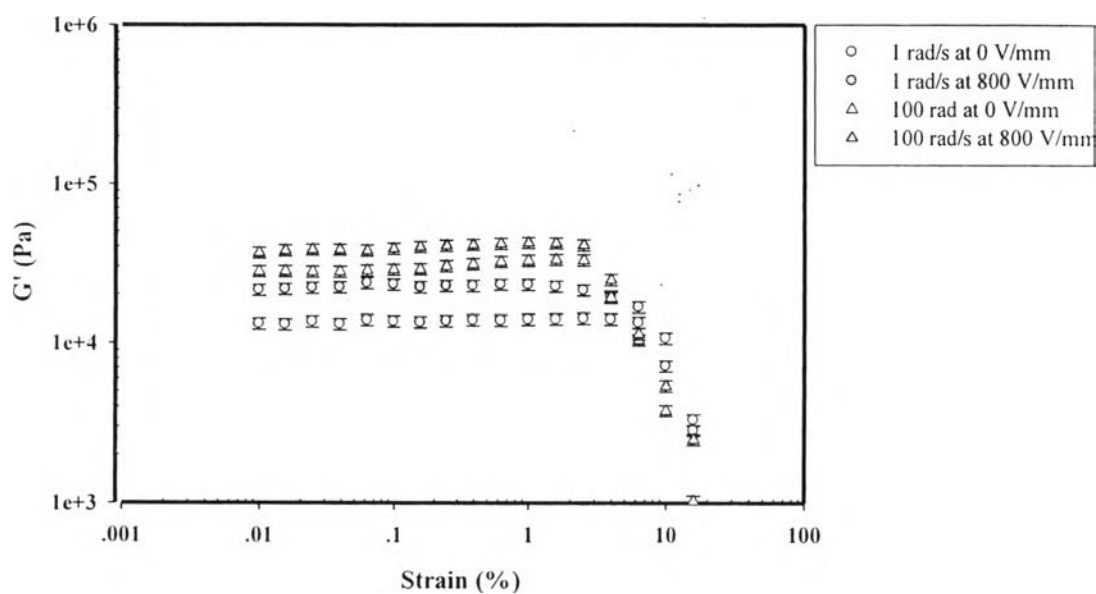
(a)



(b)

**Figure E5** Strain sweep test: (a) storage modulus; (b) loss modulus of 0.50%v/v PCB/HSA hydrogel blend with ionic crosslinking of 0.015%v/v CaCl₂ at frequency of 1 rad/s and 100 rad/s, electric field strength of 0 V/mm and 800 V/mm, sample thickness of 1.68 mm, 300 K.

**Figure E6** Temporal response test of 0.1%v/v PCB/HSA hydrogel blend with ionic crosslinking of 0.015%v/v $CaCl_2$ at frequency 100 rad/s, electric field strength 800 V/mm, sample thickness 1.65 mm, 300 K.
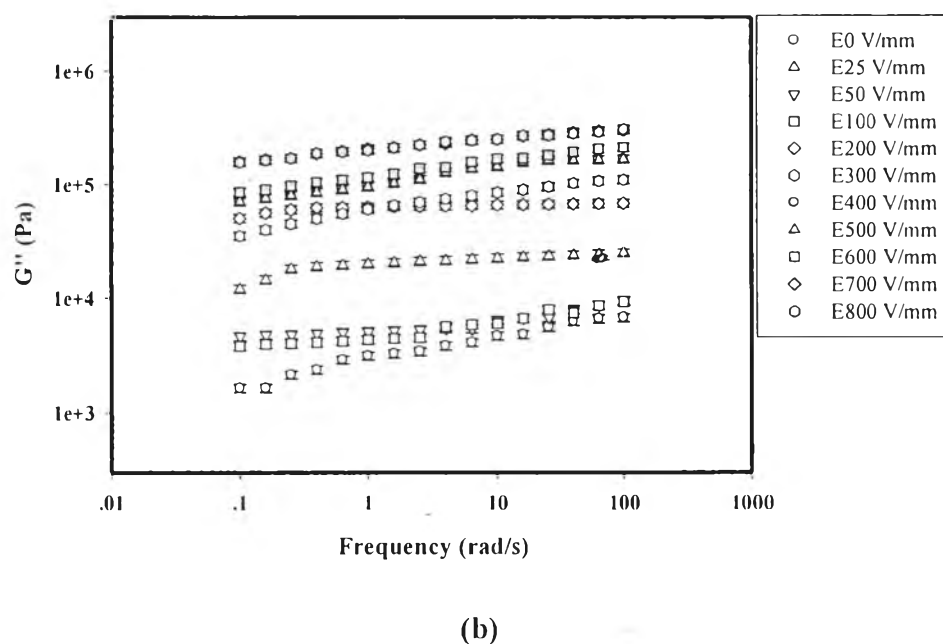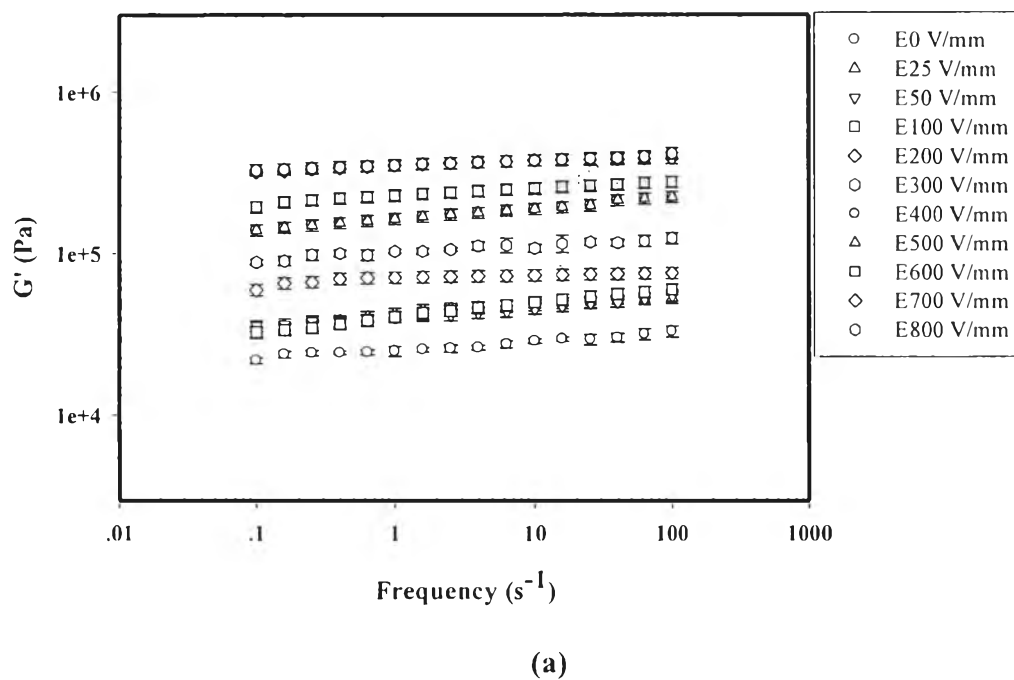
(a)



(b)

**Figure E7** Frequency sweep test: (a) storage modulus; (b) loss modulus of 0.01%v/v PCB/HSA hydrogel blend with ionic crosslinking of 0.015%v/v $CaCl_2$ at strain 0.1%, sample thickness 1.75 mm, temperature 300 K.

(a)



(b)

**Figure E8** Frequency sweep test: (a) storage modulus; (b) loss modulus of 0.05%v/v PCB/HSA hydrogel blend with ionic crosslinking of 0.015%v/v CaCl$_2$ at strain 0.1%, sample thickness 1.73 mm, temperature 300 K.

(a)



(b)

**Figure E9** Frequency sweep test: (a) storage modulus; (b) loss modulus of 0.10%v/v PCB/HSA hydrogel blend with ionic crosslinking of 0.015%v/v CaCl$_2$ at strain 0.1%, sample thickness 1.65 mm, temperature 300 K.

**(a)**



**(b)**

**Figure E10**   Frequency sweep test: (a) storage modulus; (b) loss modulus of 0.30%v/v PCB/HSA hydrogel blend with ionic crosslinking of 0.015%v/v $CaCl_2$ at strain 0.1%, sample thickness 1.65 mm, temperature 300 K.

**(a)**



**(b)**

**Figure E11**   Frequency sweep test: (a) storage modulus; (b) loss modulus of 0.50%v/v PCB/HSA hydrogel blend with ionic crosslinking of 0.015%v/v $CaCl_2$ at strain 0.1%, sample thickness 1.71 mm, temperature 300 K.
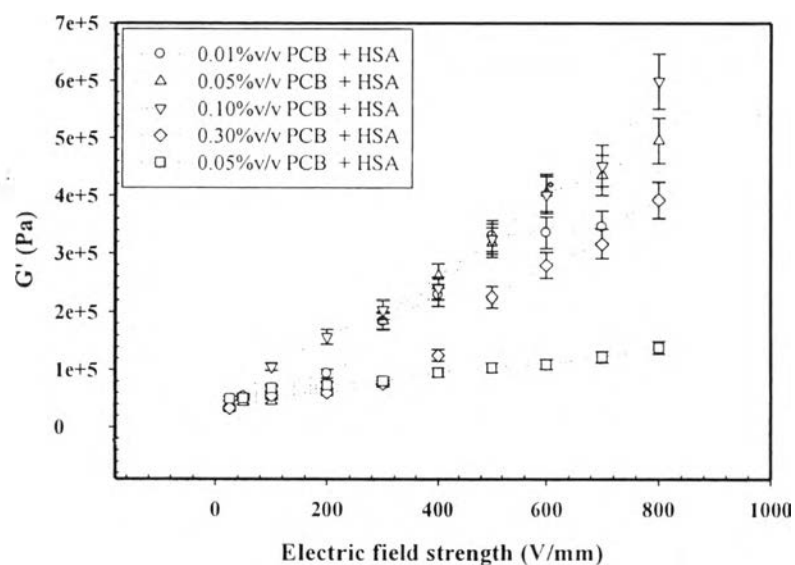
**Figure E12** The storage modulus (G') versus electric field strength of PCB/HAS hydrogel blend of various PCB concentration at strain 0.1%, frequency 100 rad/s, temperature 300 K.
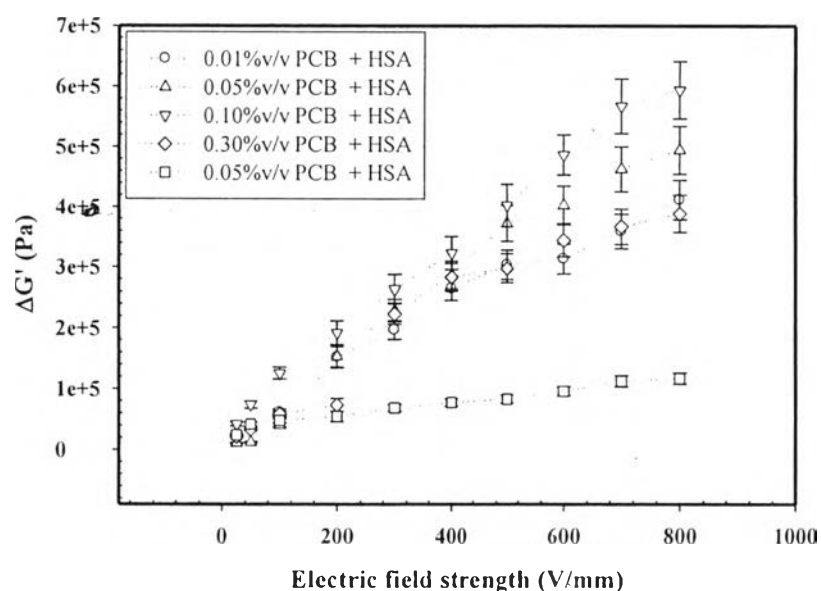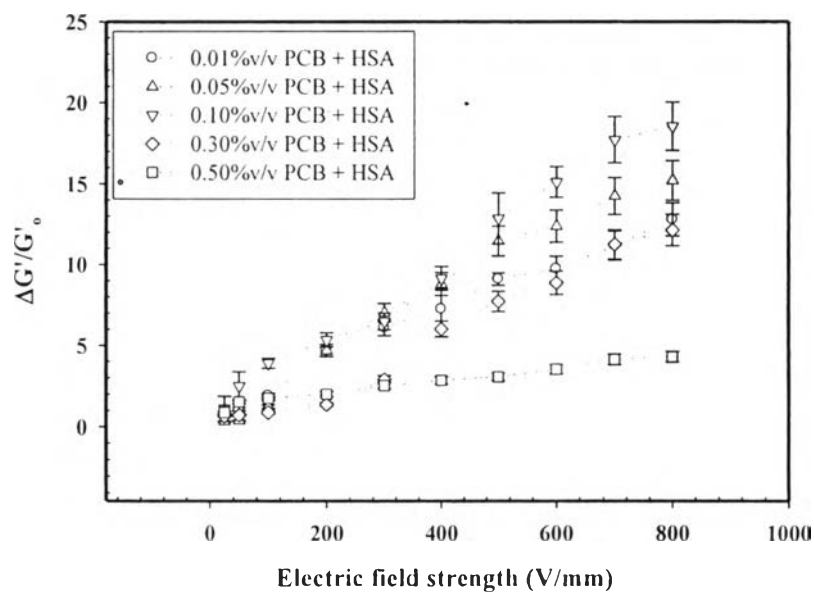


**Figure E13** The storage modulus response ($\Delta$G') versus electric field strength of PCB/HSA hydrogel blend of various PCB concentration at strain 0.1%, frequency 100 rad/s, temperature 300 K.

**Figure E14** The storage modulus sensitivity ($\Delta G'/G'_0$) versus electric field strength of PCB/HSA hydrogel blend of various PCB concentration at strain 0.1%, frequency 100 rad/s, temperature 300 K.

APPENDIX F  Deflection Responses of Pristine High Molecular Weight Sodium Alginate (HSA) Hydrogel and Polycarbazole/High Molecular Weight Sodium Alginate (PCB/HSA) Hydrogel Blends

**Table F1** Deflection angles, deflection distances, and dielectrophoresis forces of PCB/HSA blends with crosslinked by ionic crosslinking ($CaCl_2$) at electric field strength of 500 V/mm

| Materials | PCB (%v/v) | Deflection Angle (Degree) | Deflection Distance (mm) | Dielectrophoresis Fforce (mN) |
|---|---|---|---|---|
| HSA by ionic crosslinking | 0.00 | 55.58 ± 0.23 | 18.10 ± 0.57 | 1.00 ± 0.01 |
| HSA by covalent crosslinking | 0.00 | 46.15 ± 0.39 | 15.31± 0.42 | 0.75 ± 0.02 |
| PCB/HSA by ionic crosslinking | 0.01 | 40.11 ± 1.76 | 14.00 ± 0.99 | 1.78 ± 0.17 |
| PCB/HSA by ionic crosslinking | 0.05 | 40.34 ± 1.64 | 14.35 ± 0.35 | 1.83 ± 0.01 |
| PCB/HSA by ionic crosslinking | 0.10 | 44.19 ± 0.13 | 15.75 ± 0.07 | 2.76 ± 0.15 |
| PCB/HSA by ionic crosslinking | 0.30 | 36.69 ± 2.85 | 12.60 ± 0.99 | 2.18 ± 0.02 |
| PCB/HSA by ionic crosslinking | 0.50 | 24.29 ± 0.17 | 8.89 ± 0.07 | 1.06 ± 1.16 |
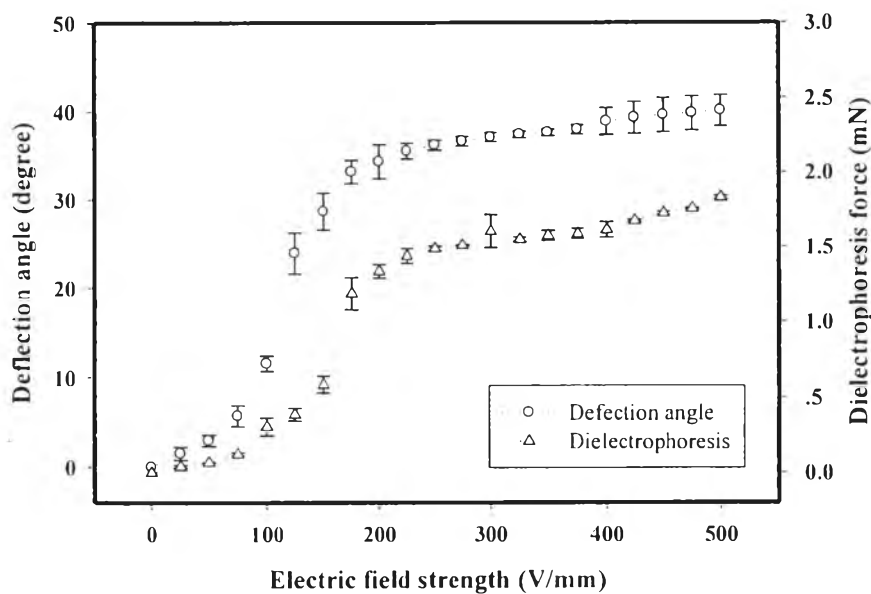
**Figure F1** Deflection angle (θ) and dielectrophoresis force (F$_d$) versus electric field strength of 0.01 %v/v PCB/HSA hydrogel blend (sample width 3 mm, sample thickness 1.5 mm, sample weight 0.21 g).
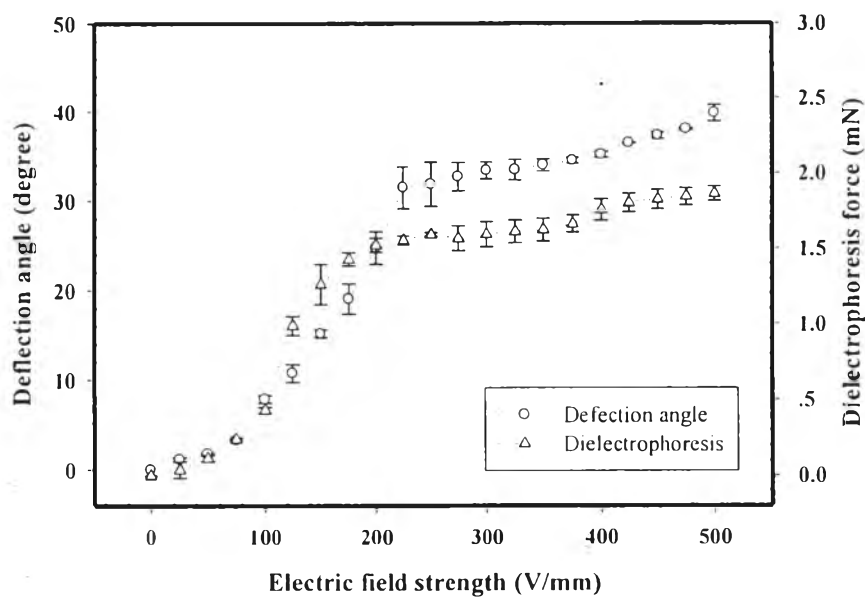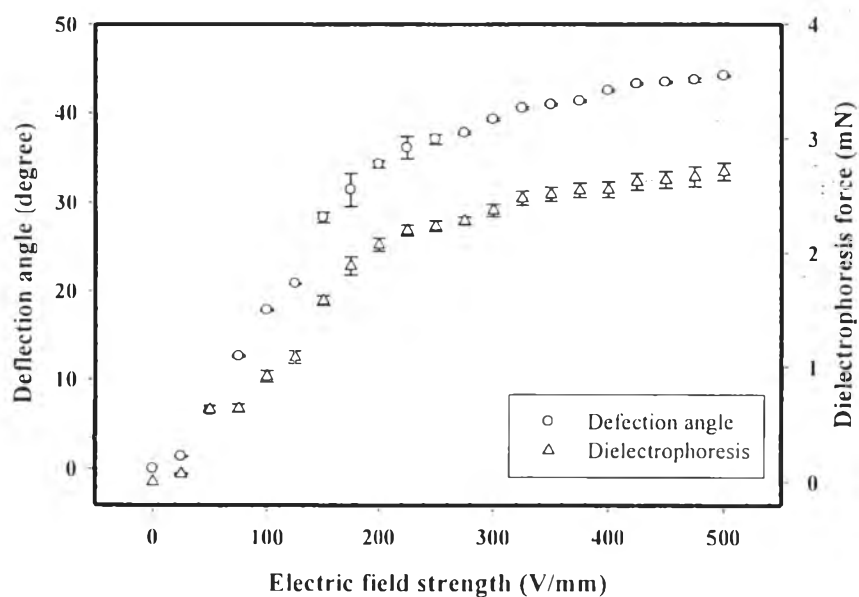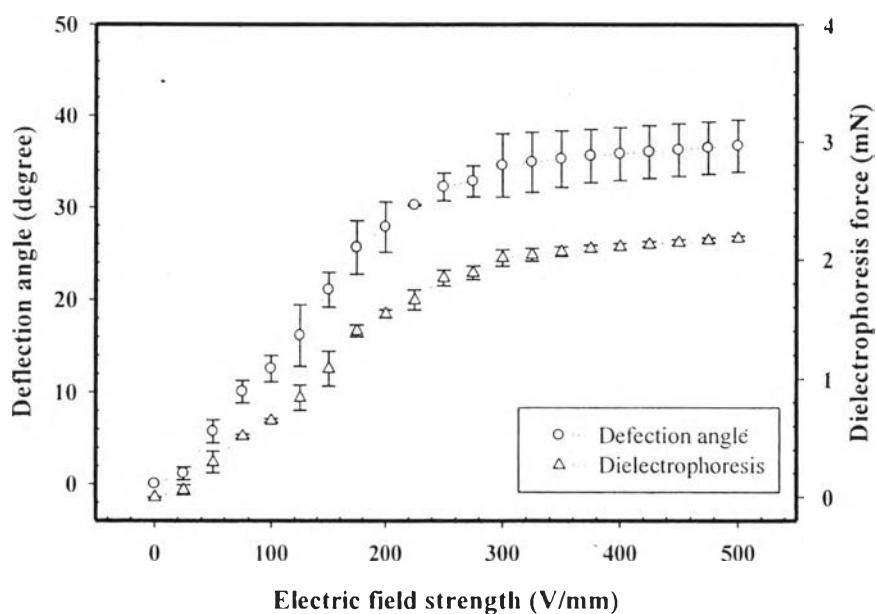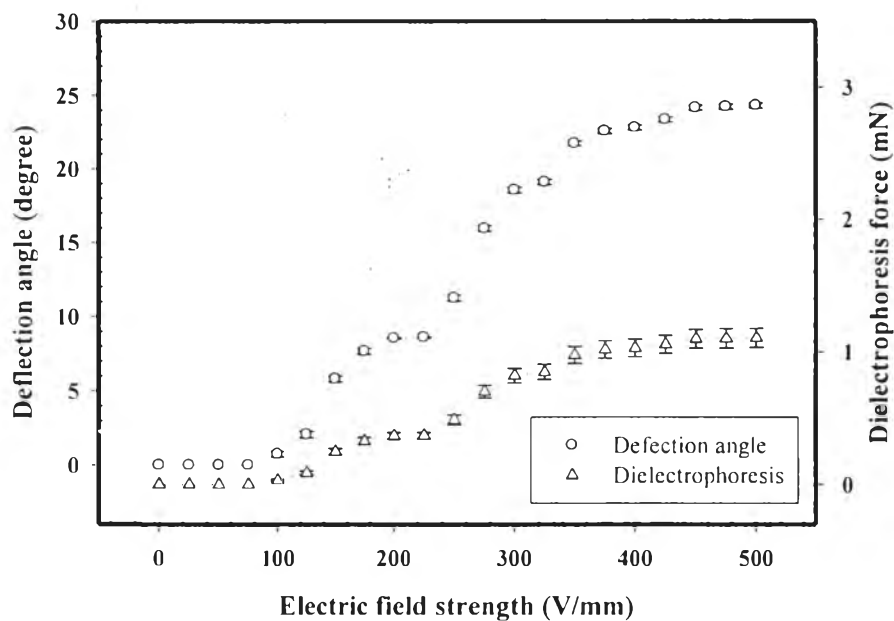


**Figure F2** Deflection angle (θ) and dielectrophoresis force (F$_d$) versus electric field strength of 0.05 %v/v PCB/HAS hydrogel blends (sample width 3 mm, sample thickness 1.5 mm, sample weight 0.22 g).

**Figure F3** Deflection angle (θ) and dielectrophoresis force ($F_d$) versus electric field strength of 0.10 %v/v PCB/HSA hydrogel blends (sample width 3 mm, sample thickness 1.5 mm, sample weight 0.28 g).



**Figure F4** Deflection angle (θ) and dielectrophoresis force ($F_d$) versus electric field strength of 0.30 %v/v PCB/HSA hydrogel blend (sample width 3 mm, sample thickness 1.5 mm, sample weight 0.29 g).

**Figure F5** Deflection angle (θ) and dielectrophoresis force (F$_d$) versus electric field strength of 0.50 %v/v PCB/HSA hydrogel blend (sample width 3 mm, sample thickness 1.5 mm, sample weight 0.26 g).
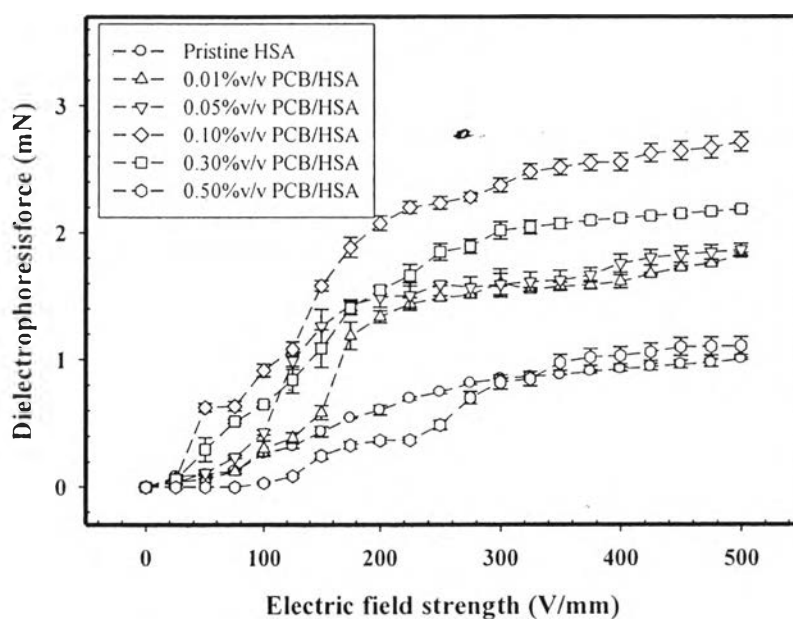


**Figure F6** Dielectrophoresis force (F$_d$) versus electric field strength of pristine HSA and PCB/HSA hydrogel blends.
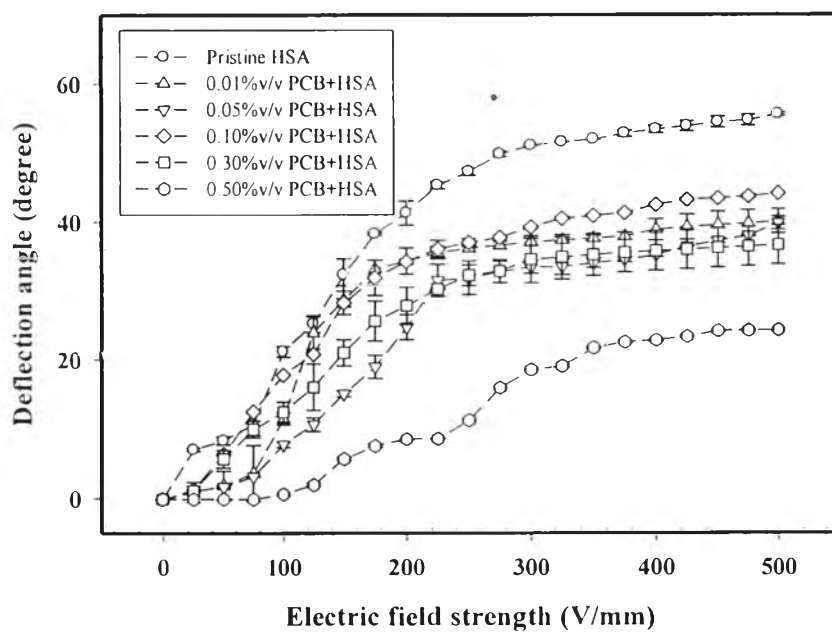
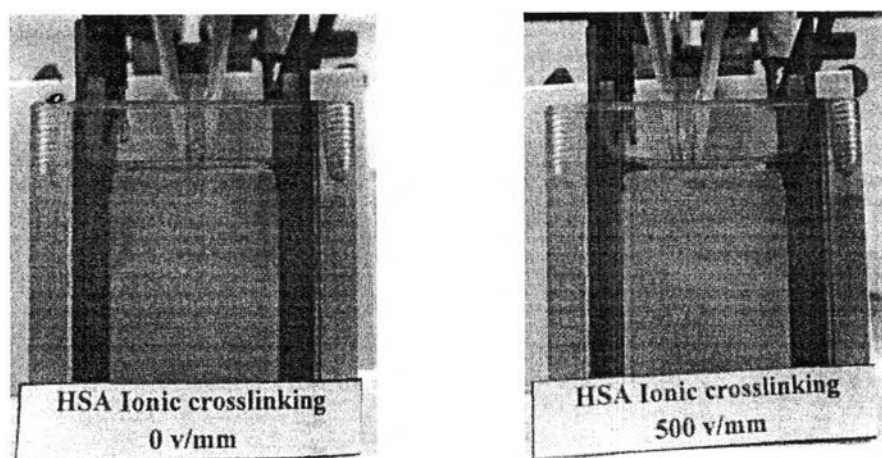**Figure F7** Deflection angle (θ) versus electric field strength of pristine HSA and PCB/HSA hydrogel blends.



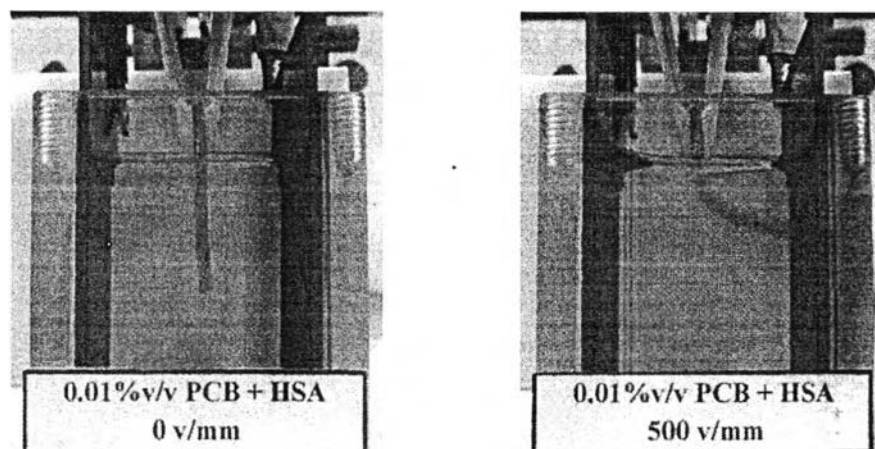**Figure F8** Bending of pristine HSA hydrogel at electric field strength 0 and 500 V/mm.

**Figure F9** Bending of pristine 0.01%v/v PCB/HSA hydrogel blend at electric field strength 0 and 500 V/mm.
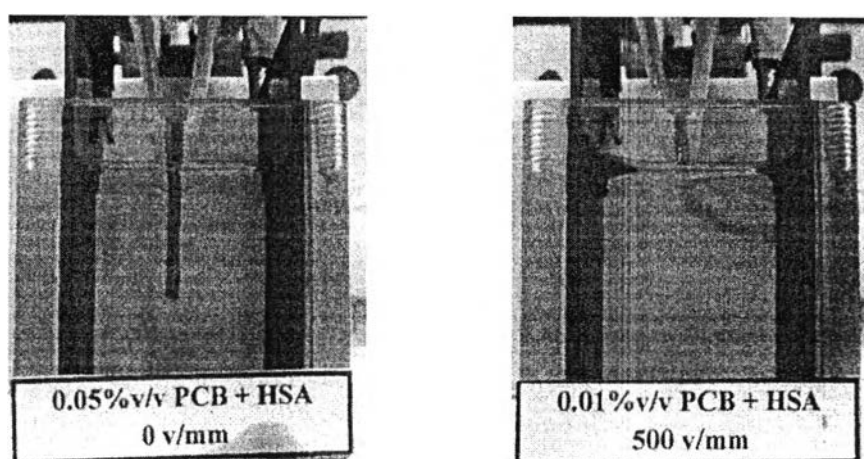


**Figure F10** Bending of pristine 0.05%v/v PCB/HSA hydrogel blend at electric field strength 0 and 500 V/mm.
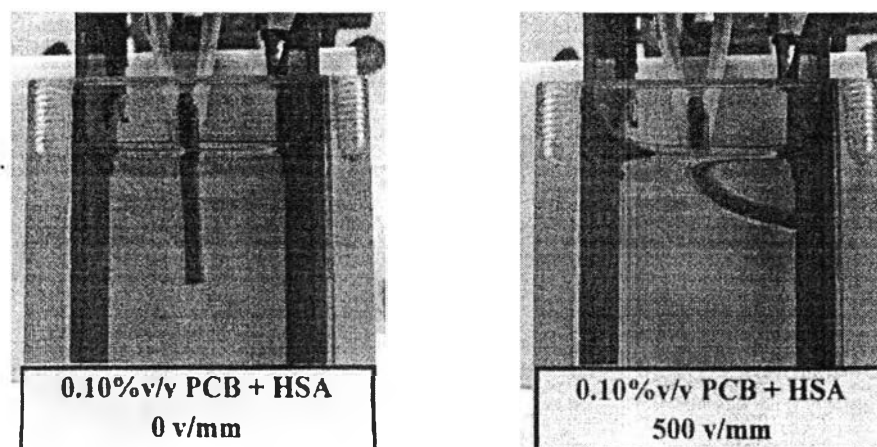
**Figure F11** Bending of pristine 0.10%v/v PCB/HSA hydrogel blend at electric field strength 0 and 500 v/mm.



**Figure F12** Bending of pristine 0.30%v/v PCB/HSA hydrogel composite at electric field strength 0 and 500 v/mm.

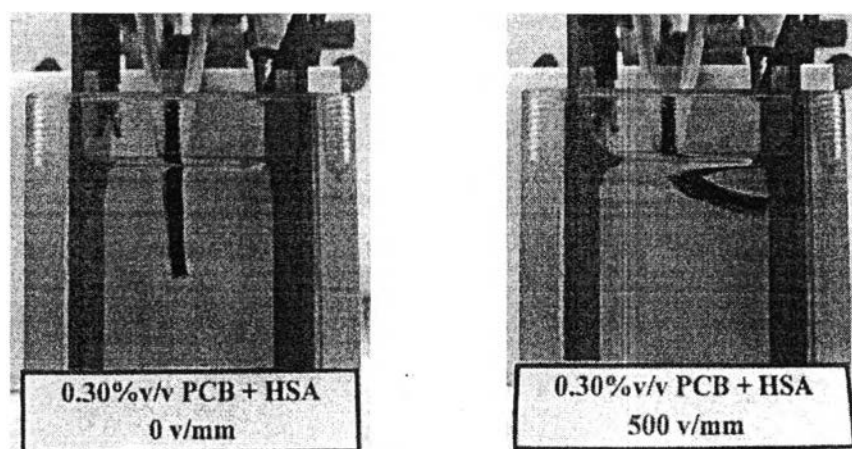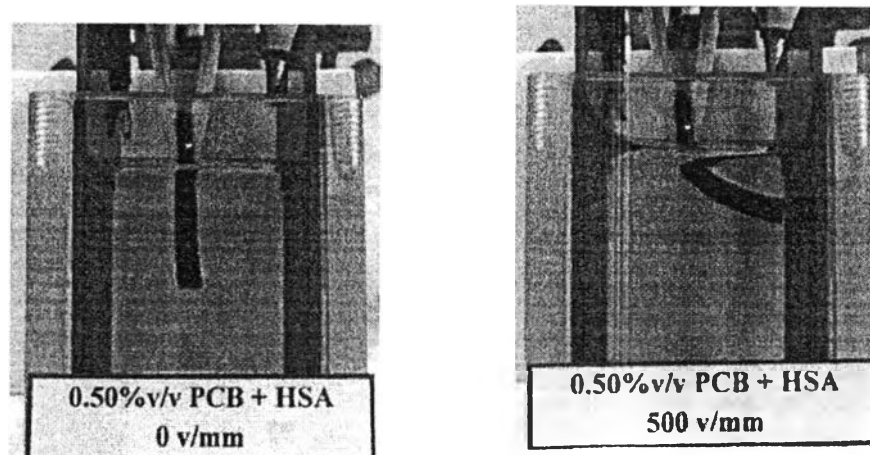**Figure F13** Bending of pristine 0.50%v/v PCB/HSA hydrogel blend at electric field strength 0 and 500 v/mm.

# CURRICULUM VITAE

**Name:**              Mr. Watchara Sangwan

**Date of Birth:**     January 10, 1990

**Nationality:**       Thai

**University Education:**

2009-2012    Bachelor Degree of Science

(B. Sc. Polymer Science), Faculty of Science Prince of Songkla University, Songkhla, Thailand

**Work Experience:**

2011              Position: Student trainee

Company name: Print Master Co., Ltd

**Proceedings:**

1.    Sangwan, W.; and Sirivat, A. (2015, April 21) Electrically Responsive Materials based on Polycarbazole/Alginate Bio-hydrogel Blends for Actuator. Proceeding of the 6$^{th}$ Research Symposium on Petrochemical and Materials Technology and the 21$^{st}$ PPC Symposium on Petroleum, Petrochemicals, and Polymers, Bangkok, Thailand.

**Presentations:**

1.    Sangwan W.; Leejarkpa T.; and Riyajan S. (2013). Effects of Parameters on the Swelling and Thermal Behavior of Epoxidized Natural Rubber/Cassava Starch Blend, Pure and Applied Chemistry, Paper presented at International Conference 2013 (PACCON 2013). , Chonburi, Thailand.

2.    Sangwan, W.; and Sirivat, A., (2015, April 21) Electrical Responsive Material based Polycarbazole/Alginate Bio-hydrogel blends as an Actuator. Paper presented at the 6$^{th}$ Research Symposium on Petrochemical and Materials Technology and the 21$^{st}$ PPC Symposium on Petroleum, Petrochemicals, and Polymers, Bangkok, Thailand.

3. Sangwan, W.; and Sirivat, A., (2015, May 21-23) Electrically Responsive Materials based on Polycarbazole/Alginate Bio-hydrogel blends for Actuator. Paper presented at the 4<sup>th</sup> International Symposium Frontiers in Polymer Science in Association with the Journal Polymer, Riva del Garda, Italy.